THE UNIVERSITY OF MICHIGAN

INDUSTRY PROGRAM OF THE COLLEGE OF ENGINEERING

P-v-T DATA FOR NEON AND HELIUM AT TEMPERATURES FROM 70° K TO 120° K AND PRESSURES TO 690 ATMOSPHERES

John A. Sullivan

A dissertation submitted in partial fulfillment
of the requirements for the degree of
Doctor of Philosophy in the
University of Michigan
Department of Mechanical Engineering
1966

February, 1966

IP-730

Doctoral Committee:

Associate Professor Richard E. Sonntag, Chairman
Associate Professor Edward R. Lady
Professor Joseph J. Martin
Assistant Professor Gene E. Smith
Professor Gordon J. Van Wylen

ACKNOWLEDGEMENTS

The author would like to express thanks to those persons and organizations who have, by their support and interest, made the completion of this research possible.

Thanks are extended to the National Science Foundation, the Ford Foundation and the Mechanical Engineering Department for personal financial support of the author and his family for the duration of the research.

Recognition for funding the research is extended to the National Science Foundation and the Mechanical Engineering Department.

Recognition for donation of the test gases is extended to the Linde Division of Union Carbide Corporation and to the Bureau of Mines. Linde Company is also to be commended for direct support of the research with contributions of liquid argon.

Special recognition for continued assistance and interest is extended to Professor Sonntag and Professor Van Wylen. Thanks are extended to the other members of the doctoral committee for their constructive criticism and helpful advice.

Special thanks are also given to Professor Herman Merte, who, although he was not directly connected with the project, was always willing to give special attention to problems which arose.

The author extends thanks to his colleague, Richard W. Crain, who served as a critic for new ideas and a sounding board for ironing out experimental difficulites.

Thanks are also extended to James Schairer for technical advice in the construction of electronic apparatus and to Jack Brigham and his staff for technical assistance in the construction and maintainance of the experimental equipment.

Finally special thanks are extended to my wife and family for sustaining the years of sacrifice and tight-budget living conditions forced upon them by the author's decision to pursue the Doctor of Philosophy degree.

TABLE OF CONTENTS

TABLE OF CONTENTS (CONT'D)

LIST OF TABLES

LIST OF TABLES (CONT'D)

LIST OF FIGURES

LIST OF FIGURES (CONT'D)

NOMENCLATURE

Arabic Symbols

A	first virial coefficient.
A'	first coefficient in the Berlin expansion.
A_e	effective area of the dead weight gage piston.
A_o	area of dead weight gage piston at zero pressure and 25° C.
B	second virial coefficient.
B^*	reduced second virial coefficient defined by Equation (57).
B'	second coefficient in the Berlin expansion.
B_{cl}	second virial coefficient obtained from corrected Boltzmann statistics.
B^*_{cl}	reduced classical second virial coefficient.
B_o	second virial coefficient for Fermi-Dirac and Bose-Einstein gases at low pressure.
B^*_o	reduced ideal gas second virial coefficient for Fermi-Dirac and Bose-Einstein gases.
B_I	first quantum correction to second virial coefficient.
B_{II}	second quantum correction to second virial coefficient.
B^*_I	reduced first quantum correction to the second virial coefficient.
B^*_{II}	reduced second quantum correction to the second virial coefficient.
b_o	reducing parameter $2/3 \; \Pi \; \tilde{N} \; \sigma^3$.
b^j, b^j_I, b^j_{II}	defined by Equations (62), (63) and (64).
C	third virial coefficient and third coefficient in Leiden expansion.
C'	third coefficient in the Berlin expansion.
D	fourth coefficient in the Leiden expansion.
D'	fourth coefficient in the Berlin expansion.

E	fifth coefficient in Leiden expansion and Young's modulus.
E'	fifth coefficient in the Berlin expansion.
E_V	error introduced into compressibilities due to incomplete evacuation of V_{II}.
F	sixth coefficient in the Leiden expansion.
F'	sixth coefficient in the Berlin expansion.
G	seventh coefficient in the Leiden expansion.
G'	seventh coefficient in the Berlin expansion.
g	gravitational acceleration.
g_c	unit conversion factor for ft, lbm, lbf, sec system.
h	Planck's constant and also height.
I	intercept on a plot of $P_j \prod_{i=1}^{j} N_i$ against P_j.
K	defined by Equation (24).
k	ratio of outside to inside radius of the Burnett cells. Boltzmann's constant.
L	defined by Equation (83).
ℓ	number of lead space volumes prior to expansion and subscript for last measured point of a partial run.
M	intercept on a plot of P_{j-1}/P_j against P_j.
m	mass, number of dead space volumes after expansion, and molecular mass.
n	number of moles.
$\tilde{N}$	Avogadro's number.
N_o	equipment constant.
N_j	defined by Equation (15).

P	Pressure.
P_m	pressure due to mass on dead weight gage.
R, $\bar{R}$	Universal gas constant. Dead weight gage resolution.
r	molecular separation.
S	slope on a plot of P_o/Z_o against N_o .
T	temperature.
T^*	reduced temperature.
V_I	volume of large Burnett cell.
V_{II}	volume of small Burnett cell.
V_{cj}	The volume the gas in the extraneous volume would occupy if at the test temperature.
V_T	total volume of Burnett cells.
V'_{co}	Corrected dead space volume at zero pressure after expansion.
V_{co}	Corrected dead space volume at zero pressure prior to expansion.
v	specific volume.
W	weight of mass on dead weight gage.
Z	compressibility factor.

Greek Symbols

β	error in $v_j(Z_j - 1)$
$\Delta (P_o/Z_o)$	error in (P_o/Z_o) due to error in N_o also total error in (P_o/Z_o) in Equations (20) and (118).
ΔV_{Ij}	volume of V_I at pressure P_j minus volume of V_I at zero pressure.
δ	extrapolation error in P_o/Z_o .

ϵ	depth of potential well.
Λ	deBroglie wavelength of relative motion.
Λ^*	defined by Equation (56).
μ	Poisson's ratio.
φ	intermolecular potential.
ρ	density.
σ	molecular separation at which the intermolecular potential becomes zero.

I. INTRODUCTION

In the past fifty years much attention has been devoted to the determination of thermodynamic properties of pure substances, and to a lesser extent of mixtures. Such investigations are indispensable to the engineer designing separation and refrigeration equipment, and in fact for any application requiring the use of a thermodynamic analysis. These basic measurements of P-v-T behavior in addition to specific heat measurements are used to fix the values of other thermodynamic variables such as enthalpy, entropy, and internal energy. This can be done graphically, but the normal procedure is to fit an appropriate equation of state to the experimental data and proceed analytically.

The virial equation of state, which is derived theoretically by employing statistical mechanics, makes it possible to determine some characteristics of the force field between molecules with the aid of accurate P-v-T data. Thus, in addition to serving the engineer, the collection of accurate P-v-T data also serves the scientist who is attempting to more fully understand the basic nature of molecular interaction and thus improve existing theories.

Presently helium is used to cool magnets and in the low temperature operation of masers in the range from about 4 to 13°K and is being considered as a prime refrigerant at temperatures to 40°K[49]. As technology advances the construction of such refrigeration devices becomes more complex and in order to determine and improve their performance it is necessary to have an accurate and consistent set of properties for helium in the temperature range from 3°K to room temperature.

Neon, as it becomes more readily available, will become an important cryogenic fluid since it has a boiling point which lies between those of nitrogen and hydrogen. Oxygen falls partially in this range but due to the precautions that must be observed to achieve safe operation it is not suitable for many applications. On the other hand, neon is suitable for such applications as magnet cooling and cooling of infra-red detectors. Neon has also been used as an intermediate fluid in hydrogen liquification.

Helium, like neon, is inert and is thus safe to work with. For both of these substances the existance of high pressure P-v-T data is very sparce. The discovery of superfluidity, the λ-point and associated phenomena tended to divert attention from the collection of P-v-T data. Also the recent work of D. White[108] indicates that the low pressure data collected for helium and used to determine the second virial coefficients is subject to question in the region covered by this research.

In view of these considerations the research carried out by the author was initiated to extend the range of existing P-v-T data on neon and helium. In carrying out the research the Burnett Method, which is a relatively new method of collecting P-v-T data, was used for the first time at liquid nitrogen temperatures.

A comparison of the data range of this research to existing data for helium is given in Figure 1. A similar comparison for neon is given in Figure 2. Figures 1 and 2 show that experimental data for neon and helium in the range from 70°K to 120°K was quite limited prior to this work.

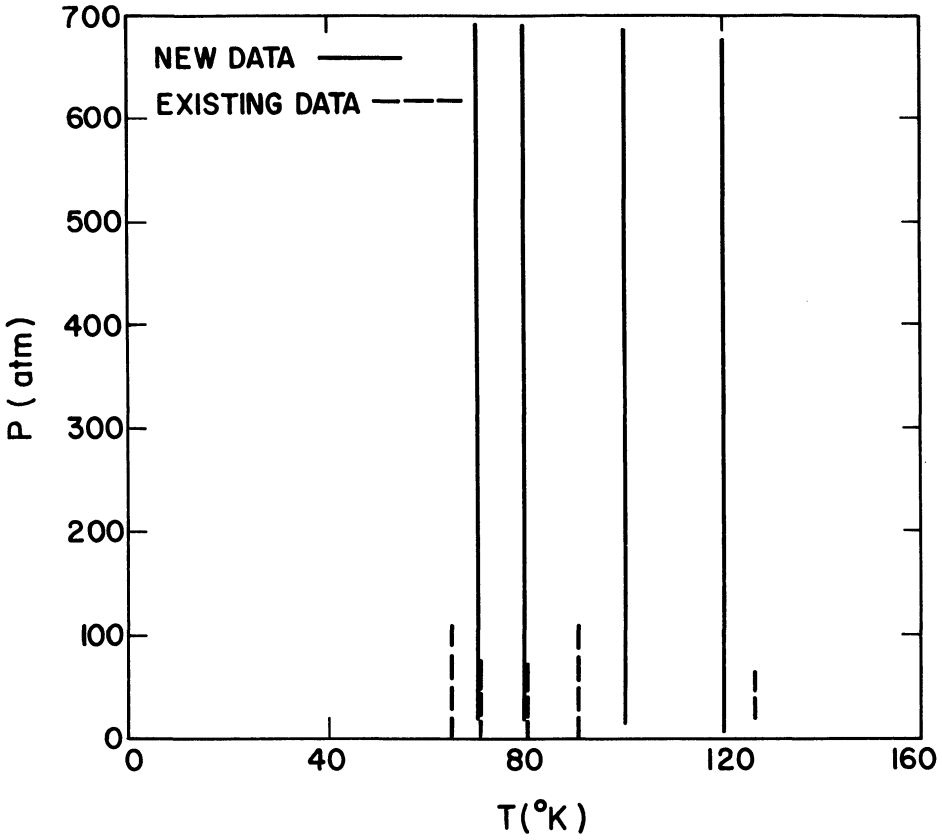

Figure 1. Isotherms of Helium Investigated in This Research

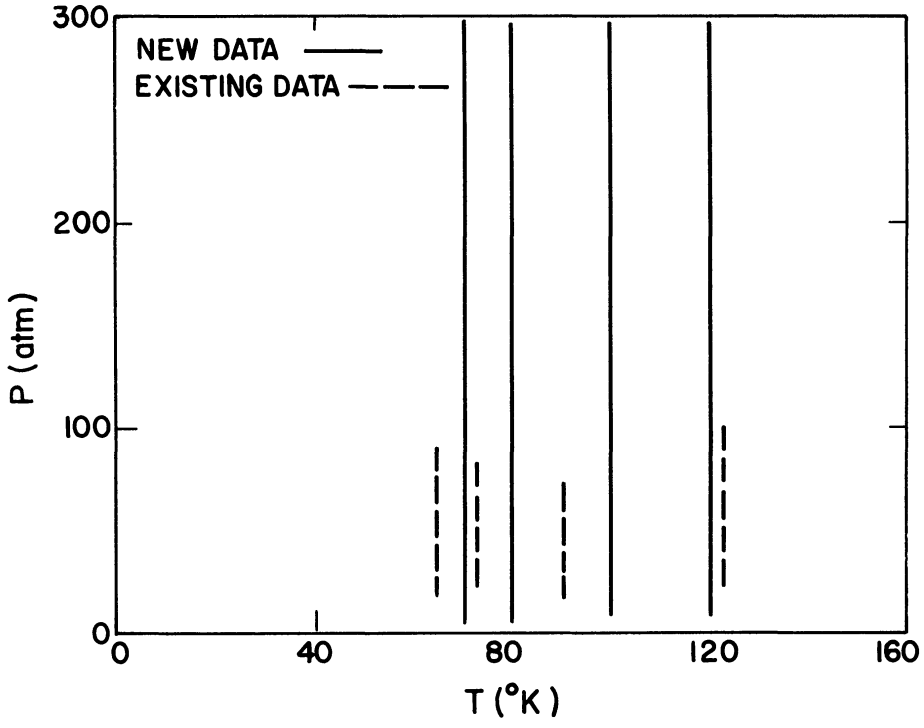

Figure 2. Isotherms of Neon Investigated in This Research.

II. LITERATURE SURVEY

A. Neon

Neon was discovered by Sir William Ramsay and Morris William Travers in 1898 when they passed an electric discharge through a sample of gas prepared by distilling argon and observed a "blaze of crimson light". Neon is a rare gas and only recently has the supply of neon exceeded the demand. As a result of the difficulties of purifying neon it is also expensive, which accounts for the relatively small amount of P-v-T data available for this substance.

Since most of the P-v-T data available for the inert gases was collected at well known laboratories, it seems appropriate to cite the references consulted under the name of the laboratory where the data was collected. In quoting the pressure ranges for the references the highest and lowest pressures measured are used. For any one particular isotherm the pressure range will lie between the limits quoted.

1. The Kamerlingh Onnes Laboratory, Leiden, Holland.

Isotherms for neon for temperatures from -217.5 to 23° C and pressures from 23 to 93 atm. were measured by H. K. Onnes and C. A. Crommelin[68] in 1915. This work was continued in 1919 by H. K. Onnes, C. A. Crommelin and J. P. Martinez[16] when isotherms of neon were measured for temperatures from -217.52 to 20° C and pressures from 21 to 93 atm.

2. The Physikalisch-Technische Reichsanstalt, Berlin, Germany.

Work at this laboratory was carried out by L. Holborn and J. Otto and consists of the following measurements:

a. Reference (32): Isotherms from 0 to 400° C and pressures from 0 to 105 atm.

b. Reference (31): Isotherms from -183 to 400° C and pressures from 0 to 105 atm.

c. Reference (30): One isotherm at -207° C at pressures from 20 to 90 atm.

Also V. W. Heuse and J. Otto[28] measured the 0° C isotherm of neon for pressures from 0.4 to 1 atm.

3. The Van der Waals Laboratory, Amsterdam, Holland.

Isotherms for neon were measured at temperatures from 0 to 100° C and pressures from 20 to 500 atm. by A. Michels and R. O Gibson[60] in 1928. Thirty years later A. Michels, T. Wassenaar, and P. Louwerse measured isotherms for neon at temperatures form 0 to 150° C and pressures from 24 to 2900 atm.

4. The National Research Council Laboratories, Ottawa, Canada.

G. A. Nicholson and W. G. Schneider[63] measured isotherms for neon for temperatures from 0 to 700° C and pressures form 10 to 80 atm. This reference is unique because the Burnett method was used to obtain P-v-T data whereas the previous references used either a piezometer or the constant volume method. The fact that the results agree within experimental accuracy shows that accurate P-v-T data can be obtained using the Burnett method, which is somewhat easier to use and eliminates the necessity of making accurate volume and mass measurements.

Other experimental P-v-T measurements for neon include the following

a. Measurement of the 0° C isotherm for pressures from 0.18 to 1.1 atm by F. P. Burt[9] in 1910.

b. Measurement of the 0° C and 100° C isotherms at pressures less than 2 atm by J. Oiski[67] in 1949.

c. Measurements by W. Ramsey and M. S. Travers[78] of isotherms from 11.2 to 237.3° C and pressures from 39 to 94 atm.

The most recent papers concerning neon P-v-T data are theoretical in that an equation of state was fitted to existing neon data and used to compute the properties for neon in those regions where no data is available. The first of these works was carried out by Yendall[102] in 1958 and consisted of fitting a twelve constant equation of state to the experimental data collected at Leiden in 1915 and 1919. The comparison of theoretically calculated values and experimental values was 1.055% maximum deviation for the Leiden points and 1.64% for those obtained by Michels and Gibson[60] in 1928. In 1962 McCarty, Stewart and Timmerhaus[59] presented a paper at the 1962 Cryogenic Engineering Conference giving compressibility factors for neon from 27 to 300° K and pressures from 0.1 to 200 atm. The data were calculated using Yendall's[102] equation of state which was fitted to existing neon data and additional reduced values calculated from data on nitrogen and argon using the theory of corresponding states. An empirical correction based on the differences in the argon-nitrogen P-v-T surfaces was made for similar differences in the P-v-T surfaces of neon and nitrogen.

A later paper by McCarty and Stewart[58] repeats the results of the above mentioned paper using the Strobridge equation of state. The accuracy to which the equation of state fitted the experimental data was comparable to the accuracy of the data. This paper extends the results of the previous work to the liquid region and gives more consistent thermodynamic properties for the entire range.

The above survey presents all the work done on P-v-T behavior of the vapor phase of pure neon. Other investigators have measured the critical constants of neon and its vapor pressure but these results are not of interest here.

B. Helium

The inert element "helium" was first discovered in 1868 when scientists observed a solar eclipse with spectrographs and found a bright yellow line near the sodium D line. Since that time helium has been the subject of many experiments and is the most widely studied inert gas. In 1942 Keesom[40] made an exhaustive literature survey on helium and published a book which discussed in detail the behavioral characteristics of helium. It would be to lengthy to cite all of the references available on helium P-v-T behavior and only those which overlap into the region of this work are given. As in the case of neon the major references will be cited under the name of the laboratory where the experimental observations were made.

1. The Kamerlingh Onnes Laboratory, Leiden, Holland.

Isotherms of helium for temperatures from -258.82° C to 100.35° C and pressures from 10 to 67 atmospheres were measured by H. K. Onnes[69], [70]

in 1907 and 1908. Later in 1924 Boks and K. Onnes[73] measured isotherms of helium for temperatures from -258.78 to 20° C and pressures from 19 to 59 atm. Isotherms for temperatures from 16.65 to 69.86° K for pressures less than 1 atm were measured by van Agt and K. Onnes[93] in 1925. Keesom and Nijhoff[65] measured isotherms of helium for temperatures of -183.07° C and -201.52° C for pressures from 3 to 8 atm in 1927. Also Nijhoff, Keesom and Illum[64] measured isotherms from -259 to -103.6° C at pressures of 1.5 to 14 atm in 1927. These latter measurements by Keesom and co-workers were made at low pressures in an attempt to more accurately determine the second virial coefficient for helium.

2. The Physikalisch-Technische Reichsanstalt, Berlin, Germany.

Measurements were made at this laboratory by Holborn and Otto over a wide range of temperature. These measurements include the following:

a. Reference (33) : Measurements for temperatures from -183 to 50° C and pressures from 0 to 105 atm in 1924.

b. Reference (34) : Measurements for temperatures from -183 to 400° C and pressures from 0 to 105 atm in 1925.

c. Reference (35) : Measurements for temperatures from -258 to -183° C and pressures from 0 to 105 atm in 1926.

Of particular interest to this work is the work of D. White[108] of Ohio State University. White measured the second virial coefficient of helium over a temperature range from 20 to 300° K. The results of his work agree favorably with older work except in the temperature range from about 60 to 150° K where his results are considerably higher than

the older values. A comparison between the results of the present work, that of White, and that of previous investigators is given in Chapter 5, section C.

Many other references on helium could be cited, but the range of P-v-T measurements for these is outside of the range of temperatures of this work. A complete listing of P-v-T references to 1942 can be found in Keesom[40] and to 1961 in Cook[14].

C. The Burnett Method

The Burnett method of obtaining P-v-T data for gases employs a technique whereby no accurate volume or mass measurements are required. The method itself will be described later in more detail. E. S. Burnett[8] first introduced his method in 1936 and from 1936 to 1949 many references appeared in the literature (see for instance[1], [11], [89], [104]) describing the use of the method by natural gas companies. The method was first used as a research tool by Schneider and co-workers[13],[48],[82],[83],[99], [103], at the National Research Council Laboratories in Canada. Their studies include work on helium. carbon dioxide, argon and neon. All of their investigations are above 0° C. Considerable improvements over the industrial models of the Burnett apparatus were introduced and the results obtained are as accurate as those obtainable by other methods. The Burnett method has also been used extensively at the University of Pennsylvania[26],[27],[76],[77], [96] where the primary emphasis has been on the study of gaseous mixtures. Other investigators who have used the Burnett method successfully are Silberberg, Kobe and McKetta[85],[86],[87]; Watsen[97]; Crain[15]; and Canfield[10] and Mueller[62] at Rice University.

D. Related Literature

Many references were consulted during the course of this research regarding design, theory, temperature control etc. These references are listed in the bibliography and will not be discussed here.

III. THEORY

A. Burnett Method

The Burnett Method is an experimental technique introduced by E. S. Burnett[8] in 1936 which makes it possible to obtain accurate P-v-T data for pure gases and gas mixtures without having to determine the volume and mass of the test gas at each experimental point. This method of collecting data has been used by several investigators[10],[13],[15],[44],[62],[82], [85] in recent years over a wide range of pressures and temperatures. In the ideal case all of the gas under observation is held at the same fixed temperature and is expanded in a series of steps from some initial pressure to some final pressure. After each expansion the pressure is measured and with the aid of analytical techniques to be discussed below it is possible to compute the compressibility factor

$$Z_j = \frac{P_j v_j}{R\,T} \qquad (1)$$

for each of the measured pressures. Knowing Z and P for a series of points along an isotherm makes it possible to determine any other thermodynamic property for that temperature by fitting the experimental data to an appropriate equation of state and calculating the desired property. In practice it is not always possible to maintain all of the gas at the same temperature and corrections to the method for such "dead space volumes" must be introduced. To implement these corrections it is necessary to accurately measure the dead space volumes and to have a fairly accurate

determination of the total volume of the cells. In addition, if the method is extended to high pressures, corrections for variations of the volumes of the Burnett cells with pressure must be included.

In the following derivation the existence of dead space volumes is assumed and the correction for variation of the cell volumes with pressure is included.

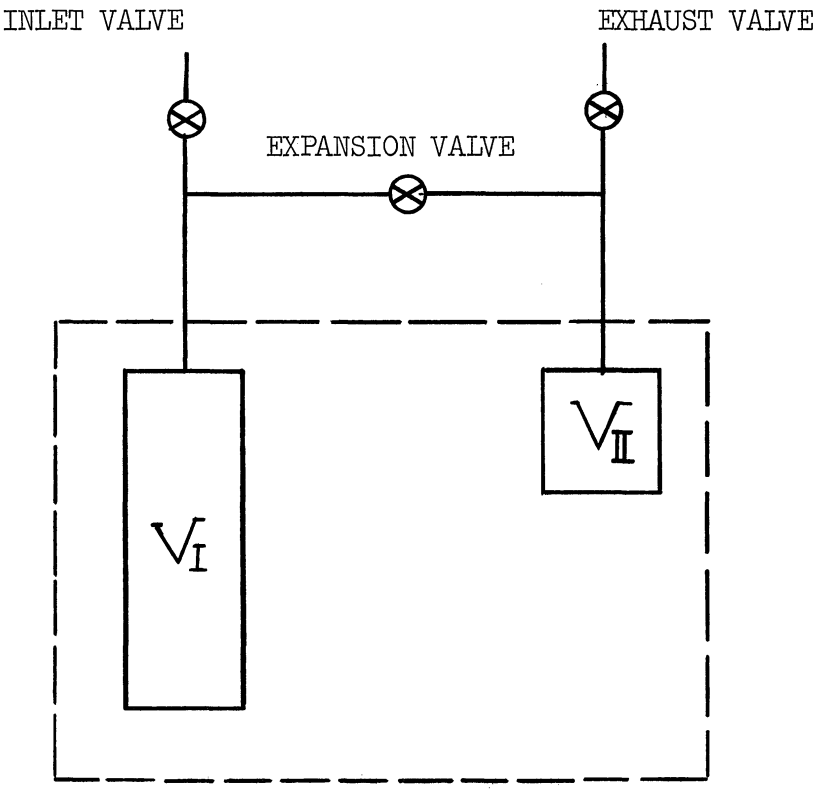

Figure 3. Schematic Illustrating the Burnett Method.

Consider the two volumes V_I and V_{II} shown in Figure 3. To initiate a series of measurements V_I is evacuated and then charged

with the test gas to some initial pressure P_o. After measuring this pressure V_{II} is evacuated, the test gas is expanded from V_I to V_{II} and the new pressure P_1 is measured.

After closing the expansion valve, V_{II} is again evacuated and a second expansion to a pressure P_2 is carried out. This process of evacuation, expansion and measurement of the pressure is continued until a low pressure is reached. The experimental data consists of the isothermally measured pressures generated by the above procedure.

To show how the experimental compressibility factors are obtained from such data let it be assumed that the Burnett cells and the portions of the inlet and exhaust lines within the dashed boundary in Figure 3 are held at the test temperature. The volume of gas in the valves and connecting lines outside of the dashed boundary is assumed to be at some temperature different from the test temperature. To simplify the analysis it will be assumed that the volumes V_I and V_{II} include the volumes of the lines within the dashed boundary. Because of its frequent appearance the quantity,

$$N_o = \frac{V_I + V_{II}}{V_I} = \frac{V_T}{V_I} \qquad (2)$$

evaluated at zero pressure, is given the symbol N_o and called the equipment constant. Equation (1) written for the condition with V_I having a pressure P_{j-1} and V_{II} evacuated is

$$Z_{j-1} = \frac{P_{j-1}\,(V_I + \Delta V_{I(j-1)} + V_{c(j-1)})}{n_{j-1}\,\overline{R}\,T} \qquad (3)$$

where $\Delta V_{I(j-1)}$ is the change in V_I due to pressurization and $V_{c(j-1)}$ is the volume the amount of gas in the lines and valves up to the expansion valve would occupy if it were at the test temperature. After expansion to the new pressure P_j, Equation (1) written for the same amount of gas is

$$Z_j = \frac{P_j(V_I + V_{II} + \Delta V_{Ij} + \Delta V_{IIj} + V_{cj})}{n_{j-1} \bar{R} T} \tag{4}$$

Dividing Equation (4) by Equation (3) and rearranging gives

$$\frac{Z_j}{Z_{j-1}} = \frac{P_j}{P_{j-1}} \frac{\left(\frac{V_I + V_{II}}{V_I} + \frac{\Delta V_{Ij}}{V_I} + \frac{V_{II}}{V_I} \frac{\Delta V_{IIj}}{V_{II}} + \frac{V_{cj}}{V_I} \right)}{\left(1 + \frac{\Delta V_{I(j-1)}}{V_I} + \frac{V_{c(j-1)}}{V_I} \right)} \tag{5}$$

For the purposes of analysis, it is assumed that the Burnett cells are thick walled cylinders with the same ratio (k) of outside to inside radius. For such cylinders the Lamé formula for volume dilatation can be used

$$\frac{\Delta V_{Ij}}{V_I} = \frac{P_j}{E} \left[2\left(\frac{k^2 + 1}{k^2 - 1} + \mu \right) + \frac{1 - 2\mu}{k^2 - 1} \right] \tag{6}$$

where E is the modulus of elasticity of the cell material and μ is Poisson's ratio. For cells of different volume but with the same value of k and made of the same material Equation (6) shows that

$$\frac{\Delta V_I}{V_I} = \frac{\Delta V_{II}}{V_{II}} \tag{7}$$

for the same change in pressure. Making use of (7) and (2) in (5) gives the result

$$\frac{Z_j}{Z_{j-1}} = \frac{P_j}{P_{j-1}} N_o \left(\frac{1 + \frac{\Delta V_{Ij}}{V_I} + \frac{V_{cj}}{V_T}}{1 + \frac{\Delta V_{I(j-1)}}{V_I} + \frac{N_o V_{c(j-1)}}{V_T}} \right) \tag{8}$$

For m dead space volumes each at a different termperature, the corrected volume is

$$V_{cj} = Z_j T \sum_{i=1}^{m} \frac{V_{ci}}{Z_{ji} T_i} \tag{9}$$

where V_{ci} is the volume of the i-th dead space, Z_j is the compressibility factor of the test gas at pressure P_j and temperature T, and Z_{ji} is the compressibility of the test gas at pressure P_j and temperature T_i.

Rearranging (8) and taking the limit as the pressure approaches zero gives

$$\lim_{p \to 0} \frac{P_{j-1}}{P_j} = N_o \lim_{p \to 0} \left(\frac{1 + \frac{V_{cj}}{V_T}}{1 + \frac{N_o V_{c(j-1)}}{V_T}} \right) \tag{10}$$

since $\Delta V_{Ij}/V_I \to \frac{\Delta V_{I(j-1)}}{V_I} \to 0$ and $Z \to 1$ as $P \to 0$. From (9) it can be seen that as the pressure approaches zero

$$V_{cj} \to T \sum_{i=1}^{m} V_{ci}/T_i = V'_{co} \tag{11}$$

and

$$V_{c(j-1)\rightarrow T} \sum_{i=1}^{\ell} V_{ci}/T_i = V_{co} \tag{12}$$

In view of (11) and (12) Equation (10) can be written as

$$\lim_{P \rightarrow 0} \frac{P_{j-1}}{P_j} = N_o \left(\frac{1 + \frac{V'_{co}}{V_T}}{1 + \frac{N_o V_{co}}{V_T}} \right) = M \tag{13}$$

From (13) it can be seen that a plot of P_{j-1}/P_j against P_j when extrapolated to zero pressure gives the numerical value of M. Knowing M makes it possible to compute N_o from

$$N_o = \frac{M}{1 + \frac{V'_{co}}{V_T} - M \frac{V_{co}}{V_T}} \tag{14}$$

Defining the quantity N_j as

$$N_j = N_o \left(\frac{1 + \frac{\Delta V_{Ij}}{V_I} + \frac{V_{cj}}{V_T}}{1 + \frac{\Delta V_{I(j-1)}}{V_I} + \frac{N_o V_{c(j-1)}}{V_T}} \right) \tag{15}$$

and substituting into (8) gives

$$\frac{Z_j}{Z_{j-1}} = \frac{P_j}{P_{j-1}} N_j \tag{16}$$

By applying Equation (16) repeatedly for the first, second, etc. expansions the following result is obtained

$$\frac{Z_1}{Z_o}\ \frac{Z_2}{Z_1}\ \cdots\cdots\frac{Z_j}{Z_{j-1}} = \frac{P_1}{P_o}\ \frac{P_2}{P_1}\ \cdots\ \frac{P_j}{P_{j-1}}\ N_1N_2\cdots\cdots N_j$$

or

$$P_j \prod_{i=1}^{j} N_i = Z_j \frac{P_o}{Z_o} \tag{17}$$

Taking the limit of (17) as the pressure approaches zero gives

$$\lim_{P \to 0} P_j \prod_{i=1}^{j} N_i = \frac{P_o}{Z_o} \tag{18}$$

Equation (18) shows that a plot of $P_j \prod_{i=1}^{j} N_i$ against P_j when extrapolated to zero pressure yields the quantity P_o/Z_o, which is called the fill constant for a run. Knowing P_o/Z_o and N_o the values of the compressibility factor at each of the other experimental points can be calculated from Equations (6), (9), (15) and (17).

It should be noted that the procedure described above implies a prior knowledge of the compressibilities to be determined. To circumvent this problem an initial guess at the values of the unknown compressibilities is made and the error is then iterated out by repeating the calculations several times.

B. Treatment of Partial Runs

Because of the nature of the Burnett method the high pressure points are widely spaced and to more accurately determine the isotherm at high pressures a partial run is desirable. To reduce the data for such a run

it is necessary to assume that the value of N_o as determined from a prior complete run at the same temperature is the same for the partial run. In addition, the data for the complete run must be used to determine the value of Z for the last measured pressure of the partial run. With this information the fill constant for the partial run can be determined from

$$\frac{P_o}{Z_o} = \frac{P_\ell}{Z_\ell} \prod_{i=1}^{\ell} N_i \tag{19}$$

and the compressibilities can be determined in the same way as for a complete run. It is apparent that any error in the values for the complete run is carried over into the determination of the values for the partial run.

C. Discussion of Errors in the Burnett Method

It can be shown (see Chapter V section C) that the total error in the compressibilities calculated by the method outlined above is given by

$$\frac{\Delta Z_j}{Z_j} = \frac{\Delta P_j}{P_j} + j\frac{\Delta N_j}{N_j} + \frac{\Delta(P_o/Z_o)}{P_o/Z_o} + \left(\frac{\partial Z}{\partial T}\right)_P \Delta T \tag{20}$$

Temperature and pressure can be very accurately measured so that the first and last terms on the right in Equation (20) are not critical. The second term in Equation (20) shows that the accuracy in the compressibility factors decreases as the number of expansions increases. It is obvious that the error in N_j must be kept to as small a value as possible. The error in N_j is a result of errors introduced by inaccurate correction

for volume dilatation and dead space corrections and the error in N_o . For a properly designed system the errors introduced by inaccurate correction for volume dilatation and dead space corrections are small compared to the error that can be introduced into N_j due to error in N_o . The error in N_o in turn is primarily due to the error in M . The magnitude of the error in M depends on the lower limit of the pressures measured and on the accuracy of the extrapolation to zero pressure on a plot of P_{j-1}/P_j against P_j . For a system with no dead space volumes M is equal to N_o and can be determined quite accurately by making a calibration run using helium. For a system with dead space volumes an accurate determination of N_o by the above method is possible only if the total volume and dead space volumes are very accurately known and their temperatures are accurately measured.

The third term in Equation (20) shows that the accuracy of the compressibilities are directly proportional to the accuracy of the determination of the intercept on a plot of $P_j \prod_{i=1}^{j} N_i$ against P_j . To accurately determine P_o/Z_o the value of N_o must be precisely known, the low pressure data must be taken with great care, and care must be exercised in choosing the degree of the equation used to fit the low pressure data.

Incomplete evacuation of V_{II} also introduces error into Z but this error can be shown to be negligible for the normal condition of evacuating V_{II} to pressures less than 50 microns of mercury.

It is extremely fortunate that the errors in N_o and P_o/Z_o can be detected and eliminated by the technique developed in Chapter III, section E. Thus, the prime sources of error in the Burnett Method can be restricted to errors in pressure, temperature, correction for volume dilatation, and corrections for dead space volumes.

D. Review of Present Data Treatment Techniques

Data collected using the Burnett method can be reduced by employing analytical approaches as described by Silberberg, Kobe and McKetta[86]. However for systems with dead space volumes such analytic techniques would be difficult to apply.

Recently Canfield, Leland and Kobayashi[10] proposed a method of determining N_o using only the experimental results for the gas under investigation, thus eliminating the necessity of making calibration runs. The principal assumptions of this method are that a plot of $v_j(Z_j - 1)$ against $1/v_j$ will be linear over some density range ρ_1 to ρ_2, that experimental points for densities less than ρ_1 exhibit large non-random deviations from linearity due to the physical nature of the dead weight gage and that the error introduced in extrapolating a plot of $P_j \prod_{i=1}^{j} N_i$ against P_j to zero pressure does not significantly affect the value of N_o. References (10) and (37) indicate that an incorrect value of N_o will cause a plot of $v_j(Z_j - 1)$ against $1/v_j$ (virial plot) to become non-linear after the fashion indicated in Figure 4.

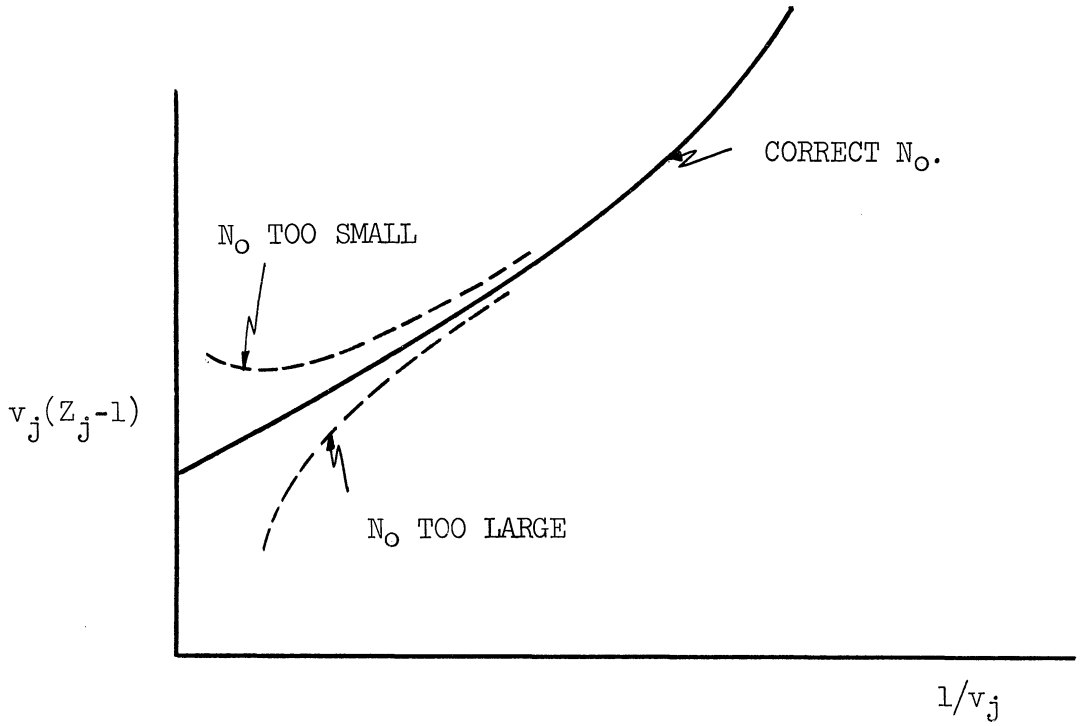

Figure 4. Effect of Varying N_o According To (10).

In attempting to employ this method it was found that it was not possible to select a unique N_o and that the extrapolation error in P_o/Z_o influenced the choice of N_o .

This discovery lead to the realization that the correct N_o could not be found unless the extrapolation error in P_o/Z_o could be eliminated. It is also apparent from the nature of the equations for reduction of the data that a small error in N_o creates an additional error in P_o/Z_o of considerable magnitude.

The mathematical analysis presented below shows that errors in P_o/Z_o and N_o both influence the nature of the non-linearities on a virial plot. The analysis also shows that the error in N_o and the extrapolation error in P_o/Z_o combine in such a manner that a virial

plot exhibits non-linearities very much different from those indicated in Figure 4.

An important conclusion that can be drawn from the analysis is that the non-linearities in the low pressure points are not due to the physical behavior of the dead weight gage. In fact, the method proposed here assumes that the percent error in the pressure measurements is essentially constant with pressure. The method shows that the non-linearities exhibited by the low pressure data on a virial plot can be used as a powerful tool for eliminating small errors in N_o and P_o/Z_o .

E. The Exact Method for Determining N_o and P_o/Z_o

To demonstrate the assertions made in section D above, let it be assumed that the true values of N_o and P_o/Z_o are known so that the true values of the compressibilities are given by Equation (17). Let N_o be varied by an amount ΔN_o causing P_o/Z_o to change an amount $\Delta (P_o/Z_o)$. Let it also be assumed that the intercept I on a plot of $P_j \prod_{i=1}^{j} N_i$ against P_j differs from P_o/Z_o by an amount $\Delta (P_o/Z_o) + \delta$ where

$$I = P_o/Z_o + \delta + \Delta (P_o/Z_o) \tag{21}$$

The error in Z_j due to the above errors can be computed from Equation (17). To a first approximation this error can be derived from

$$\frac{P_j \left(1 + j \frac{\Delta N_o}{N_o}\right) \prod_{i=1}^{j} N_i}{P_o/Z_o + \delta + \Delta (P_o/Z_o)} = Z_j + \Delta Z_j \tag{22}$$

Solving for ΔZ_j in Equation (22) yields

$$\Delta Z_j = K Z_j \tag{23}$$

where

$$K = \frac{j \frac{\Delta N_o}{N_o} - \frac{\delta + \Delta (P_o/Z_o)}{P_o/Z_o}}{1 + \frac{\delta + \Delta (P_o/Z_o)}{P_o/Z_o}} \tag{24}$$

From experience it is known that P_o/Z_o varies approximately linearly with N_o, so that

$$\Delta (P_o/Z_o) = S \Delta N_o \tag{25}$$

where S is the slope on a plot of P_o/Z_o against N_o. The slope S is always positive and has a magnitude which depends on the number of points taken for a given run. Substituting (25) into (24) gives

$$K = \frac{j \frac{\Delta N_o}{N_o} - \frac{\delta + S \Delta N_o}{P_o/Z_o}}{1 + \frac{\delta + S \Delta N_o}{P_o/Z_o}} \tag{26}$$

The error in v_j brought about by error in Z_j is given by

$$\Delta v_j = K v_j \tag{27}$$

so that the error in $v_j(Z_j - 1)$ can be shown to be

$$\beta = v_j (1 + K)[Z_j(1 + K) - 1] - v_j(Z_j - 1) = K v_j(2Z_j - 1) \tag{28}$$

where it has been noted that $K^2 << 2K$ for small errors. The true nature of the effect of errors in N_o and P_o/Z_o on a virial plot can be demonstrated by plotting β against $1/v_j$ (β - plot). The effect of errors in $1/v_j$ will not be considered here. These errors are small and would shift the abscissa of the points slightly but would not significantly change the shape of the curves on a β - plot. The consideration of errors in N_o and P_o/Z_o can be divided into the following cases:

Case 1. No error in N_o

For no error in N_o Equation (26) becomes

$$K = \frac{-\delta}{P_o/Z_o + \delta} \tag{29}$$

Equation (29) in conjunction with Equation (28) shows that β is positive for δ negative ($I < P_o/Z_o$) and negative for δ positive ($I > P_o/Z_o$) with the exception of the region for which Z_j is less than 0.5. For a substance such as helium (or a typical substance for temperatures greater than the Boyle temperature), the variation of β with $1/v_j$ is shown by the curves labeled C1 in Figure 5.

A β - plot for a typical substance for isotherms with a region where Z_j is less than 0.5 is shown in Figure 6.

Case 2. No Extrapolation Error in P_o/Z_o

For the case where $\delta = 0$, Equation (26) becomes

$$K = \frac{\left(j - \frac{S\,N_o}{P_o/Z_o} \right) \frac{\Delta N_o}{N_o}}{1 + \frac{S\,\Delta N_o}{P_o/Z_o}} \tag{30}$$

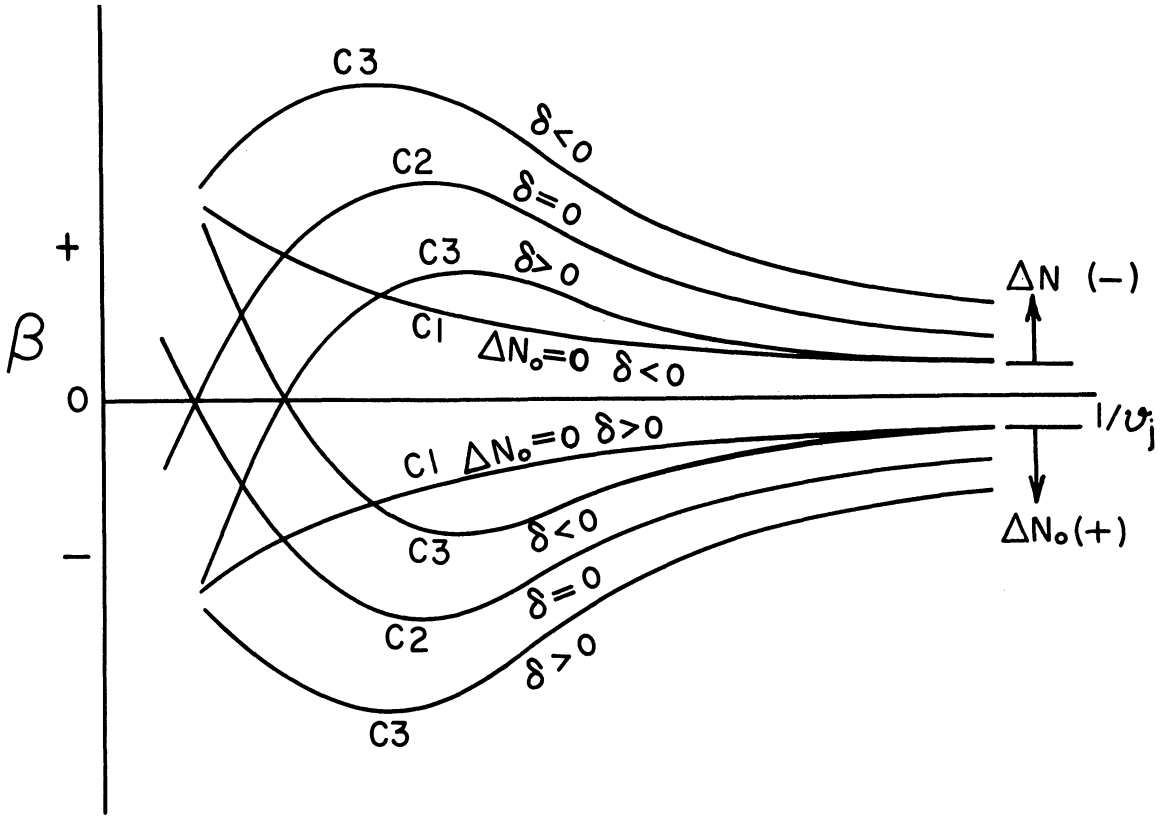

Figure 5. β-Plot For Helium.

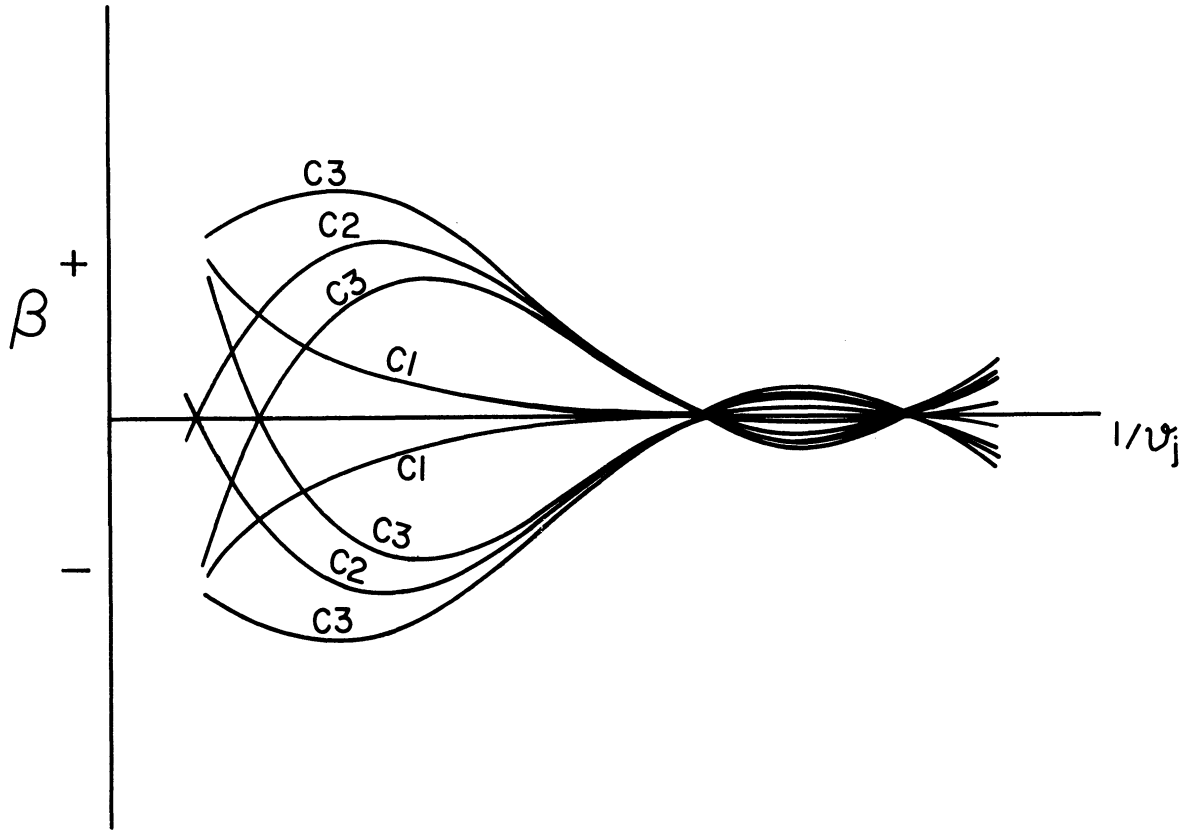

Figure 6. β-Plot For A Typical Substance For Isotherms With A Region Where $Z < 0.5$.

Examination of (30) and (28) indicates that there are three places where the error will be approximately zero. For isotherms which have values of $Z_j < 0.5$, the error will be close to zero at $Z_j = 0.5$, which occurs at two places and for all isotherms the error will be near zero for

$$j \cong \frac{S\ N_o}{P_o/Z_o} \tag{31}$$

Equation (30) shows that for $j < \frac{S\ N_o}{P_o/Z_o}$ and ΔN_o negative (N_o too small), β will be positive except for the range where Z_j is less than 0.5. For $j > S\ N_o/P_o/Z_o$ and ΔN_o negative, the sign of β is reversed. A similar argument applies for ΔN_o positive (N_o too large).

The curves labeled C2 in Figures 5 and 6 show the variation of β with $1/v_j$ for the case where $\delta = 0$.

Case 3. Error in both P_o/Z_o and N_o

For this case, which is the normal situation, a β - plot takes on appearances which result from the four possible combinations of the curves for Cases 1 and 2. The true nature of the curves will depend on the relative magnitudes of δ and ΔN_o . The general appearance of the curves is shown in Figures 5 and 6 for the same δ and ΔN_o which gave rise to the Case 1 and Case 2 curves.

It should be noted that Figures 5 and 6 are drawn to indicate the trends predicted by the equations derived in this section and thus may be distorted somewhat from the appearance of actual experimental data. The position of the Case 3 curves is a function of the relative magnitude of ΔN_o and δ . In general they will be positioned above and below

the axis as indicated in Figures 5 and 6, but for the cases where δ is the governing error the generalization does not hold.

A β - plot for the 100° K isotherm of helium as measured in this research is shown in Figure 7. The plot was generated by imposing the errors indicated in the figure on the final experimental results which deviated from linearity with a standard deviation of 0.647×10^{-3} in $v_j(Z_j - 1)$ for densities less than half the critical density.

Figure 7 shows the same trends as Figure 5 and thus demonstrates that the theory presented here gives a close approximation to the true nature of the effects of errors in P_o/Z_o and N_o .

Figure 8 is a β - plot for the 80° K isotherm of Neon. This β - plot for neon shows that the isotherms of a substance for temperatures less than the Boyle temperature will be S-shaped on a virial plot if incorrect values of N_o and P_o/Z_o are used.

The development presented here shows that to obtain the true values of P_o/Z_o and N_o the deviation of the low pressure points from linearity must be minimized with respect to these parameters. This is equivalent to finding the minimum point of a surface generated by plotting the deviation from linearity as the elevation above the $N_o - P_o/Z_o$ plane. Due to the amount of work required to find such a minimum point for Burnett data the task can be performed readily only with the aid of a digital computer.

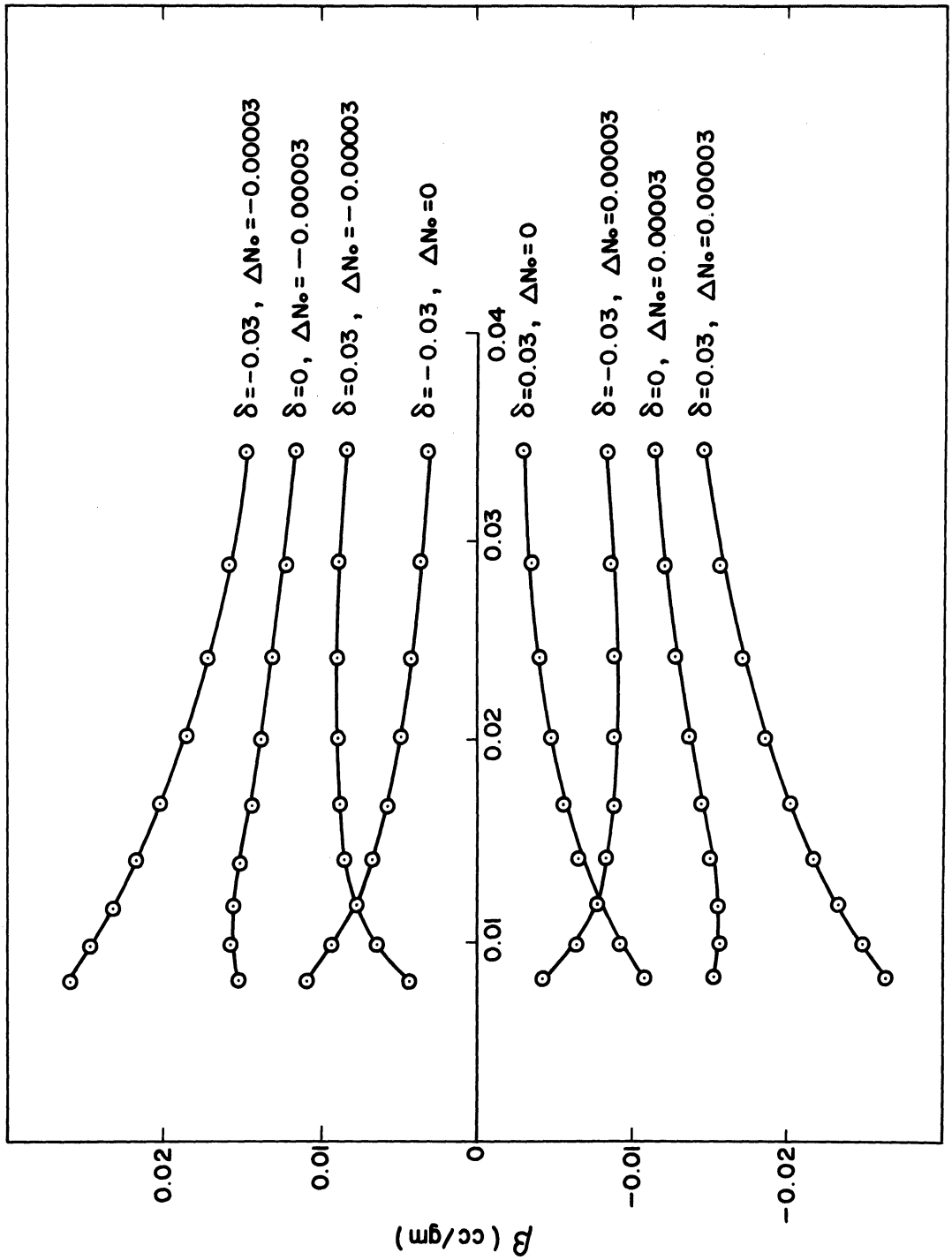

Figure 7. β-Plot For 100° K Helium Isotherm (δ in atm).

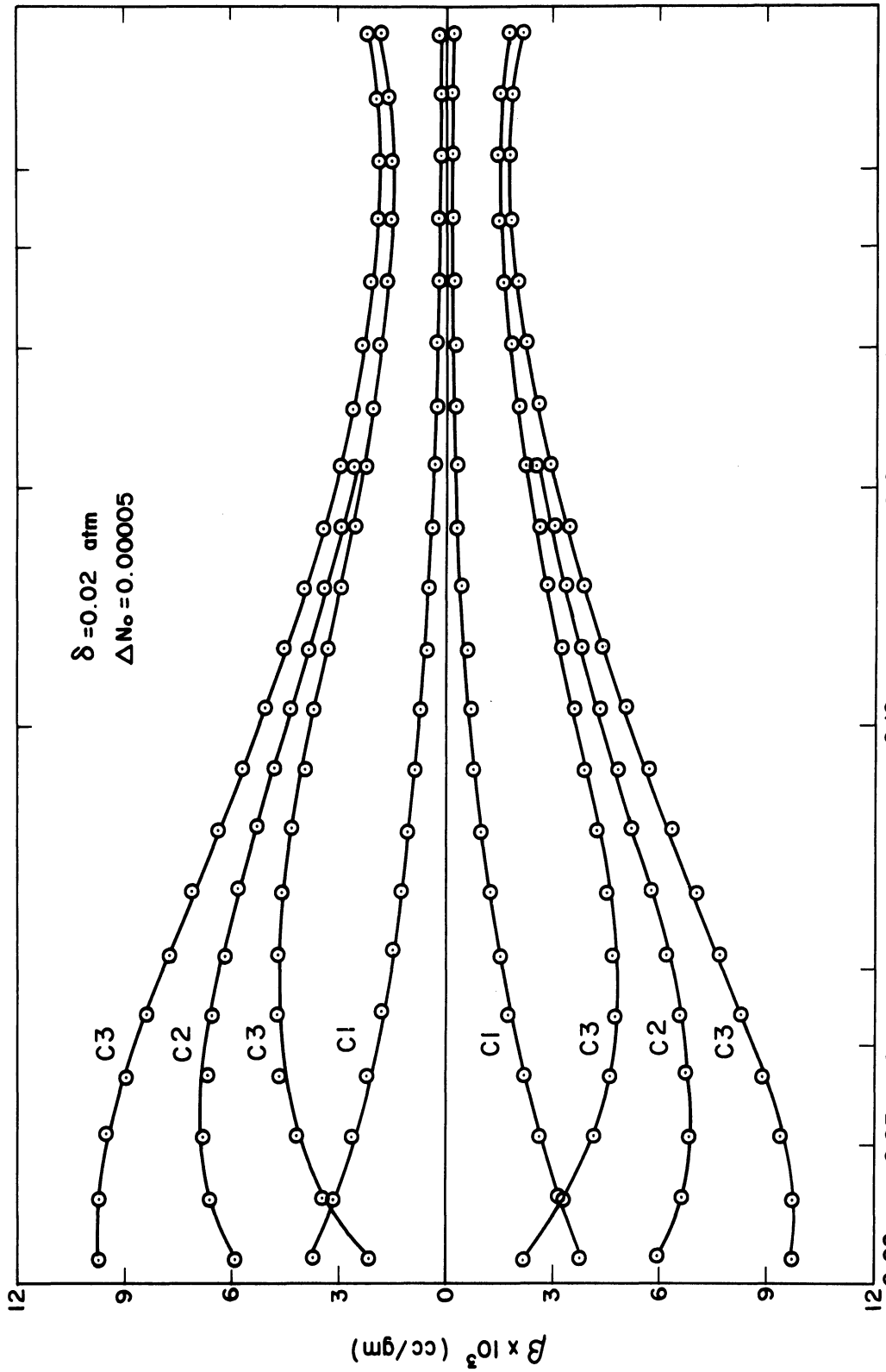

Figure 8. β-Plot For 80° K Neon Isotherm.

As opposed to the technique introduced by Canfield, Leland and Kobayashi[10] the technique introduced here permits the reduction of the experimental data with no chance of bias on the part of the investigator. The values of N_o and P_o/Z_o are unique using this method and the values of the second virial coefficient are obtained from the low density points. This technique eliminates the necessity of resorting to the theory presented in Reference (37) to obtain accurate virial coefficients from Burnett data.

Finally the overall accuracy of the final data is greatly improved due to the simultaneous minimization of error in N_o and P_o/Z_o .

In using the technique proposed here for eliminating errors in N_o and P_o/Z_o the natural curvature of an isotherm on a virial plot plays an important role. If experimental points above the linear section of an isotherm are included in the linearization erroneous values of N_o and P_o/Z_o will result. In addition it is apparent that the value of N_o will be affected by any other errors which introduce non-linearities into the isotherms on a virial plot.

Thus, for a system with dead space volumes, exact repeatability of N_o cannot be expected. In the light of the above remarks it is apparent that for a system with dead space volumes N_o is not strictly an equipment constant as defined by Equation (2). For systems with dead space volumes N_o assumes the additional role of a linearizing factor for the low pressure data points.

F. The Virial Equation of State

The routine of fitting experimental P-v-T data in terms of a series expansion of the form

$$\frac{Pv}{RT} = A + \frac{B}{v} + \frac{C}{v^2} + \ldots . \qquad (32)$$

was first introduced by H. K. Onnes[71] in 1901. The number of terms necessary in (32) to obtain a satisfactory fit to experimental data increases as the density increases. This form of equation of state attained special significance when developments in statistical thermodynamics made it possible to arrive at (32) from a purely theoretical standpoint. Statistical thermodynamics shows that (32) can be obtained from the relation between the pressure and the partition function

$$P = k\,T \left(\frac{\partial \ln Z_N}{\partial V} \right)_T = k\,T \sum_{\ell} b_\ell d^\ell \qquad (33)$$

where P is pressure, k is the Boltzmann constant, T is temperature, Z is the partition function and V is the volume. The factor d is called the active number density and is equal to the product of the activity and the number density

$$d = \frac{N}{V} a \qquad (34)$$

where N is the number of molecules of the system. The activity as used here is the ratio of the fugacity at a given state to the fugacity at the standard state. As shown in Chapter 3 of Hirschfelder, Curtiss and Bird[29],

d can also be expressed as

$$d = \frac{N}{V} e^{-\sum_{i=1}^{\infty} \beta_i \frac{N}{V}} \tag{35}$$

The b_ℓ in (33) are cluster integrals defined by

$$b_\ell = \frac{1}{V\, \ell!} \int U_\ell(\vec{r}_1, \vec{r}_2, \ldots, \vec{r}_\ell) d\vec{r}_1 d\vec{r}_2 \ldots d\vec{r}_\ell \tag{36}$$

with the integration limits being the dimensions of the containing volume V.

The U functions are in turn defined in terms of the Boltzmann factor by

$$W_N(\vec{r}^N) = \sum_{(\Sigma\, \ell m_\ell = N)} \prod U_\ell(\vec{r}^{\lambda}) \tag{37}$$

The summation in (37) is over all possible divisions of N molecules into m_ℓ groups of ℓ molecules with the restriction that $\Sigma\, \ell m_\ell = N$. The superscripts indicate sets of N and λ molecules respectively. The Boltzmann factor can also be written as

$$W_N(\vec{r}^N) = e^{-\Phi(\vec{r}^N)/kT} \tag{38}$$

where Φ is the potential energy of the system of N molecules. Expansion of (38) yields the following relations

$$W_1(\vec{r}_i) = U_1(\vec{r}_i) = 1 \tag{39}$$

$$W_2(\vec{r}_i, \vec{r}_j) = U_2(\vec{r}_i, \vec{r}_j) + U_1(\vec{r}_i)\, U_1(\vec{r}_j) \tag{40}$$

which gives the Boltzmann factor for one, two, etc., molecules alone in volume V. Inverse relations from (39) and (40) expressing the U functions in terms of the Boltzmann factors are easily obtained. Thus

$$U_1(\vec{r}_i) = W_1(\vec{r}_i) = 1 \tag{41}$$

$$U_2(\vec{r}_i,\vec{r}_j) = W_2(\vec{r}_i,\vec{r}_j) - W_1(\vec{r}_i)\, W_1(\vec{r}_j) \tag{42}$$

etc.

From (36), (38), (41) and (42) the cluster integrals can be written as

$$b_1 = \frac{1}{V} \int d\,\vec{r}_1 = 1 \tag{43}$$

$$b_2 = \frac{1}{2V} \iint [W_2(\vec{r}_1,\vec{r}_2) - W_1(\vec{r}_1)\, W_2(\vec{r}_2)]\, d\,\vec{r}_1\, d\,\vec{r}_2$$

$$= \frac{1}{2} \int_0^\infty (e^{-\varphi(r)/kT} - 1)\, 4\,\Pi\, r^2 dr \tag{44}$$

etc.

Returning now to (35) and noting that the β_i are functions of the cluster integrals given by

$$\beta_1 = 2\, b_2$$

$$\beta_2 = 2\, b_3 - 6\, b_2^2 \tag{45}$$

etc.

Equations (35) and (33) can be combined to give the following form for the virial equation of state.

$$\frac{PV}{NkT} = 1 - \sum_{i=1}^{\infty} \frac{i\,\beta_i}{i+1} \left(\frac{N}{V}\right)^i \tag{46}$$

or

$$\frac{Pv}{RT} = 1 - \sum_{i=1}^{\infty} \frac{i\,\tilde{N}\,\beta_i}{(i+1)v^i} \tag{47}$$

where $\tilde{N}$ is Avogadro's number. Expansion of (47) gives

$$\frac{Pv}{RT} = 1 - \frac{\tilde{N}}{2}\frac{\beta_1}{v} - \frac{2}{3}\tilde{N}\frac{\beta_2}{v^2} - \ldots. \tag{48}$$

Equation (48) is normally written in the form of Equation (32) and the coefficients B, C, etc., which represent the deviation from ideal behavior when interactions between two, three, etc. molecules become important, are called virial coefficients. By direct comparison of (32) and (48) and with the aid of (43), (44) and (45) the virial coefficients A and B are

$$A = 1$$

$$B = -\frac{\tilde{N}}{2}\beta_1 = -\tilde{N}b_2 = -\frac{\tilde{N}}{2}\int_0^{\infty} (e^{-\varphi(r)/kT} - 1)4\Pi r^2 dr \tag{49}$$

In order to be able to evaluate (49) the intermolecular potential $\varphi(r)$ must be known. The most widely used intermolecular potential is the Lennard-Jones 6-12 potential, which is

$$\varphi(r) = 4\epsilon\left[\left(\frac{\sigma}{r}\right)^{12} - \left(\frac{\sigma}{r}\right)^{6}\right] \tag{50}$$

In Equation (50), σ is the intermolecular distance at which the potential passes through zero and ϵ is the depth of the potential well. These quantities are determined from experimental data on the second virial coefficient, from viscosity data, or heat of sublimation data. The determination of the intermolecular force parameters from P-v-T data requires that the data be very accurate.

Since helium and neon both exhibit quantum deviations in the range of the experimental data covered in this research, the classical development of the virial equation as presented above must be modified. In order to make the previous development applicable in quantum mechanics it is necessary to replace the Boltzmann factor by the Slater sum and the partition function by the quantum mechanical partition function as shown in Chapter 16 of Hirschfelder, Curtiss, and Bird[29]. The Slater sum is given by

$$W_N(\vec{r}^N) = N!\,\lambda^{3N} \sum_q \varphi_q^*(\vec{r}^N)\varphi_q(\vec{r}^N)\, e^{-H/kT} \qquad (51)$$

where the functions $\varphi_q(\vec{r}^N)$ are a complete orthonormal set of eigenfunctions, $\lambda^2 = h^2/2\Pi mkT$ and H is the quantum mechanical Hamiltonian operator. By replacing $W_2(\vec{r}_1, \vec{r}_2)$ in the equation just prior to Equation (44) by the Slater sum and noting that $W_1(\vec{r}_1) = W_2(\vec{r}_2) = 1$ the second virial coefficient using quantum corrections becomes

$$B = -\frac{\tilde{N}}{2V} \iint [W_2(\vec{r}_1,\vec{r}_2) - 1]\, d\vec{r}_1 d\vec{r}_2 \qquad (52)$$

where use has also been made of Equation (49). After subtracting the second virial for ideal behavior from (52) and writing the Slater sum for two particles and substituting this into (52) the following expression for B is obtained

$$B = \left[B_{c\ell} + \frac{h^2}{m} B_I + \left(\frac{h}{m}\right)^2 B_{II} + \ldots \right] \pm \left(\frac{h^2}{m}\right)^{3/2} B_o(T) \qquad (53)$$

in which $B_{c\ell}$ is given by (49) and

$$B_I = 2\Pi \tilde{N} \left(\frac{1}{48\Pi^2 \; k^3 \; T^3} \right) \int_o^\infty e^{-\varphi(r)/kT} \left(\frac{d\varphi}{dr}\right)^2 r^2 dr \qquad (54)$$

$$B_{II} = 2\Pi \tilde{N} \left(\frac{1}{1920\Pi^4 k^4 \; T^4} \right) \int_o^\infty e^{-\varphi(r)/kT} \left[\left(\frac{d^2\varphi}{dr^2}\right)^2 + \frac{2}{r^2} \left(\frac{d\varphi}{dr}\right)^2 + \frac{10}{9kTr} \left(\frac{d\varphi}{dr}\right)^3 - \frac{5}{36k^2T^2} \left(\frac{d\varphi}{dr}\right)^4 \right] r^2 dr \qquad (55)$$

The term $(h^2/m)^{3/2} \; B_o(T)$ which is the second virial coefficient for ideal behavior is added for Fermi Dirac gases and substracted for Bose Einstein gases.

The solution to (49), (54) and (55) has been carried out by J. DeBoer and A. Michels[21] for the Lennard-Jones potential. The method used involves the expansion of B , B_I and B_{II} in rapidly converging series in powers of Λ^* where

$$\Lambda^* = \frac{\Lambda}{\sigma} = \frac{h}{\sigma \sqrt{m\epsilon}} \qquad (56)$$

The quantity Λ is the deBroglie wavelength of relative motion of two molecules at a temperature where the mean relative kinetic energy is ϵ, and is an indication of the significance of quantum effects. The result is

$$B^* = [B^*_{\ell} + \Lambda^{*2} B^*_{I} + \Lambda^{*4} B^*_{II} + \ldots] \mp \Lambda^{*3} B^*_{o} \tag{57}$$

wherein

$$B^*_{c\ell} = \sum_{j=o}^{\infty} b^j T^{*\,-(3 + 6_j)/12} \tag{58}$$

$$B^*_{I} = \sum_{j=o}^{\infty} b^j_{I} T^{*\,-(13 + 6_j)/12} \tag{59}$$

$$B^*_{II} = \sum_{j=o}^{\infty} b^j_{II} T^{*\,-(23 + 6_j)/12} \tag{60}$$

$$B^*_{o} = \left(\frac{3}{32\ \Pi^{5/2}}\right) T^{*\,-3/2} \tag{61}$$

and the coefficients b^j, b^j_I, and b^j_{II} are given by

$$b^j = -\left(\frac{2^j + 1/2}{4\ j!}\right) \Gamma\left(\frac{6_j - 3}{12}\right) \tag{62}$$

$$b^j_I = \left(\frac{36_j - 11}{768\ \Pi^2}\right)\left(\frac{2^j + 13/6}{j!}\right) \Gamma\left(\frac{6_j - 1}{12}\right) \tag{63}$$

$$b^j_{II} = -\left(\frac{767 + 4728\ j + 3024\ j^2}{491520\ \Pi^4}\right)\left(\frac{2^j + 23/6}{j!}\right) \Gamma\left(\frac{6j + 1}{12}\right) \tag{64}$$

The reduced virial coefficient given by (57) is related to that of (53) by

$$B^* = B / b^o \tag{65}$$

where $b^o = 2/3\ \Pi \tilde{N} \sigma^3$. The quantity T^* is the dimensionless temperature given by

$$T^* = \frac{k\ T}{\epsilon} \tag{66}$$

Use is made of the developements of this section in Chapter VII, section A where the determination of the intermolecular force parameters using the results of this research is discussed.

IV. EXPERIMENTAL APPARATUS AND PROCEDURES

A. Experimental Apparatus

1. General Description

The experimental apparatus used consisted of the Burnett Cells suspended in the lower portion of a cryostat insulated with multilayer insulation. The temperature of the cells was determined with a platinum resistance thermometer which was embeded in the Burnett cell block between the two gas chambers. The pressure of the test gas in the cells was measured by means of a Ruska dead weight gage with the null point determined with a differential pressure diaphragm. The Burnett cells were connected by means of appropriate valves and tubing to a piston type pressure intensifier and to a vacuum system. A differential thermocouple referenced to the location of the resistance thermometer was located in each cell. In addition, two other differential thermocouples were placed on the cells, one with its junctions on the top and the side and the other with its junctions on the bottom and the side of the cells. Resistance heaters were located around the cell and connected to an automatic temperature controller which was actuated by a wafer type resistance thermometer attached to the cells.

Cooling of the cells when required was achieved by controlling the vapor pressure of the bath fluid. Uniformity of the temperature of the bath was achieved by means of a magnetic stirring arrangement.

2. Design of the Burnett Cells

The design of the Burnett cells was dictated by the following criteria

a. Ease of construction.

b. Temperature range of the data.

c. Pressure range of the data.

d. Desired accuracy.

These considerations will be discussed below.

a. Ease of Construction.

Some consideration was initially given to making the cells spherical, but due to the difficulty of machining spherical cells this idea was discarded in favor of cylindrical cells. This decision caused the cells to have greater mass for the same total volume which is detrimental in terms of temperature response. The choice of thick walled cylinders makes it possible to determine the volume change of the cells with pressure by means of the Lamé formula for thick walled cylinders. The Lamé formula is

$$\frac{\Delta V}{V} = \frac{P}{E}\left[2\left(\frac{k^2+1}{k^2-1} + \mu\right) + \frac{1-2\mu}{k^2-1}\right] \qquad (67)$$

With the values of P, E and μ being dictated by the type of material and the pressure range of the data the only variable which can be chosen to help the design is the ratio of the outer to the inner radius. The larger the value of k the less will be the volume dilatation for a given pressure. A plot of $\Delta V/V/P/E$ against k showed that a value of $k = 3$ was sufficiently large to minimize volume dilatation and a value of $k = 2$ was as small as one should go. To minimize the mass of the cells and thus achieve better temperature response the design value $k = 2$ was chosen. The length of the cells was dictated by the dimensions of the cryostat and by necessity of achieving uniform temperature. With the total volume determined by consideration d , the inside radius was arbitrarily set at 3/4 inches and it was found that the length was not excessive. The wall thickness of the cells was checked and found to conform with the ASA code for pressure piping. Each of the three stresses in the cylinder wall was checked and the tangential stress at a pressure of 1.5 times the working pressure of 680 atm was found to be about half the yield strength of type 347 stainless steel. Type 347 stainless was chosen for its high yield strength and because of the necessity of avoiding structural metals which become brittle at low temperatures.

b. Temperature Range of the Data.

At the outset of the research it was proposed that the system be designed to cover the temperature range from 20 to 100° K with the range from 70 to 100° K being obtained by immersing the cells in liquid nitrogen and the lower range being obtained by using an adiabatic calorimeter technique with the system immersed in liquid hydrogen. The upper range offers no problems other than the mass be kept small enough so that the system will come to temperature equilibrium with the bath in a reasonable amount of time. For the lower range it is necessary to keep the cell mass to as small a value as possible to minimize the amount of liquid hydrogen to be used and to achieve good temperature response between the heater shield and the cells. It was not possible to satisfy this consideration and at the same time satisfy considerations c and d .

c. Pressure Range of the Data.

The maximum desired pressure of 10,000 psi necessarily forces the cells to be quite bulky for a given total volume. Also a margin of safety is necessary to assure that the cells will not yield at some point and make the use of the Lamé formula invalid, or rupture creating unknown hazards because of the large quantity of liquid hydrogen surrounding the cells.

One of the serious shortcomings of the Burnett method is the spacing of the data points for a given isotherm. At high pressures the data points are far apart and at low pressures they become very dense. The larger the ratio of the total volume to the volume of the larger cell the greater the separation of the points at high pressures. On the other hand a small cell constant forces one to take a large number of data points which reduces the accuracy of the final results of the method, and lengthens the time necessary for completion of an isotherm. It was found after careful consideration that a cell constant of 1.2 would be suitable for the proposed pressure range. Even with this value it was necessary to make a short run on the high pressure end of the isotherms to fill in the gaps.

d. Desired Accuracy.

Because it was found necessary to locate the valves and the differential pressure diaphragm, which separates the test gas from the oil of the dead weight gage, outside of the cryostat it was impossible to construct a system with no dead space volume. Since the dead space volume is one of the governing errors when using the Burnett method it is essential to keep it as small as possible relative to the total volume of the system. In view of the work of previous investigators it was decided to hold the dead space volume to about 0.2% of the total volume. After careful design of the valves and selection of tubing size it was found that the dead space volume would be about 0.5 cm^3. This made the design value of the total cell volume 250 cm^3 which was arbitrarily increased to 260 cm^3 . The initial pressure measurement system which involved the use of a mercury U-tube proved to be unfeasible and had to be replaced by a differential pressure diaphragm. This increased the dead space volume to about 0.8 cm^3 which is 0.3% of the total volume.

With all of the above considerations the Burnett cells shown in Figure 9 were arrived at. Later it was decided to loosely clad the cells with 1/4 inch copper to help in the attainment of uniformity of temperature. A view of the exterior of the cells suspended in place is shown in Figure 10. The volumes of the cells after assembly and insertion of the thermocouples turned out to be

$$V_I = 211.5 \ cm^3$$

$$V_{II} = 41.1 \ cm^3$$

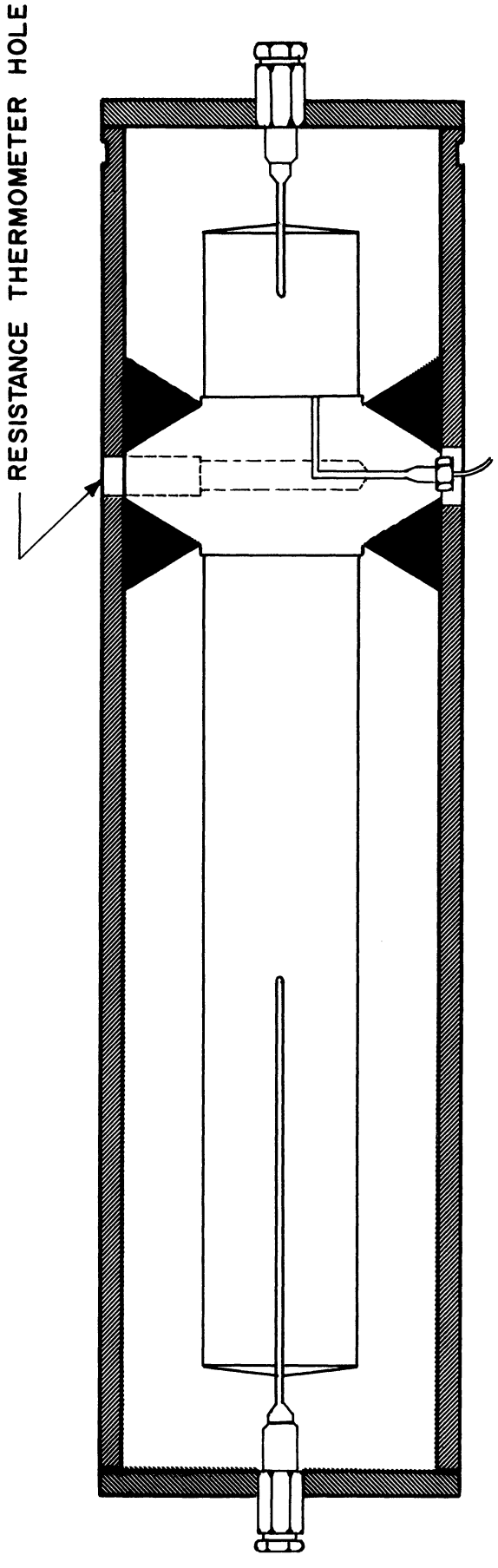

Figure 9. Cross-section Drawing of the Burnett Cells.

Figure 10. Photograph of The Burnett Cells.

Thus the total volume is 252.6 cm^3 and the cell constant is roughly 1.194 for the temperature range of thisresearch.

3. Pressure Measurement System

The pressure was measured with a type 2400.1 Ruska dead weight gage. The gage was calibrated by intercomparison with Ruska Instrument Corporation's master gage No. 7544 which in turn was calibrated by the National Bureau of Standards. The gage is equipped with two pistons, one covering the range from 30 to 12,240 psi and the other the range from 6 to 2428 psi. The high range piston was used to measure pressures from 2000 to 10,000 psi and the low range piston was used for pressures below 2000 psi. The change of pistons was made to take advantage of the higher degree of accuracy attainable using the low range piston for pressures below 2000 psi. The oil of the dead weight gage was separated from the test gas by a Ruska model 2416.1 differential pressure indicator. The location of the differential pressure indicator (DPI) resulted in an oil leg of 4.882 inches, which was determined with a K & E precision level. The gas side of the DPI was connected to the inlet valve to the large cell with 100.75 inches of .006 I. D. capillary tubing. This connection was made just below the seat so that the large cell was at all times in communication with the DPI. The pressure as determined by the mass placed on the dead weight gage and the oil leg is subject to several corrections which are discussed in Chapter V, section A. The dead weight gage is shown in Figure 11.

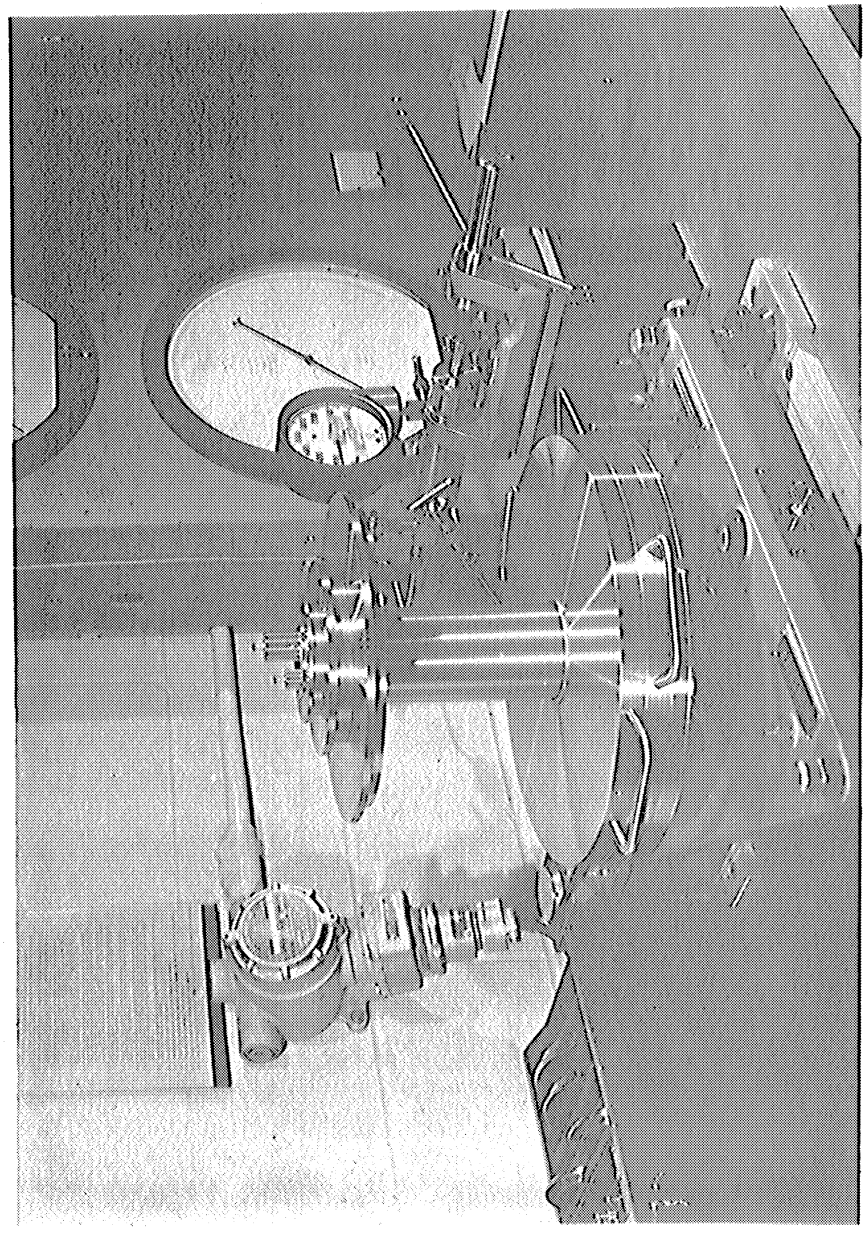

Figure 11. Photograph of The Dead Weight Gage.

4. Temperature Measurement

The temperature was measured with a Leeds & Northrup No. 8164 platinum resistance thermometer which was placed in a 7/32 diameter hole drilled in the cell material between the two chambers as indicated in Figure 9. The thermometer was placed at a depth such that only the wire leads showed outside of the cell. Number thirty copper wire was attached to the thermometer leads and wound once around the cell before being joined to No. 24 copper wire which was used as lead out wire to a terminal strip at the top of the cryostat. To connect the leads to the Leeds & Northrup type G-2 Mueller bridge, which was used to measure the resistance, about 20 feet of No. 14 copper wire was used. The thermometer was calibrated by the National Bureau of Standards to five significant figures. The Mueller bridge is capable of reading a change of 0.0001 ohms which is roughly 1/1000 of a degree Kelvin. All temperature measurements were made with the resistance within $\pm$ .0003 ohms of the value determined by the calibration for the given temperature.

Four copper-constantan difference thermocouples were used to detect temperature gradients on the cells. A difference thermocouple referenced to the location of the resistance thermometer was located in each cell and two other thermocouples were used to detect temperature differences between the top and side and the bottom and side of the cells. On the thermocouples located in the cells one wrap of the lead wires was made around the cell before they were led out through the neck tube to a Conax gland in the gland holder at the top of the cryostat. In addition

to the four difference thermocouples on the cell four additional copper-constantan thermocouples were used to measure dead space volume temperatures.

One thermocouple with its reference junction in the bath fluid was located four inches down from the gland chamber at the top of the cryostat in the tube containing all of the lead-in wires and the inlet and exhaust lines to the cells. Another thermocouple was located on the exhaust tube at the point where it left the gland holder. The remaining two were located on the valves and the DPI. Thus, on the inlet and exhaust tubes where the greatest gradient in temperature occurs, four known temperatures are available for the computation of a meaningful average tube temperature. To be able to check the liquid level in the cryostat three difference thermocouples with their reference junctions at the bottom of the lead-in tube on the cryostat were located at 3-3/4, 9-1/2 and 12 inches from the bottom of the cryostat lid. The emf output of the thermocouples was measured with a Leeds & Northrup Wenner Potentiometer. The smallest reading possible with the Wenner Potentiometer is one-tenth of a microvolt. For copper-constantan at 70° K the output of a thermocouple is about 16 microvolts per degree Kelvin. Thus it was possible to detect gradients on the cell of the order of $\pm$ 0.005° K. The difference thermocouples normally produced readings in the range from zero to $\pm$ .3 microvolts. The Mueller bridge and Wenner potentiometer in conjunction with the indicating suspension type galvanometers are shown in Figure 12.

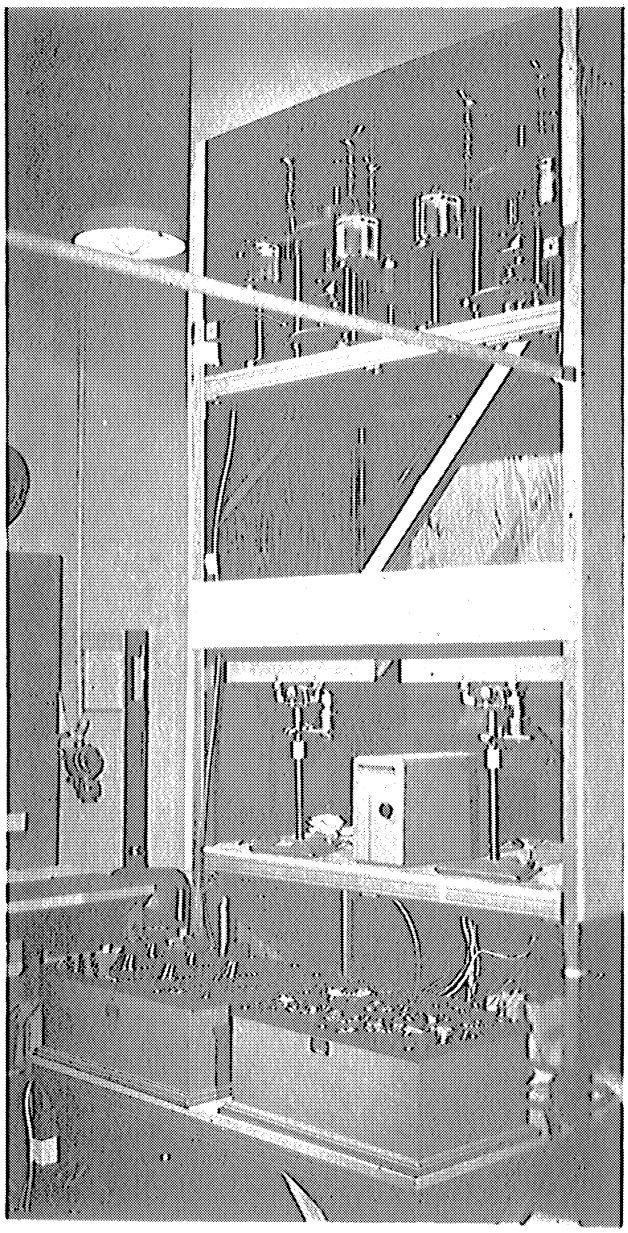

Figure 12. View of The Mueller Bridge and Wenner Potentiometer and Associated Galvanometers.

5. Test Gas System.

The test gas system is shown schematically in Figure 13.

A Ruska piston type pressure intensifier was used to attain the initial pressure of 10,000 psi used in taking the data for helium. This unit consists of a single piston having different diameter heads on each end with the space separating the two gas chambers vented to the atmosphere. The ratio of the areas of the piston heads is nine to one. This made it possible to achieve output pressures of 10,000 psi by using bottled nitrogen gas at 2200 psi as the working gas.

The test gas system is set up so that expansion of the gas from V_{II} can be directed back to the intensifier and recompressed into a storage chamber. This feature made it possible to cut the waste of valuable neon gas to a tolerable amount. It can be seen from Figure 13 that the entire test gas system except the volume in the intensifier can be evacuated. This made it relatively easy to clear the system of any foreign gases prior to filling the large Burnett chamber. All lines except the line leading from the exhaust valve on Cell II to the vacuum pump and the lines connecting the cells to the valves and the DPI were 1/8 O. D. x 0.040 I.D. stainless steel. The tubing connecting the valves and the cells was 1/16 O. D. x 0.020 I. D. stainless and the tube running to the DPI was 1/16 O. D. x 0.006 I. D. stainless. The vacuum line running from the exhaust valve was 1/4 O. D. x 1/8 I. D. for the high pressure portion and 1/4 O. D. copper line for the low pressure section.

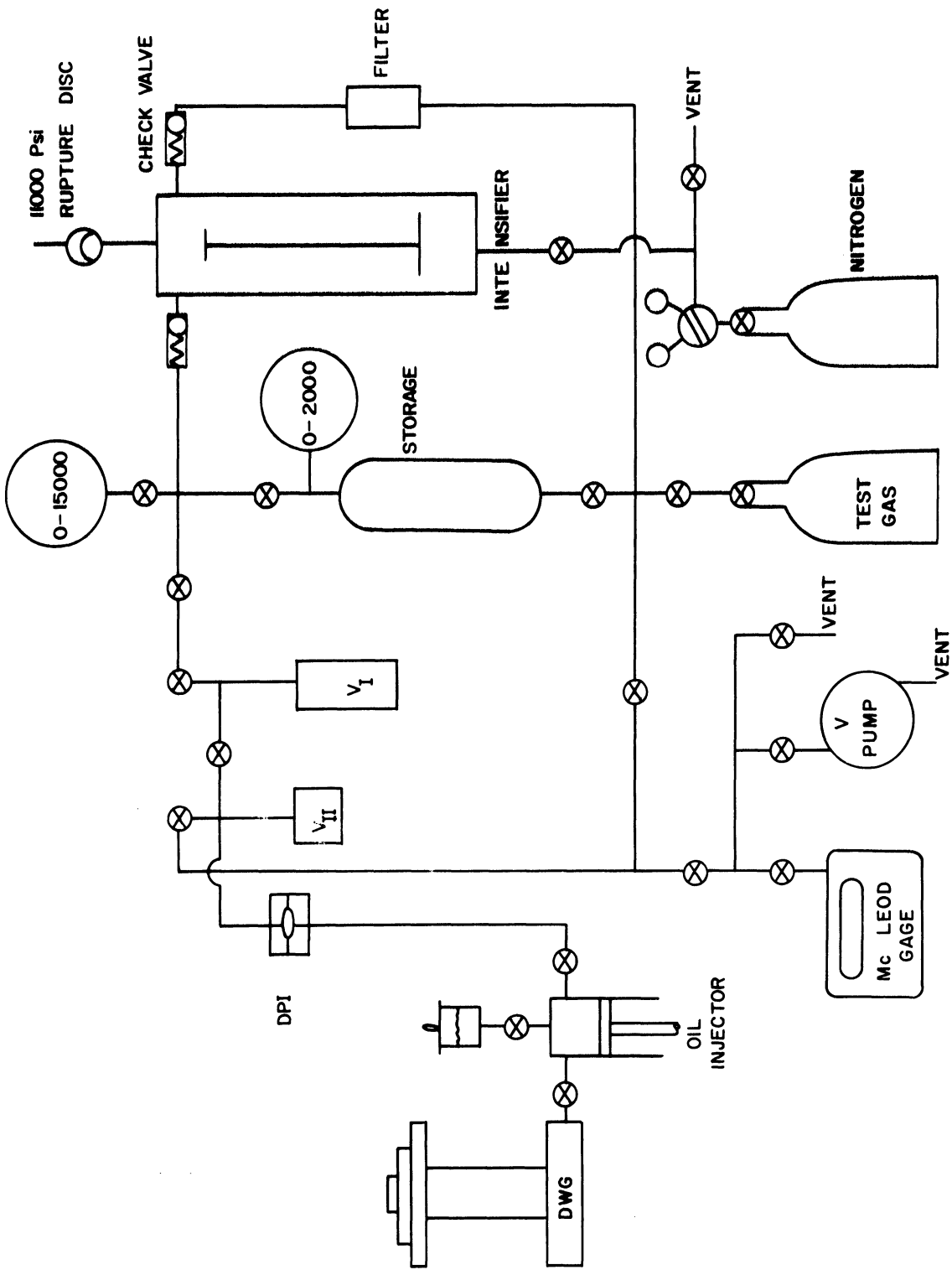

Figure 13. Schematic Diagram of the Test Gas System.

In order to hold down the dead space volume, the expansion, inlet and exhaust valves had to be specially designed. The inlet and exhaust valves utilized the bonnets from Dragon model 808 extended stem valves with the stem tip modified to a 22 degree included angle. The stem material on these valves is 17-4 PH and the bodies were made from type 316 stainless steel. The expansion valve was designed similar to High Pressure Equipment Companies midget series valves, with the stem length increased to accommodate additional packing and with the stem tip angle reduced to 22 degrees. The expansion valve was of the non-rotating stem type, whereas the inlet and exhaust valves had rotating stems. Since the valves were operated at room temperature teflon packing served quite well and no problems with leakage were encountered.

The noxious volumes introduced by the connecting lines, the DPI, and the valves were measured using the technique described by Kaminsky and Blaisdell[105] and Crain[15]. The vacuum pump used to evacuate V_{II} was a Welch Scientific Company model 1402 duo seal vacuum pump. With this unit the pressure in V_{II} could be reduced to 20 microns of mercury in 20 minutes. Vacuum readings were made with a Folsdorf type Stokes Mcleod gage.

6. Temperature Control System.

The temperature of the cells was maintained constant by setting the vapor pressure of the bath fluid such that a very slight cooling tendency prevailed and then offsetting the cooling with automatically controlled heaters. The bath was stirred constantly with a magnetic stirring arrangement.

a. Heater Design

A schematic diagram of the heater circuit is shown in Figure 14. The neck heater was made by winding bare No. 28 Chromel-A wire on a 1 inch O. D. wooden dowel. The output of this heater was from zero to a maximum of about 4 watts. The inner, middle, and outer heaters were made by winding No. 28 Chromel-A resistance wire on a cage constructed from three formica rings and six 3/8 O. D. x 13-1/2 inch long wooden dowels. The middle heater was wound around the cage with 8 turns per inch from top to bottom and the inner and outer heaters were made by passing the resistance wire from the top formica ring to the bottom ring and back in intervals of 30 degrees. The output of the middle heater ranged from zero to 20 watts depending on the control setting. The outer and inner heaters had miximum outputs of about 5 watts. By means of the controls indicated in Figure 14 the output of each heater could be controlled. The total heat input was controlled with the variac. The clearance between the heater cage and the cells was 1/2 inch.

The heater system was originally designed for control of the cell temperature under adiabatic conditions and was modified by making the heaters described above. Figure 15 shows the physical appearance of the heaters described above and also shows their location in relation to the Burnett cells.

The input to the heaters came from a Hallikainen Instrument Company Thermotrol temperature controller. The temperature controller was actuated with a wafer type resistance thermometer attached to the side

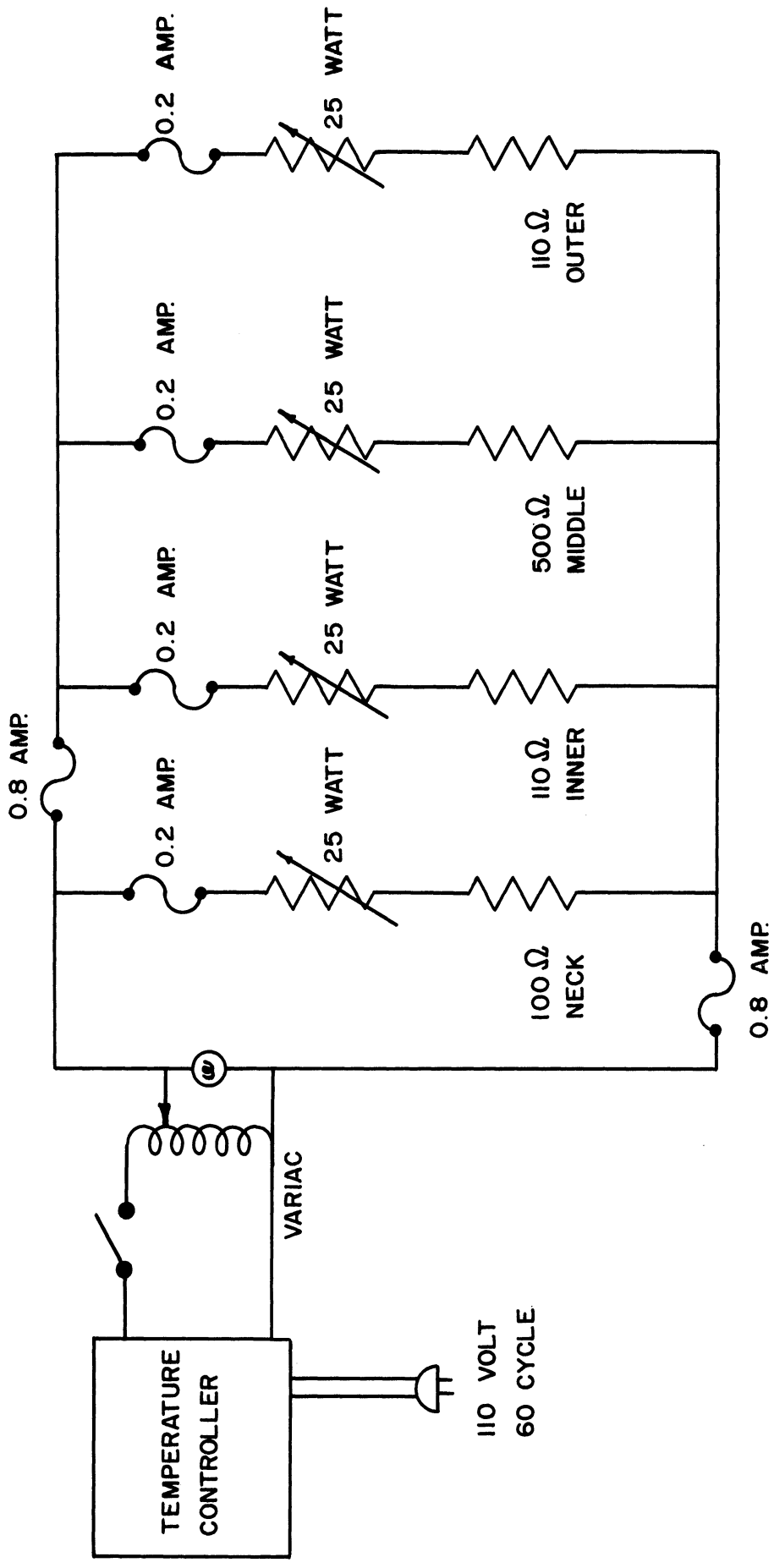

Figure 14. Circuit Diagram of the Heater System.

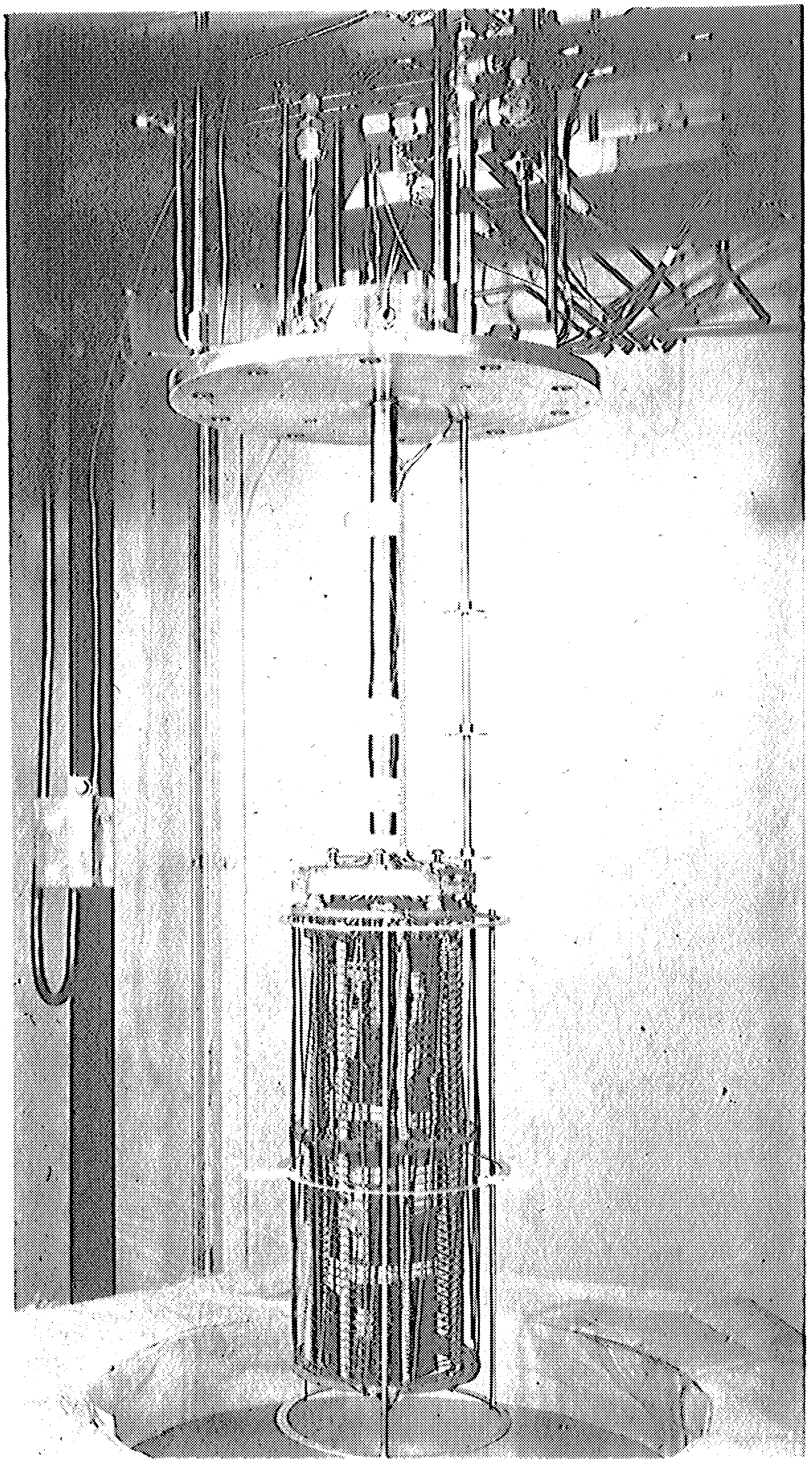

Figure 15. View of The Burnett Cells With The Heaters and Stirrer in Place.

of the Burnett cells. The width of the temperature band to which the controller would control could be varied by adjusting the gain in the instrument. For the system employed it was found that the controller operated best with the gain set at 8 and the reset dial set at 60 seconds. This setting corresponded to an on-off temperature band of about 0.005° C.

The temperature controller and heater control unit are visible in the lower center of Figure 16.

b. Vapor Pressure Control System.

The vapor pressure control system is shown schematically in Figure 17.

In operation the gas from the cryostat was throttled by means of the metering valve and bypass valve until the desired operating pressure was reached. The valve across the small mercury U-tube was then closed causing the cryostat pressure to communicate with the pressure in the insulated volume by means of the small U-tube. The U-tube is equipped with mercury contacts and serves as a switch to operate the solenoid valve on the panel which is normally closed. Gas was either introduced into or taken out of the control volume in small slugs until the desired operating temperature was reached. In operation the controls were set so that the mercury rose very slowly in the left leg of the U-tube switch. When the mercury reached the upper contact the solenoid opened and allowed a small slug of gas to escape, thus dropping the pressure slightly and causing the switch to break contact. The circuit diagram for control of the solenoid is shown in Figure 18.

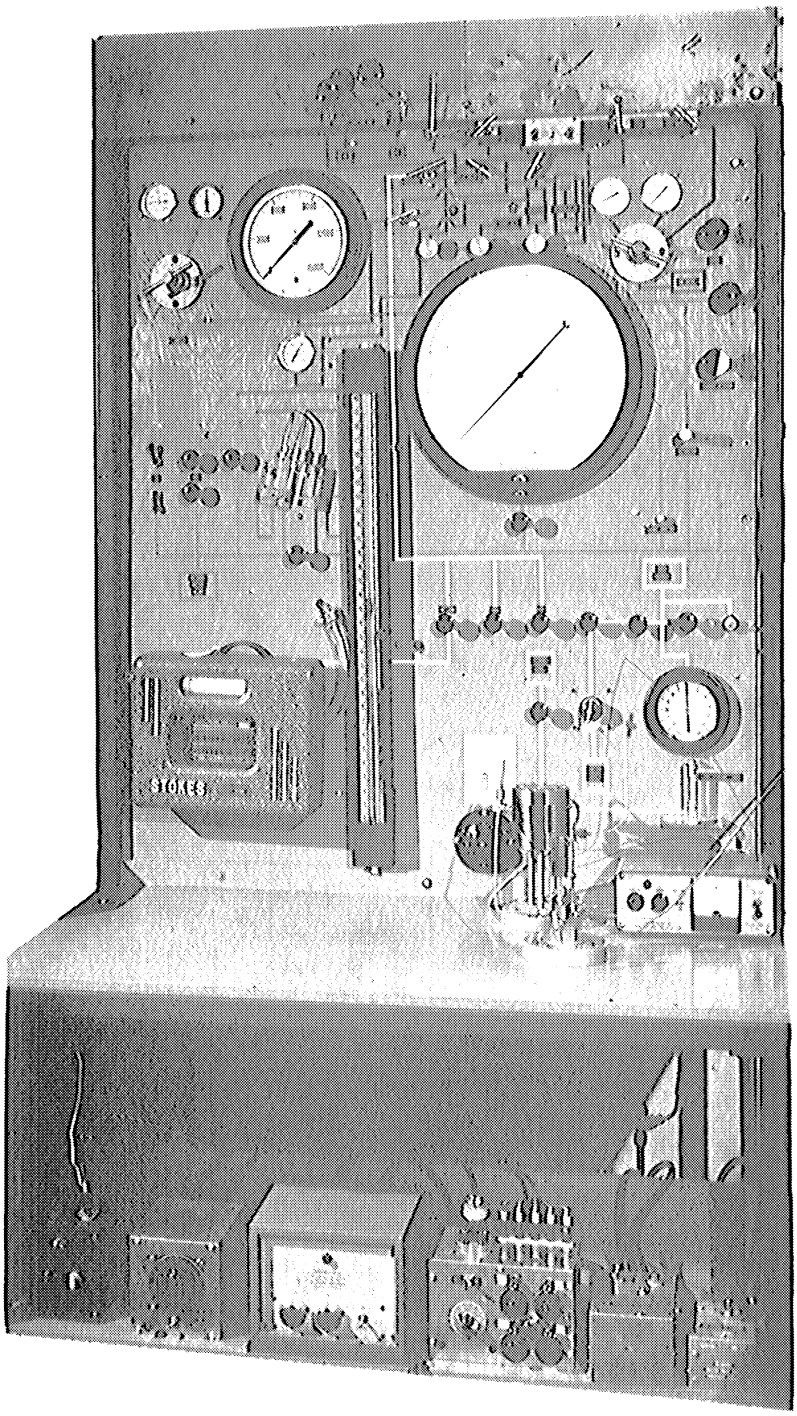

Figure 16. View of The Control Panel.

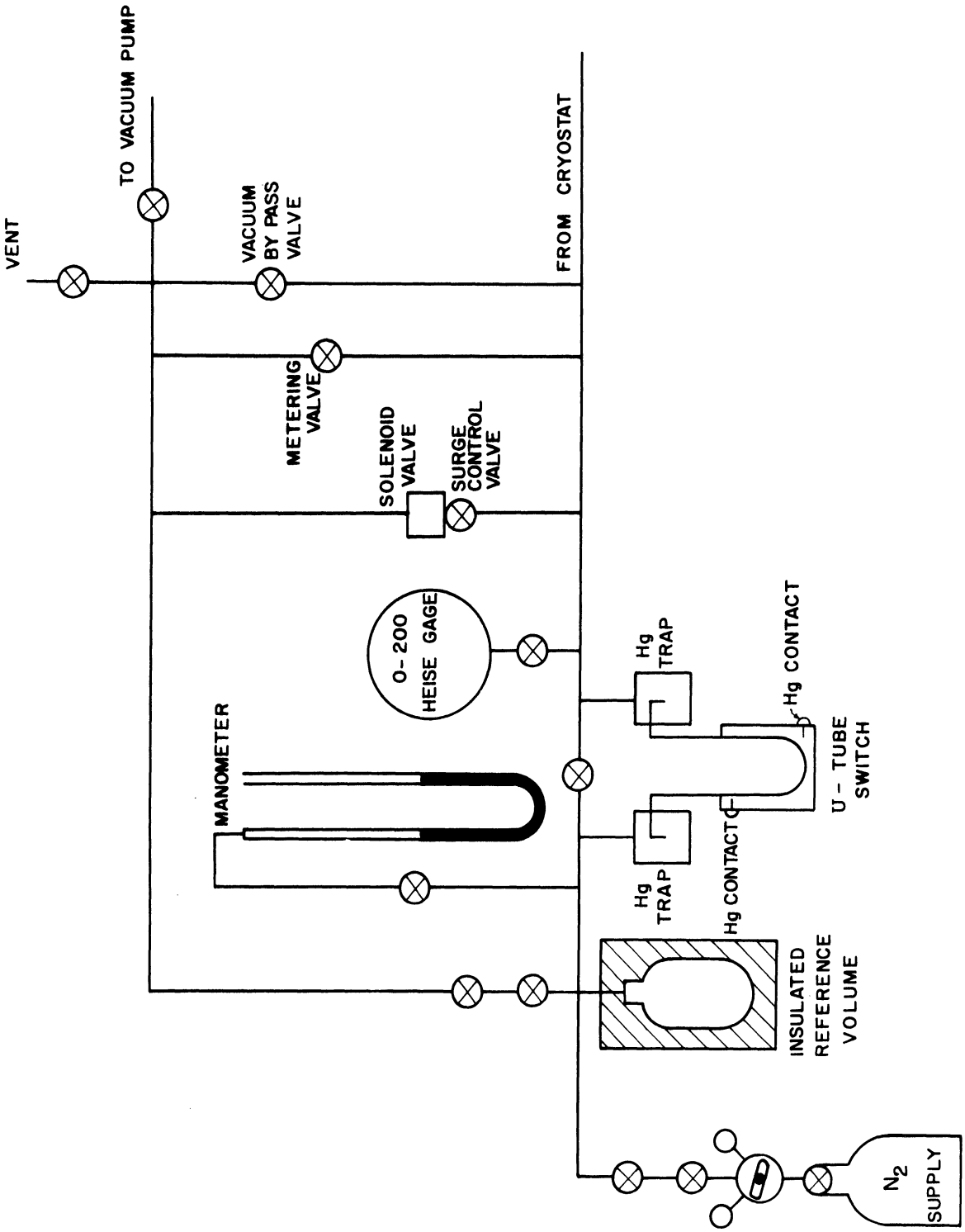

Figure 17. Schematic Diagram of the Vapor Pressure Control System.

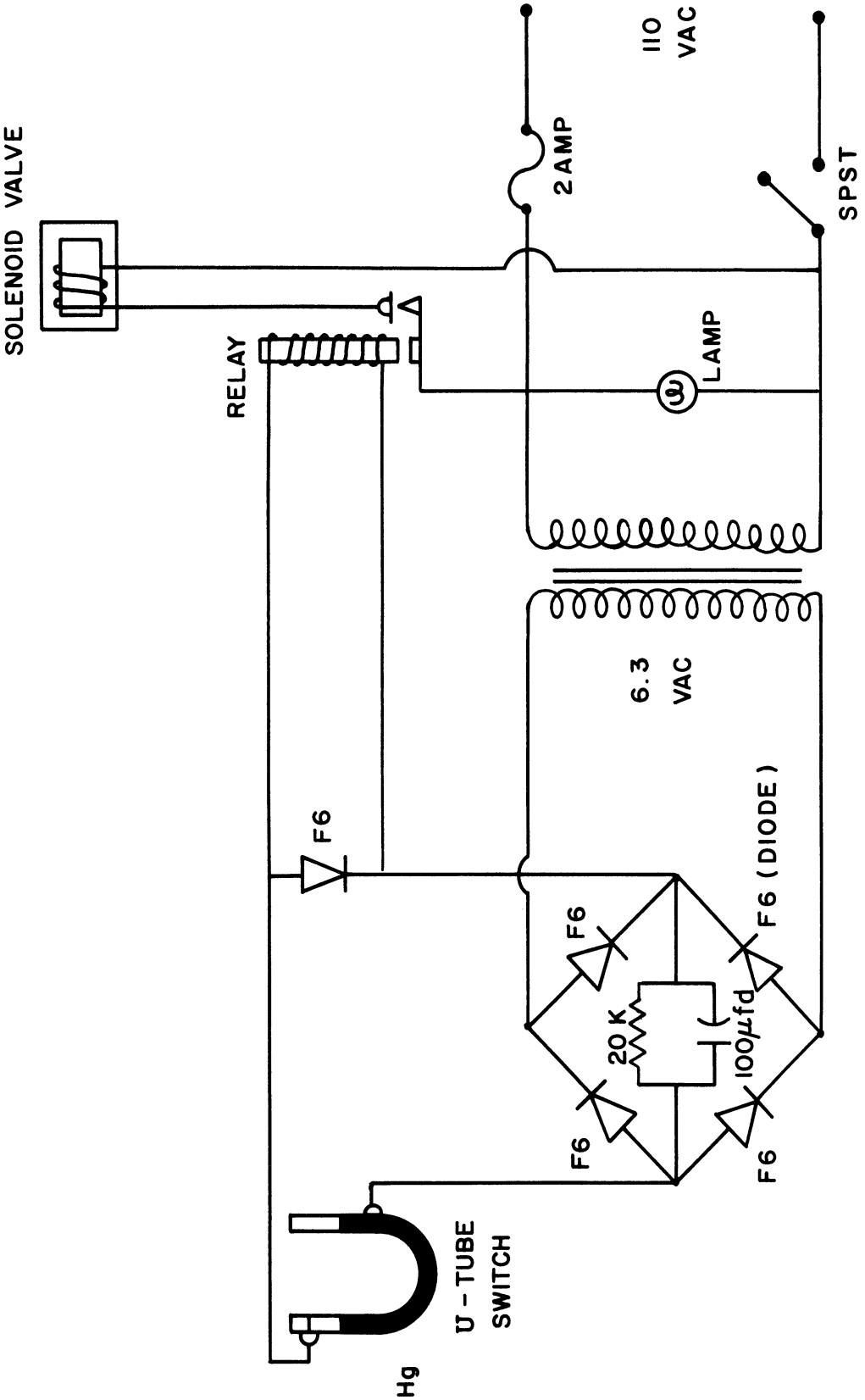

Figure 18. Circuit Diagram For The Solenoid Control System.

The mercury switch operates with a d. c. voltage of from 4 to 6 volts. The system was designed to give a minimum spark in the U-tube switch since it was originally intended to operate the system with hydrogen as the bath fluid. In the actual taking of the data it was found that the heating effect upon expansion was severe enough to cause the mercury to be blown from the U-tube switch and the system could not be operated as described above under such unsteady state conditions. However, by carefully manipulating the metering valve very satisfactory vapor pressure control could be attained and the cell temperature could be maintained within 0.005° K of the desired value for extended periods of time without using the U-tube switch and solenoid.

c. Stirring Mechanism

The bath stirrer consisted of three aluminum rings, 7-1/2 inch outside diameter 5/16 inch wide, connected together with 3/16 O. D. aluminum tubing and was located outside of the heater assembly in the lower portion of the cryostat. A 1/4 O. D. thin walled stainless steel tube was attached to the top ring and passed up through the cryostat lid through the outlet pipe. The upper end of the stirrer rod was silver soldered to a soft iron core 5/8 O. D. x 2 inches long. The core was housed in a 3/4 O. D. stainless steel tube which was counterbored to produce a seat for the core. A 115 volt 60 cycle coil was mounted on the outside of the stainless steel core housing in such a position as to cause the core to rise about 1 inch when the coil was actuated. The coil was housed in a copper cylinder wound with 1/4 inch copper tubing. Water was continuously

circulated around the coil to keep it cool during operation. The lower portion of the stirrer is visible in Figure15. A timer motor and micro switch actuated the coil approximately once every second causing the stirrer to pass through the bath twice per second. In addition to the three large rings on the lower section of the stirrer three 1-1/2 inch diameter aluminum discs were placed on the stirrer rod in the upper chamber of the cryostat and three teflon guides were mounted on the center ring of the lower section. The magnetic stirring arrangement was chosen to eliminate the necessity of sealing a rotating shaft in the cryostat lid and for its simplicity in design, construction, and maintainance. With the stirring arrangement described no gradients in the bath could be detected except near the top of the liquid where the vapor, which is at a much higher temperature than the liquid, causes heating of the liquid. The stirrer controls are visible in Figure 16.

7. Cryostat

The cryostat was designed by the author and contracted for construction to the Linde Company. A simple schematic outline of the cryostat appears in Figure 19. The unit is capable of holding about 50 liters of bath fluid with about 15 liters in the lower chamber when the cells are in place. The inner shell is made from 3/16 inch thick 304 stainless and the outer shell is made from 1/8 inch 304 stainless. The space separating the two shells was filled with Linde super-insulation. The cryostat was designed with the small diameter at the bottom to keep from wasting expensive cryogenic fluids since the fluid in the bottom section

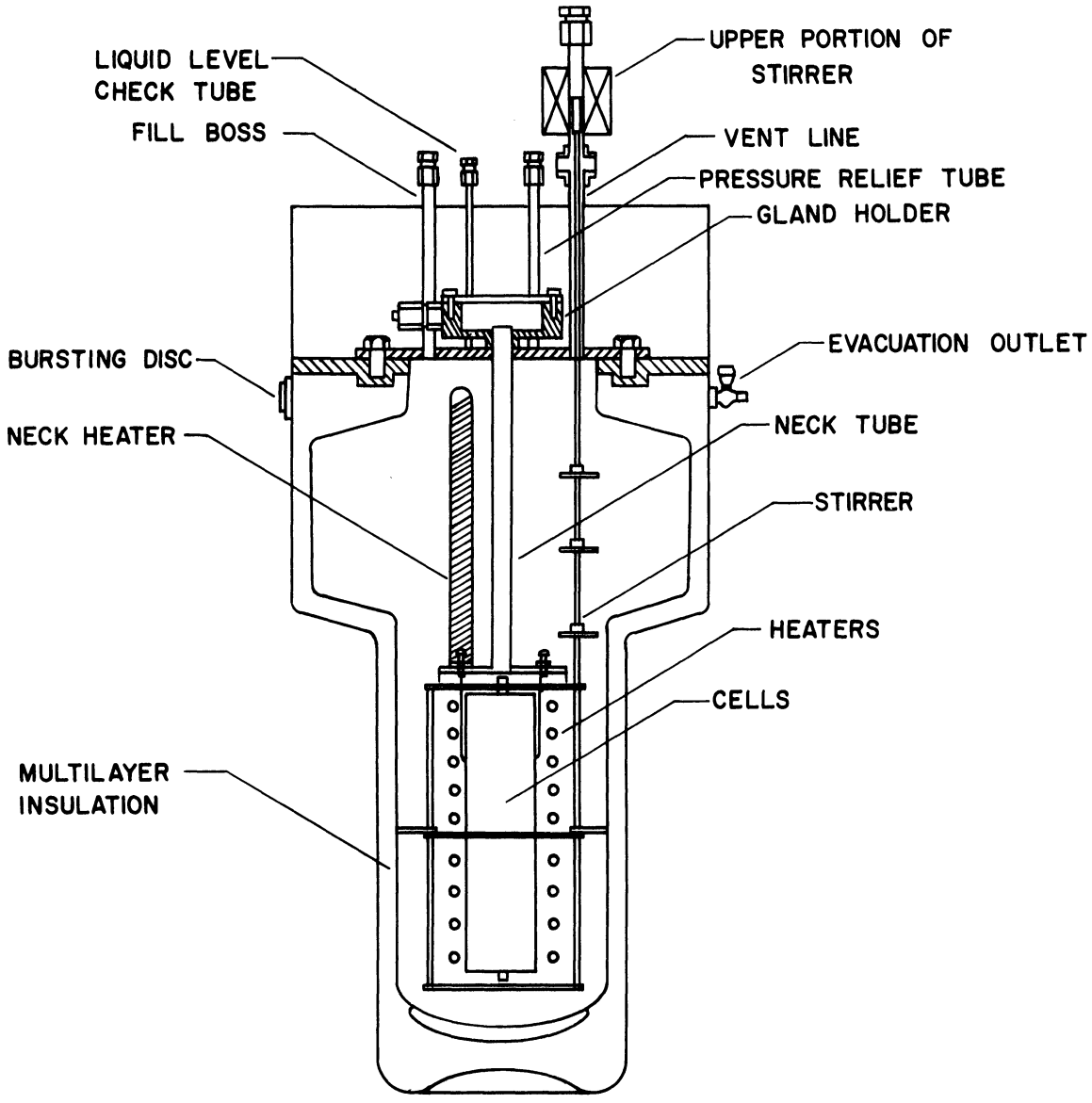

Figure 19. Schematic Drawing of the Cryostat.

is unused when the unit is shut down. A cylindrical 6 inch O. D. x 1-5/8 inch deep can mounted on a 1 inch O. D. tube which extends through the lid serves as a gland holder. All tubes and lead out wires are brought up through the neck tube and passed through conax glands to the outside. The cover plate is a 1/2 inch thick 14 inch O. D. stainless plate secured in place by ten 3/4 O. D. bolts. The unit is sealed with a United Aircraft Products teflon coated self energized O-ring. The cover on the gland holder is a 6 inch O. D. 5/16 inch thick stainless plate secured by eight 3/8 inch bolts and sealed with a United Aircraft O-ring. The outer shell of the cryostat extends about 7 inches above the cryostat top forming a large reservoir which can be filled with insulation or with liquid nitrogen if hydrogen is placed in the cryostat. In the temperature range from 70 to 120° K the top reservoir was filled with a vermiculite insulation. A plywood housing was constructed around the cryostat. The space between the plywood and the outer shell was insulated with styrofoam to a depth of 10 inches from the top. Below that foam glass insulation was used down to the small diameter of the cyrostat. The space surrounding the lower portion of the cryostat was filled with Zonolite insulation. The plywood housing was screwed to two 2 by 8 by 22 inch planks which were in turn bolted to a Unistrut framework. The cryostat lid with all the connecting lines and the cells mounted in place was suspended from a unistrut framework with the lid about 6 ft. from the floor. A system of pulleys and a small wench were attached to the framework and four nylon ropes were tied to the framework around the cryostat. With this lifting

arrangement the cryostat could be raised up to the cover plate and bolted in place. The above arrangement made it possible to make repairs on the experimental package without having to disconnect the wires and lines attached to the test cells and cryostat lid. The cryostat and lifting arrangement are visible in Figure 20.

Four stainless steel tubes were arc-welded to the cryostat lid. These consisted of a 1/2 inch O. D. fill tube, a 1/4 O. D. tube available for insertion of a liquid level probe, a 1 inch O. D. tube for exhaust, and a 1/2 inch O. D. tube connected to a 200 psi rupture disc. The 1 inch O. D. tube was equipped with a cross with the stirrer mounted on the upper port, a Conax gland containing the lead out wires from the liquid level thermocouples mounted in one side port, and the 3/4 O. D. copper vent line connected to the other side port. The cryostat was designed for a maximum operating pressure of 200 psi and tested to 300 psi by Linde Company.

B. Experimental Procedures

1. Cleaning the Cells

Before putting the cells into use they were cleaned by flushing them repeatedly with trichloroethylene, benzene, and acetone. The cells were first flushed with trichloroethylene until no discoloration of the solvent was apparent. Then the same flushing procefure was carried out using benzene. Finally the cells were flushed repeatedly with acetone. Care was taken when connecting the lines to the cells and inserting the thermocouples to assure that no foreign matter entered the cells.

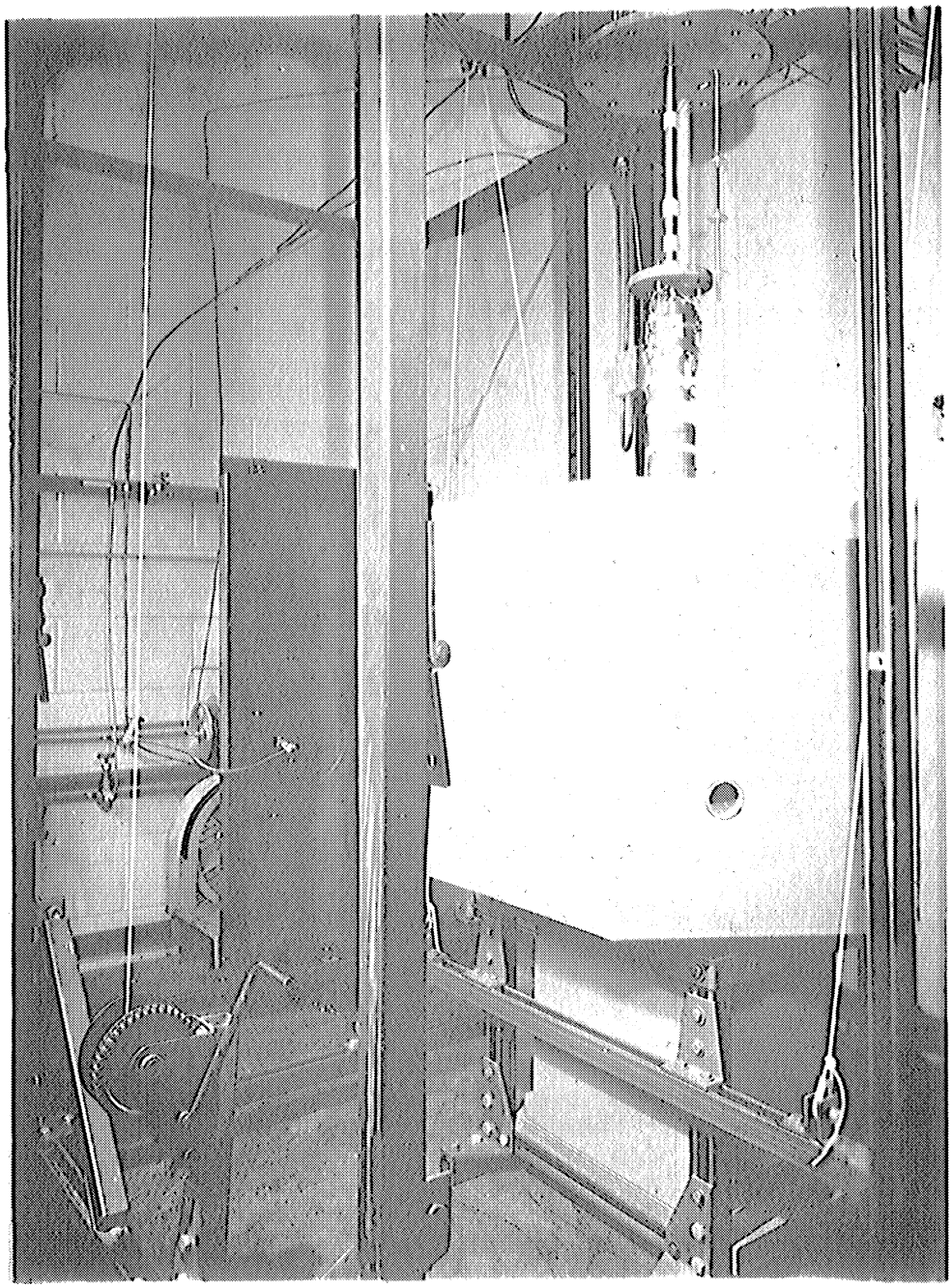

Figure 20. View of The Cryostat Showing The Lifting Mechanism.

2. Charging the Burnett Cell.

Prior to making the initial run the electronic null detector on the DPI was zeroed by opening both sides of the diaphragm to the atmosphere. The test gas system was then evacuated to 10 microns of mercury or less and purged with the test gas. This procedure was repeated again and then the cells were re-evacuated and pressurized to 200 to 300 psig. After attaining the proper temperature the large cell was then charged to the desired initial pressure with the pressure intensifier. On subsequent runs the electronic null detector was normally rezeroed prior to initiating the run. However, it was found from experience that the null position on the indicator changed only slightly over long periods of time and on runs which were made close together the rezeroing procedure was not deemed necessary.

3. Pressure Measurement.

A typical pressure measurement was made by first obtaining a close guess of the pressure to be measured and then placing enough mass on the dead weight gage to create a pressure slightly above this. This was done to assure that the DPI was always overpressurized from the same side. The manufacturer recommended this in view of the possibility of causing the null point of the DPI to shift under frequent changes of direction of overpressure. After placing enough mass on the gage to create a pressure exceeding the pressure to be measured the valve isolating the weight table was opened and weights were removed until the null detector indicated too little mass. Then small weights were added and removed as required until a rough balance was attained. The rough balance was maintained until

the cells had been at the proper temperature for 10 to 15 minutes. After this waiting period the pressure was balanced and the expansion valve was closed. After closing the expansion valve the pressure was re-balanced within the limits of the accuracy of the gage.

4. A Typical Data Point

The temperature of the cells was frequently checked and the controls were manipulated so as to force the cells to remain at the desired temperature during the time required to take a point (roughly 20 to 30 minutes after expansion). The difference thermocouples were also monitored and when it was decided that equilibrium had been achieved the expansion valve was closed and the final null of the dead weight gage was carried out. Then the valve isolating the weight table and oil injector from the DPI was closed and the pressure on the weight table was reduced to zero. Immediately following this the exact temperature reading was taken, the difference thermocouples on the cells were read and then the thermocouples on the noxious volumes were read. Following this the barometer reading was recorded and the gas was expanded from V_{II} and evacuation initiated. The room temperature and the temperature of the oil in the piston housing on the dead weight gage were then recorded. Finally to complete the data necessary for a single point the weights used on the dead weight gage were recorded. The average total time for one data point was about 1 hour and 10 minutes.

C. Difficulties Encountered.

1. Design of the Cells.

The problems encountered in designing the cells were previously pointed out. Several unforseen problems arose due to the geometry of the cells. First it was difficult to tighten the fittings connecting the inlet and outlet lines to the cell and a special wrench had to be made for that purpose. The cells were heavy and difficult to put in place due to the necessity of threading the inlet and exhaust lines up through the neck tube before the cells could be raised to their mounting position. The cells were also difficult to clean since no large openings were provided.

2. Valves.

Initially the valves were tested in liquid nitrogen and after breaking one specially designed stem in the expansion valve and noting that the freeze-up problem was very severe in the inlet and exhaust valves it was decided to discard the idea of placing the valves in a liquid nitrogen bath.

Since the valves could not be placed in the bath the dead space volume they introduced had to be kept small. No commerical valves which had small enough dead space volumes were available, so the valve bodies were specially designed. Some difficulty in machining the valves was encountered because of the small holes and close tolerences. The seats on the valves were made with a 22° cone which was coated with lapping compound and repeatedly forced against the seat. The stem points were

polished to a mirror finish before installing them in the valves.

3. Initial Pressure Measurement System.

Initially it was intended that a mercury U-tube would be used to separate the test gas from the oil of the dead weight gage. This unit was constructed of 1/4 O. D. high pressure stainless steel tubing and fitted with mercury contacts at the upper end of each leg and in the center of one leg. It was possible by closing a valve at the bottom of the leg on the gas side to isolate the oil side from the gas side. The gas side leg was in continuous communication through a Ruska gage separator with a 15,000 psi Heise gage filled with oil. The intended method of taking a pressure reading was to note the pressure on the gas side with the above mentioned gage and then impose a pressure slightly smaller on the oil side by means of the oil injector on the dead weight gage. Then the valve on the gas side leg was opened and the pressure was balanced with a differential pressure diaphragm located between the U-tube and the dead weight gage. Weights were then placed on the dead weight gage that would correspond to a pressure equal to that indicated by the gages.

The valve isolating the weight table was then opened and weights were added or subtracted until the differential pressure diaphragm again indicated null. Finally a bypass valve around the DPI was opened and the level of the mercury in the U-tube was adjusted until the level reached one of the upper contacts. Weights were to be placed on or taken off of the weight table and the mercury injector manipulated until a balance was reached. Balance was to be determined by the smallest weight that would cause one contact to make when placed on the weight table and the other to make when taken off.

While the system described above offered the advantage of very small dead space volume it was very cumbersome and hard to operate. Also it was found that upon evacuation of the cells mercury was drawn up through the capillary line leading to the cells and the entire assembly had to be disassembled and cleaned.

This system was discarded in favor of the more simple and direct method of using a single DPI with an electronic null indicator even though this caused a doubling of the dead space volume.

4. Stirring Mechanism.

The original stirrer coil was an 850 ohm d. c. coil powered by a 150 volt d. c. power supply. The coil was taken from a magnetic radio speaker. The unit functioned satisfactorily during the taking of data for two isotherms. Then when the system was tested with hydrogen enough moisture collected in the coil housing to short the unit out and a replacement coil could not be readily located. The coil was replaced with a 115 volt 60 cycle a. c. coil. This second coil overheated excessively and water cooling was necessary for continuous operation. Also the a. c. coil interfered with the temperature controller and had to be shielded. The capacity of the stirrer was increased at every opportunity, first by increasing the passes per second through the bath and the length of the stroke. In addition the three aluminum discs on the stirrer rod were added. In the final configuration used the stirring was adequate and no gradients could be detected in the lower chamber of the cryostat and only slight gradients were present in the upper chamber near the surface of the bath.

5. Temperature Control.

A problem that was encountered in the temperature control was the difficulty of finding a suitable setting for the gain and reset dials on the temperature controller. The unit would not always turn on the heaters at the same temperature and a small overshoot or undershoot sometimes occurred.

It was found that the vapor pressure could be controlled very nicely without using the elaborate automatic system that was built for that purpose. In fact, manual control was desirable in view of the upset in vapor pressure that occurred when an expansion was made.

6. Thermocouples.

The main difficulty encountered with thermocouples was the grounding out of the lead wires and the commercial Conax thermocouples used in the cells. The lead wires were No. 24 teflon coated copper wire. With the system at room temperature the thermocouple circuits could be checked and found to be ungrounded. A similar check with the cryostat full, however, showed the thermocouples to be grounded. It was found that this was due to moisture collecting on the wires at points where the insulation was damaged slightly when the wires were threaded through the porcelain guides on the Conax glands. It was finally necessary to reinsulate all of the thermocouple wires to eliminate the problem. The Conax thermocouples originally placed in the cells proved to be very unreliable and were finally replaced with units made by the author.

A Leeds & Northrup thermocouple selector switch was initially used to switch from one thermocouple to another. It was found that the switch produced a signal large enough to make very small readings (0.2 to 0.3 microvolts) meaningless. The switch was replaced with DPDT copper knife switches which eliminated the problem. Shielded leadwire was used to connect the knife switches to a terminal board on the back of the instrument panel, since this section of leadwire had to pass near the a. c. control units for the stirrer and heaters. It was also necessary to use shielded wire to connect the potentiometer and the galvanometer in order to eliminate a slight zero shift of the galvanometer.

7. Thermometer Leads.

The experience of Crain[15] with the resistance thermometer leads indicated that some way of avoiding breakage of the platinum leads on the thermometer was to be desired. Accordingly, short pieces of teflon tubing were slipped over the leads and bound together with thread. A 90 degree bend was made in the leads about 1/4 inch from the butt of the thermometer and the thread winding was continued just beyond the bend. Finally the thread wound portion which extended from the bend up over the glass nipple to a point just behind where the leads enter the glass was coated with epoxy. This made a very sound unit which could be easily handled without fear of lead breakage and never offered any problems.

V. DATA REDUCTION AND EXPERIMENTAL RESULTS

A. Data Reduction.

1. Pressure Calculation.

Because of the nature of the dead weight gage the calculation of the numerical value of a measured pressure was quite involved. For accurate pressure determination an accurate value of the local gravitational acceleration is required. The value used was calculated using a formula taken from reference 106 since no actual measurement at the location of the laboratory was available. The formula was checked by comparing it to the value of local gravity published in reference 107 for Selfridge Air Force which is 66miles N.E. of Ann Arbor, at Mt. Clemens, Michigan, and found to agree within 0.006 cm/sec^2.

For a free floating piston the pressure exerted by a given mass is

$$P_m = \frac{W}{A_e} = \frac{m}{A_e} \frac{g}{g_c} \tag{68}$$

where m is the mass of the weights and A_e is the effective area of the piston.

Since the mass of the stainless steel weights was determined by comparing them with brass standards, a correction for the difference between the air buoyancy force for brass and stainless steel must be introduced. The actual mass is given by

$$m = m_a \left(1 - \frac{\rho_a}{\rho_b} \right) \tag{69}$$

where m_a is the apparent mass obtained from the comparison with the brass standards, ρ_a is the air density of that location, and ρ_b is the density of brass.

The effective area varies with pressure due to elastic distortion of the housing and piston and also varies with temperature. The correction for variation of the effective area with pressure and temperature results in the equation

$$A_e = A_o(1 + bP)(1 + C\Delta T) \tag{70}$$

where b and C are functions of the materials used in the construction of the gage and A_o is the area of the piston at zero pressure and a temperature of 25° C. Substituting (69) and (70) into (68) gives

$$P_m = \frac{m_a\, g \left(1 - \frac{\rho_a}{\rho_b} \right)}{A_o\, g_c\, (1+bP)(1+C\Delta T)} \tag{71}$$

For the apparatus used in this investigation the DPI was lower than the reference mark on the dead weight gage and a small positive pressure on the test gas due to the oil leg was always present. In addition, the final balance of the gage involves the use of small weights that are calibrated by the manufacturer to indicate pressure directly. The pressure indicated by a given mass on the gage is thus given by

$$P = P_m + P_{oil} + P_{wt} + P_{bar} + P_{dpi} \tag{72}$$

where P_{oil} is the pressure due to the oil leg, P_{wt} is the pressure determined by the small weights used, P_{bar} is the barometric pressure and P_{dpi} is a small correction for the difference in pressure between the two chambers of the DPI.

For calculation of the pressure due to the oil leg the density of the oil was assumed constant and the following formula was used.

$$P_{oil} = \rho_{oil} \frac{g}{g_c} h_{oil} \tag{73}$$

The barometric pressure was determined from the equation

$$P_{bar} = \rho_{hg} \frac{g}{g_c} h \tag{74}$$

where ρ_{hg} is the density of mercury at 0° C and h is corrected for temperatures other than 0° C by means of a chart supplied by the manufacturer.

At null of the DPI the pressure in the lower chamber (gas side) is greater than the pressure in the upper chamber by the amount

$$P_{dpi} = 3.56 \times 10^{-6} P \tag{75}$$

where P is in lbf/in^2.

The values used in the above formulas were

$g = 32.1618$ ft/sec^2

$g_c = 32.1740$ lbm-ft/lbf-sec^2

$\rho_a = 0.0012$ gm/cm^3

$\rho_b = 8.4$ gm/cm^3

$A_o = 0.0260417 \text{ in}^2$
$b = -3.6 \times 10^{-8} \text{ /psi}$
$C = 1.6 \times 10^{-5} \text{ / }^{\circ}\text{C}$
} High range piston

$A_o = 0.130220 \text{ in}^2$
$b = -5.4 \times 10^{-8} \text{ /psi}$
$C = 1.6 \times 10^{-5} \text{ / }^{\circ}\text{C}$
} Low range piston

$\rho_{oil} = 0.85 \text{ gm/cm}^3$

$\rho_{hg} = 13.5951 \text{ gm/cm}^3$

When the above values are substituted into (71), (73) and (74) the following equations are obtained.

$$P_m = 0.999479 \frac{m_a}{A_e} \tag{76}$$

$$A_{eH} = 0.0260417(1-3.6\times10^{-8}P)(1+1.6\times10^{-5}\Delta T) \tag{77}$$

$$A_{eL} = 0.130220(1-5.4\times10^{-8}P)(1+1.6\times10^{-5}\Delta T) \tag{78}$$

$$P_{oil} = 0.030696 \ h_{oil} \tag{79}$$

$$P_{bar} = 0.0193295 \ h \tag{80}$$

where h_{oil} is in inches and h is in mm of mercury. The area A_{eH} is the effective area for the high range piston and A_{eL} is the effective area for the low range piston. The oil head is 0.04 inches greater for the high range piston due to a slight shift in the balance reference for the gage. The measured value of the oil leg was 4.882 inches.

Using the above formulas a computer program was written to carry out the necessary computations. The value of pressure required in (77) and (78) was obtained from

$$P = P_m + P_{wt} + P_{bar}$$

where P_m was computed without correcting the effective area for pressure and temperature variation. With the aid of the computer program the pressure for seventeen data points could be computed in about one second. The orders of magnitude of the terms in (5) are

P_m = 6 psi to 10,000 psi

P_{oil} = 0.15 psi

P_{wt} = 0.002 psi to 0.595 psi

P_{bar} = 14.3 psi

P_{dpi} = 0.0005 psi to 0.036 psi

An error analysis which discusses the magnitude of error in pressure measurement is presented in section C of this chapter.

2. Determination of Dead Space Temperatures

The total dead space volume was broken into two parts. The valves and DPI and the connecting line between them were all at room temperature and constituted one dead space volume. The lines running from the valves to the cells constituted the second dead space volume. These volumes are slightly different prior to an expansion than they are after an expansion. In this respect there are four separate dead space volumes to be considered; two prior to an expansion and two after expansion. The temperature of the

DPI and the valves was measured for each point on an isotherm. The microvolt readings of these temperatures was averaged for the entire run and the average temperatures of the units was determined from this. These average temperatures were normally within 0.5° K of each other. The temperature of the dead space volume in the valves and DPI and the line joining them was obtained by averaging the average temperature of the valves and of the DPI. This temperature was used for all points of the run. Four known temperatures were available for computing the average temperature of the volume in the lines connecting the valves and the cells. The microvolt readings of the thermocouples on the lines were first averaged for the entire run and the average temperatures computed from these. Each line was divided into four sections of different length. The first section which ran from the cells to the lowest liquid level thermocouple was assumed to be at the test temperature and its volume was thus added to the total volume of the cells and not treated as a dead space volume. The uppermost ten inches of each line was at room temperature and was added into the dead space volume of the valves and DPI. A weighted average temperature was computed for each of the two remaining sections by averaging the temperatures at the ends of the section and multiplying the result by the length of the section divided by the total length of line from the lowest liquid level thermocouple to a point 10 inches from the valves. These weighted average temperatures were then added to obtain the average line temperature for a run.

3. Dead Space Corrections.

To carry out the correction for dead space volumes outlined in Chapter III, section A, it is necessary to know the compressibility factor for each measured pressure. To obtain these compressibilities for helium the data tables published by D. B. Mann[49] were used. A linear least squares fit of the data to an equation of the form

$$Z = C_1 + C_2 P \tag{81}$$

was made for each different average dead space temperature. These equations were then used to calculate compressibilities at the experimental pressures. Since the Tables mentioned only extend to 100 atm this involves linearly extrapolating to obtain compressibilities at the higher pressures. For helium at the temperatures of the dead space volumes (about 200° K and 300° K) the isotherms are so close to being linear that Equation (81) gives a very good value for Z even at the highest pressures measured. In fact, even for a linear fit of the data of this research which extends to 690 atm and is at much lower temperatures the standard deviation in Z was only 0.5×10^{-2} .

For neon the dead space compressibilities were obtained by fitting the data of McCarty, Stewart and Timmerhaus[59] to an equation of the form

$$Z = C_1 + C_2 P + C_3 P^2 + C_4 P^3 + C_5 P^4 \tag{82}$$

The data in (59) extends to 200 atm and since the pressure range of this research extends to 300 atm for neon the compressibilities of the highest pressures were obtained by extrapolating Equation (82). The average standard deviation in Z using (82) was 0.2×10^{-4} for all dead space temperatures. The initial guess of the experimental compressibilities required to start the calculations was obtained by fitting existing data (19) and (59) to (81) and (82) for the test temperatures.

4. Correction for Volume Dilatation.

The properties of 347 stainless steel required in the Lamé formula were obtained through correspondence with F. Garfalo of U.S. Steel. Since this data was at room temperature and above it had to be linearly extrapolated to the temperatures covered in this research. This extrapolation yielded the following result

$$L = \frac{1}{E}\left[2\left(\frac{k^2+1}{k^2-1}+\mu\right) + \frac{1-2\mu}{k^2-1}\right] = \left[1.818 + \frac{0.767T}{1000}\right]\times 10^{-6} \quad (83)$$

where T is in °K and L is in atm^{-1}. The values of L for each isotherm were obtained from (83).

5. Calculation of Compressibilities.

A computer program based on the equations presented in Chapter III, section A, and on the information in section E was written to handle the calculation of the compressibility factors. The computer program was set up to obtain an initial value of N_o and P_o/Z_o by proceeding exactly as outlined in Chapter III, section A. Starting with these initial values

P_o/Z_o was held fixed and N_o was varied until a minimum deviation from linearity was obtained for points below a predetermined density on a virial plot. For helium points below half the critical density were used and for neon points below four-tenths of the critical density were used for the minimization. For each small change of N_o the calculation of the compressibilities was repeated three times using the results of the previous computation each time. This was done to iterate out the error in the dead space corrections that would arise if the values of Z for the initial N_o were used.

This procedure of finding an N_o which gives a minimum deviation from linearity on a virial plot for points below four tenths of the critical density was repeated for two values of P_o/Z_o below the initial value and two values of P_o/Z_o above the initial value. The above procedure produces five sets of N_o and P_o/Z_o . The deviation from linearity for these sets of N_o and P_o/Z_o was compared and the pair with the smallest deviation was taken as the initial values to be used for a repetition of the above procedure. If the value of P_o/Z_o for this new pair fell inside the extreme of P_o/Z_o the step intervals of P_o/Z_o and of N_o were halved. If the value of P_o/Z_o for the new pair was at one of the extremes the step intervals were left unchanged. In either event the above method of varying P_o/Z_o and N_o was continued until the step size in P_o/Z_o reached 0.003 atm.

The initial step sizes in P_o/Z_o and N_o were chosen such that the step size in N_o was nearly zero when the step size in P_o/Z_o reached

0.003 atm. The values of P_o/Z_o and N_o obtained from the above minimization procedure were taken as the final answers and used to calculate the compressibilities. The maximum total variation in N_o using this method was 0.06% of the initial value.

B. Error Analysis

1. Temperature

The prime error in temperature measurement is the uncertainty in the uniformity of temperature of the cells.

The Leeds & Northrup Mueller bridge used to determine the resistance reading of the resistance thermometer is capable of indicating changes as small as $\pm$ 0.0001 ohms which corresponds to temperature changes of $\pm$ 0.001° K. All experimental points were taken with the resistance reading within $\pm$ 0.0003 ohms of the calibrated value for a given temperature. Thus the temperature readings are within $\pm$ 0.003° K of the calibrated values.

Nonuniformity of temperature of the cells was indicated by the difference thermocouples located on them. The output of the difference thermocouples was read with a Leeds & Northrup Wenner potentiometer which is capable of detecting emf's as small as $\pm$ 0.1 microvolts. All experimental points were taken with difference thermocouples 1 and 2 which are located in the cells and referenced to the resistance thermometer showing values of 0.25 microvolts or less. In most cases the readings were 0.2 microvolts or less. The output of a copper-constantan thermocouple at the lowest measured temperature (70° K) is about 16 microvolts per degree Kelvin. Thus the maximum temperature gradient which could have existed

for a point is $\pm$ 0.015 ° K. In view of the above considerations it is felt that the temperature measurement is good to better than $\pm$ 0.015° K. The international temperature scale is known to the nearest $\pm$ 0.01° K so the above maximum possible temperature error is quite satisfactory.

2. Pressure

Of the various factors that affects the accuracy of the pressure measurement, the most critical is the accuracy to which the area of the dead weight gage piston can be determined. This will become apparent in the following discussion.

a. Gage Resolution.

The resolution of the dead weight gage, which is the smallest change in mass on the weight table that will produce a measurable change in the condition of equilibrium is quoted by the manufacturer as being less than 5 ppm for both the high and low range pistons for all calibrating test points. Through experience with the gage it was found that a more meaningful resolution would be 10 ppm. The numerical value of the resolution is expressed as the ratio of the change in mass to the total mass

$$R = \frac{\Delta m}{m} = \pm 10^{-5} \tag{84}$$

Expressing (84) in terms of pressure yields

$$R = \frac{\Delta P}{P} = \pm 10^{-5} \tag{85}$$

Equation (85) represents the resolution of the gage for both pistons for the range 6 to 12,000 psi.

b. Oil Leg.

Due to the location of the DPI relative to the dead weight gage a small oil leg was present in the system. Errors in the correction applied for the oil leg arise from inaccuracy of determination of the oil leg and from fluctuations in the room temperature. The height of the oil leg was measured to $\pm$ 0.015 inches, making the uncertainty in the correction $\pm$ 0.0005 psi. For maximum room temperature fluctuations of 3° C the error in the oil leg correction is $\pm$ 0.0009 psi. The total error due to error in oil leg correction is then about $\pm$ 0.0014 psi.

c. Error in Reading the Gage.

The point at which the line on the weight table and the reference line on the gage exactly line up is determined by eye and could be in error by as much as $\pm$ 0.015 inches. This introduces an error of $\pm$ .0015 psi into the pressure measurement.

d. Gas Leg.

Due to the physical arrangement of the DPI relative to the cells, the line connecting the two has a considerable temperature gradient imposed upon it, with the result that the actual pressure in the cells is slightly higher than the pressure in the DPI. From calculations made on the gas leg, which was not corrected for, the error introduced was found to be

$$\frac{\Delta P}{P} \simeq 2 \times 10^{-6} \qquad (86)$$

e. Error in Correction for DPI Pressure Differential.

Since an estimated value of the pressure was used to determine the correction for pressure difference between the two chambers of the DPI, a slight error was introduced. The estimated pressure was found by calculating, the pressure without correcting the piston area for temperature and pressure and adding the barometric pressure and the pressure due to the small weights. The maximum possible error in the estimated pressure is

$$\frac{\Delta P_e}{P} = 4 \times 10^{-4} \tag{87}$$

The error in the correction for difference in pressure in the DPI is then

$$\frac{\Delta P_{dpi}}{P} = 3.56 \times 10^{-6} \frac{\Delta P_e}{P} = 1.5 \times 10^{-9} \tag{88}$$

f. Error in Local Gravity.

The effect of error in local gravity on the pressure can be estimated by estimating the maximum error in the weight of the mass on the weight pan of the gage. The equation relating mass and weight is

$$W = \frac{mg}{g_c} \tag{89}$$

The error in W due to an error in g is given by

$$\frac{\Delta W}{W} = \frac{\Delta g}{g} \tag{90}$$

and the resulting error in the gage pressure is

$$\frac{\Delta P_m}{P} = \frac{\Delta g}{g} \tag{91}$$

The estimated accuracy in g is $\pm$ 0.006 cm/sec^2 so that the resulting error in P_m is

$$\frac{\Delta P_m}{P} = 6 \times 10^{-6} \tag{92}$$

g. Error in Barometric Pressure.

The barometric pressure was read to the nearest 0.1 mm of mercury. The total error in the barometric pressure due to reading error and to error in local gravity is given by

$$\Delta P_{atm} = \left(\frac{\Delta g}{g} + \frac{\Delta h}{h} \right) P_{atm} \tilde{=} \pm 0.002 \text{ psi} \tag{93}$$

h. Error in Effective Piston Area.

The uncertainty in the area of the pistons for the dead weight gage is reported as 10^{-4} in.^{2} In addition to this constant uncertainty, errors in the gage temperature and errors in the estimated pressure used to calculate the final pressure affect the precise determination of the effective area. The effective area of the piston can be very closely approximated by the equation

$$A_e = A_o (1 + bP_e + C\Delta T) \tag{94}$$

where b and C are constants for the gage, A_o is the piston area at zero pressure and 25° C and ΔT is the gage temperature minus 25° C. The total error in the effective area due to errors in estimated pressure, temperature, and measured piston area is

$$\Delta A_e = A_e \frac{\Delta A_o}{A_o} + A_o b P_e \frac{\Delta P_e}{P_e} + A_o C \, \Delta(\Delta T) \tag{95}$$

Assuming $A_e \tilde{=} A_o$ and $P_e \tilde{=} P$ Equation (95) becomes

$$\frac{\Delta A_e}{A_e} = \frac{\Delta A_o}{A_o} + b \, P \, \frac{\Delta P_e}{P} + C \, \Delta(\Delta T) \tag{96}$$

The error in pressure due to error in A_e can be estimated from the equation

$$P_m = \frac{W}{A_e} \tag{97}$$

From (97) the error in P_m due to an error in A_e is given by

$$\frac{\Delta P_m}{P_m} = - \frac{\Delta A_e}{A_e} \tag{98}$$

Using $\Delta A_o / A_o = \pm 10^{-4}$ and Equation (87) for $\Delta P_e / P$ the error in P_m becomes

$$\frac{\Delta P_m}{P_m} = 1.08 \times 10^{-4} + 1.44 \times 10^{-11} \, P \tag{99}$$

Since the second term in this equation is negligible

$$\frac{\Delta P_m}{P_m} \simeq \frac{\Delta P_m}{P} = 1.08 \times 10^{-4} \qquad (100)$$

i. Total Error in Measured Pressure.

The total error in the pressure which is computed from the equation

$$P = P_m + P_{atm} + P_{oil} + P_{dpi} + P_{wt} + (\text{others})$$

is given by

$$\Delta P = \Delta P_m + \Delta P_{atm} + \Delta P_{oil} + \Delta P_{dpi} + (\text{others}) \qquad (101)$$

Using the values obtained in the previous discussion in Equation (101) gives

$$\Delta P = 1.26 \times 10^{-4} \; P + 0.004 \; \text{psi} \qquad (102)$$

From the previous discussion it is seen that the maximum uncertainty in the pressure results from the uncertainty in the piston area. It should also be noted that Equation (102) does not represent the limits of repeatability of the pressure measurement, but the degree to which the measured pressure might deviate from the exact pressure if it could be measured. The repeatability of the pressure measurements can be computed from the above analysis by neglecting the uncertainty in the piston area.

3. Error in Total Volume and Dead Space Volumes.

The maximum possible error in the total volume is estimated to be no greater than 6 cm^3. The volume was experimentally measured at 80° K.

The volume measurement was repeatable to $\pm$ 2 cm^3. This makes

$$\frac{\Delta V_T}{V_T} = \frac{6}{252.6} = 0.024 \tag{103}$$

The dead space volumes were measured to within 0.002 cm^3.

4. Error in N_j .

The value of N_j is influenced by the value of N_o , the dead space volume correction and the correction for volume dilatation due to pressurization. The equation for N_j is

$$N_j = N_o \left(\frac{1 + \frac{\Delta V_{Ij}}{V_I} + \frac{V_{cj}}{V_T}}{1 + \frac{\Delta V_{I(j-1)}}{V_I} + N_o \frac{V_{c(j-1)}}{V_T}} \right) = \frac{N_o G_j}{G_{j-1}} \tag{104}$$

From (104) the total error in N_j can be shown to be

$$\frac{\Delta N_j}{N_j} = \left(1 - \frac{N_o V_{c(j-1)}}{V_T G_{j-1}} \right) \frac{\Delta N_o}{N_o} + \frac{\left(\frac{\Delta V_{Ij}}{V_I} \right)_j}{G_j} - \Delta \left(\frac{\frac{\Delta V_{I(j-1)}}{V_I}}{G_{j-1}} \right)_{j-1}$$

$$+ \frac{\Delta V_{cj}}{G_j V_T} + N_o \frac{\Delta V_{c(j-1)}}{G_{j-1} V_T}$$

$$+ N_j \left(\frac{V_{c(j-1)} - V_{cj}}{V_T} \right) \frac{\Delta V_T}{G_j V_T} \tag{105}$$

a. Error in Volume Dilatation Correction.

Writing the Lame formula as

$$\frac{\Delta V_{Ij}}{V_I} = L\, P_j \tag{106}$$

where L is given by (83). The error in the correction is given by

$$\Delta\left(\frac{\Delta V_{Ij}}{V_I}\right)_j = L\,\Delta P_j + P_j \Delta L + E_j \tag{107}$$

In Equation (107) E_j is the error introduced due to neglecting end effects and is estimated to be about 1% of the total volume change. The value of L is believed to be good to better than 5%. Using $L = 1.879 \times 10^{-6}$ /atm and Equation (102) for ΔP_j, Equation (107) becomes

$$\Delta\left(\frac{\Delta V_{Ij}}{V_I}\right)_j = 7.68 \times 10^{-9}\, P_j \tag{108}$$

where P_j is in lbf/in^2.

Similarly

$$\Delta\left(\frac{\Delta V_{I(j-1)}}{V_I}\right)_{j-1} \cong 7.68 \times 10^{-9}\, P_{j-1} \tag{109}$$

In taking the difference in the errors for volume dilatation in Equation (105) the error in pressure due to area in piston area and the error in L and E cancel out leaving

$$\Delta\left(\frac{\Delta V_{Ij}}{V_I}\right)_j - \Delta\left(\frac{\Delta V_{I(j-1)}}{V_I}\right)_{j-1} \cong L\,(P_{j-1} - P_j) \times 10^{-5} \cong 0 \qquad (110)$$

b. Error in Dead Space Volume Correction.

The dead space volume correction is determined from

$$V_{cj} = Z_j T \sum_{i=1}^{m} \frac{V_{ci}}{Z_{ji}\, T_i} \qquad (111)$$

Assuming no error in Z_j and T the error in the corrected dead space volume is given by

$$\frac{\Delta V_{cj}}{V_{cj}} = Z_j T\left(\sum_{i=1}^{m} \frac{1}{Z_{ji}\, T_i}\right) \frac{\Delta V_c}{V_{cj}} + \frac{\Delta Z_{ji}}{Z_{ji}} +$$

$$Z_j T \sum_{i=1}^{m} \left(\frac{V_{ci}\ \Delta T_i}{Z_{ji}\ T_i^2}\right) \qquad (112)$$

The maximum error in Z_{ji} is 1% and the maximum error in the dead space temperature for the dead space volume outside of the cryostat is $\pm$ 1° C. The uncertainty in the temperature of the tubes leading from the valves to the cells is probably no worse than $\pm$ 20° C.

Substituting actual values into (112) and assuming $Z_j \approx Z_{ji}$ gives

$$\frac{\Delta V_{cj}}{V_{cj}} \cong 0.03 \qquad (113)$$

and

$$\frac{\Delta V_{c(j-1)}}{V_{c(j-1)}} \simeq 0.021 \qquad (114)$$

By taking

$$V_{cj} = 0.321$$

$$V_{c(j-1)} = 0.423$$

$$\frac{\Delta V_{Ij}}{V_I} = 0.000253$$

$$\frac{\Delta V_{I(j-1)}}{V_I} = 0.000332$$

and $N_o = 1.194875$, which are average values for the 80° K isotherm of helium, the following values of G_j , G_{j-1} and N_j are obtained

$$G_j = 1.00153$$

$$G_{j-1} = 1.00234$$

$$N_j = 1.193908$$

Estimating the maximum error in N_o to be 5×10^{-5} and using the approximate values given above in addition to Equations (103), (113), and (114) in Equation (105) gives the result

$$\frac{\Delta N_j}{N_j} = (5 + 3.61 + 4.25 + 1.73) \times 10^{-5} \qquad (115)$$

The order of the appearance of the terms in (115) is the same as in (105) with the volume dilatation terms deleted due to (110). Equation (115) shows that the errors are all of the same order of magnitude. This result also shows that the accuracy of the Burnett method is highly dependent upon the accuracy to which N_o can be determined and to a large extent upon the accuracy of the determination of dead space corrections. For the case where N_o can be accurately determined the dead space corrections dominate as shown by (115). The error in N_o due to error in total volume is about one- half of the combined errors due to dead space correction errors. When all of the terms in Equation (115) are added the final result is

$$\frac{\Delta N_j}{N_j} = 1.5 \times 10^{-4} \tag{116}$$

5. Total Error in Compressibility.

The error in the compressibility factors will be determined from

$$Z_j = \frac{P_j \prod_{i=1}^{m} N_i}{P_o/Z_o} \tag{117}$$

From Equation (117) the error in Z_o is given by

$$\frac{\Delta Z_j}{Z_j} = \frac{\Delta P_j}{P_j} + j\frac{\Delta N_j}{N_j} + \frac{\Delta(P_o/Z_o)}{P_o/Z_o} + \left(\frac{\partial Z}{\partial T}\right)_P \Delta T + E_v \tag{118}$$

where it has been assumed that $\frac{\Delta N_1}{N_1} = \frac{\Delta N_2}{N_2} = \ldots = \frac{\Delta N_j}{N_j}$. The term E_v

has been added to account for incomplete evacuation of V_{II} and is given by

$$E_V = P_r \frac{Z_o}{P_o} \left(\prod_{i=1}^{j} (N_i) - 1 \right) \qquad (119)$$

Normally V_{II} was evacuated to pressures less than 30 microns of mercury so that Equation (119) gives

$$E_V \cong 0.4 \times 10^{-5} \qquad (120)$$

for twenty successive expansions.

For helium the rate of change of Z with temperature at constant pressure is approximated as

$$\left(\frac{\partial Z}{\partial T} \right)_P \cong - 0.00174/^oK \qquad (121)$$

The error in P_o/Z_o is not in excess of $\pm$ 0.02 atm and the uncertainty in N_o is estimated to be $\pm 5 \times 10^{-5}$. Using these estimates and Equations (102), (116), and (121) in (118) gives

$$\frac{\Delta Z_j}{Z_j} = (1.26 + 1.5\ j + 0.6 + 0.26 + 0.04) \times 10^{-4} \qquad (122)$$

or

$$\frac{\Delta Z_j}{Z_j} = (2.16 + 1.5\ j) \times 10^{-4} \qquad (123)$$

Equation (123) shows that for the first expansion of a run the error in Z is 3.66×10^{-4} or about 0.04% and for twenty expansions

the error is about 3.2×10^{-3} or 0.32%. These error estimates are based on the 80° K isotherm for helium.

It should be noted Equation (123) represents an estimate of the maximum error in the compressibilities.

The actual errors in compressibilities are expected to be less than indicated by Equation (123).

VI. EXPERIMENTAL RESULTS

A. Experimental Results for Helium

1. Compressibilities

The isotherms for helium were investigated using high purity helium supplied by the Bureau of Mines helium plant at Amarillo, Texas. The purity of the helium conformed to the specifications listed in Table 1.

TABLE 1

HELIUM PURITY

Contaminant	Amount (ppm)
H_2	< 0.4
CH_4	0.0
H_2O	< 0.5
Ne	< 14.0
N_2	< 4.0
O_2	< 0.8
Ar	Trace
CO_2	< 0.1

Table 1 shows that the maximum amount of impurities in the helium did not exceed 20 ppm.

The experimentally determined values of the compressibilities for helium are listed in Table 2 along with the computed values of the specific volumes. The number of experimental points for each isotherm is composed

of the points from a complete run from 680 atm down to about 17 atm and the points for a partial run (6 or 8 points) at high pressures. The compressibilities for the data points of a partial run were obtained by fitting the reduced data for the full run to a fifth or sixth order polynomial in pressure and computing the compressibility factor for the last measured pressure of the partial run and proceeding as outlined in Chapter III, section B. The consistency of the helium data is demonstrated by the compressibility diagrams presented as Figures 21 and 22.

Table 3 is a comparison of the experimental compressibilities for helium with published values for selected values of pressure. The values of compressibility listed from the work of Holborn and Otto were obtained by linearly interpolating between the isotherms studied by them. The values published by Mann[49] were arrived at by fitting the Strobridge equation to existing data in the temperature range from 3 °K to 300 °K. The values of compressibility listed from this work were obtained by fitting each isotherm to a fifth or sixth degree polynomial in pressure and computing the compressibilities for the even values of pressure listed in Table 3. Table 3 shows that in the range from 0 to 100 atm the compressibilities from this work agree with the results of Holborn and Otto to within 0.3%. The agreement with the calculated results of Mann is somewhat better than 0.15%.

TABLE 2

EXPERIMENTAL RESULTS FOR HELIUM

T = 70° K			T = 80° K		
P(atm)	Z = Pv/RT	v(cc/gm)	P(atm)	Z = Pv/RT	v(cc/gm)
684.8179	2.38703	5.00180	693.3695	2.21331	5.23494
575.2362	2.17780	5.43269	601.2871	2.05939	5.61682
477.0025	1.98494	5.97132	492.1884	1.87656	6.25266
408.8116	1.84789	6.48630	433.8434	1.77490	6.70927
346.0660	1.71950	7.12996	362.1074	1.64925	7.46938
301.4177	1.62691	7.74528	323.3245	1.58022	8.01520
259.2827	1.53844	8.51432	274.2133	1.49211	8.92375
228.6351	1.47372	9.24944	247.1254	1.44302	9.57613
199.1316	1.41104	10.1682	212.1853	1.37949	10.6620
177.2556	1.36451	11.0463	192.5948	1.34369	11.4417
155.8527	1.31895	12.1438	166.9379	1.29679	12.7394
139.7372	1.28472	13.1928	152.3615	1.27013	13.6712
123.7492	1.25079	14.5038	133.0322	1.23480	15.2221
111.5619	1.22502	15.7569	121.9451	1.21469	16.3356
99.3449	1.19934	17.3229	107.0731	1.18756	18.1890
89.9440	1.17961	18.8196	86.8495	1.15102	21.7345
80.4433	1.15988	20.6902	70.8718	1.12237	25.9715
65.5593	1.12903	24.7123	58.1139	1.09975	31.0348
53.7108	1.10481	29.5167	47.8305	1.08162	37.0854
44.1820	1.08549	35.2552	39.4923	1.06718	44.3159
36.4628	1.07001	42.1097	32.6789	1.05524	52.9565
30.1718	1.05755	50.2972	27.0986	1.04566	63.2819
25.0185	1.04743	60.0767	22.5058	1.03777	75.6209
20.7789	1.03908	71.7578	18.7183	1.03142	90.3659
17.2845	1.03240	85.7105			

TABLE 2 (CONT'D)

EXPERIMENTAL RESULTS FOR HELIUM

T = 100° K			T = 120° K		
P(atm)	Z = Pv/RT	v(cm^3/gm)	P(atm)	Z = Pv/RT	v(cc/gm)
685.9706	1.96335	5.86729	692.8584	1.81597	6.44750
596.0191	1.84474	6.34483	518.3546	1.62214	7.69817
503.0904	1.71951	7.00653	396.7062	1.48243	9.19245
442.7845	1.63667	7.57728	309.0784	1.37927	10.9776
379.2859	1.54826	8.36801	244.2293	1.30160	13.1101
337.2588	1.48891	9.05005	195.1435	1.24208	15.6575
292.2335	1.42483	9.99488	157.3013	1.19579	18.7003
261.9459	1.38129	10.8098	127.6941	1.15939	22.3350
228.9879	1.33360	11.9387	104.2411	1.13043	26.67652
206.5452	1.30100	12.9125	99.1653	1.12411	27.8852
181.8324	1.26498	14.2612	85.4788	1.10716	31.8624
164.8037	1.24004	15.4246	81.3971	1.10206	33.3059
145.8905	1.21241	17.0360	70.3492	1.08834	38.0568
132.7315	1.19305	18.4259	67.0455	1.08422	39.7808
118.0002	1.17145	20.3510	58.0692	1.07302	45.4557
107.6887	1.15632	22.0117	55.3808	1.06970	47.5147
96.0702	1.13935	24.3116	45.8487	1.05776	56.7526
78.6122	1.11376	29.0434	38.0308	1.04798	67.7868
64.5923	1.09325	34.6964	31.5946	1.03990	80.9666
53.2492	1.07670	41.4500	26.2807	1.03319	96.7094
44.0156	1.06324	49.5186	21.8844	1.02764	115.513
36.4623	1.05223	59.1580	18.2393	1.02301	137.974
30.2599	1.04324	70.6741	15.2130	1.01918	164.802
25.1502	1.03587	84.4323	12.6974	1.01605	196.847
20.9281	1.02978	100.869			
17.4326	1.02477	120.506			

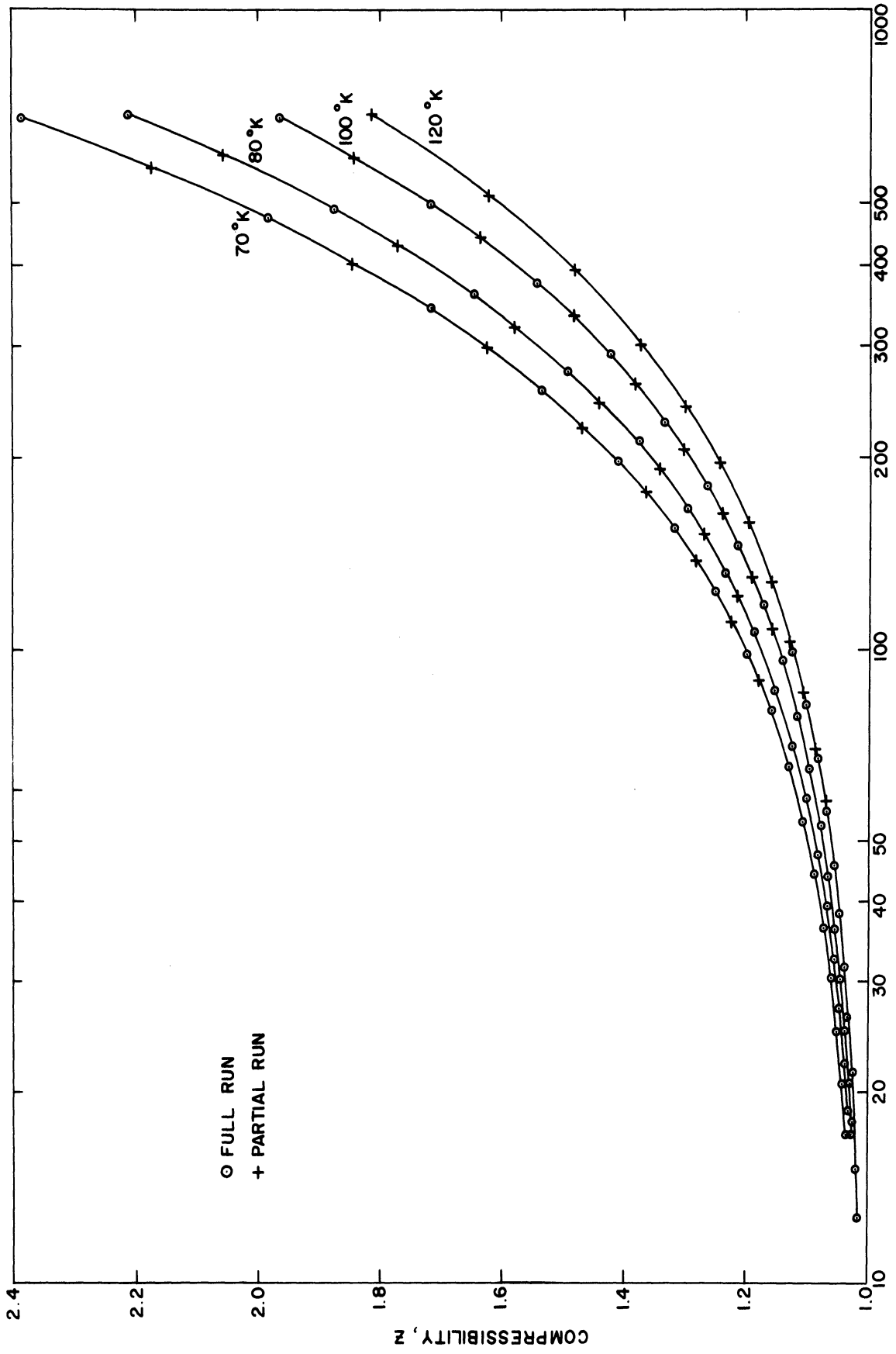

Figure 21. Compressibility Diagram For Helium Showing The Experimental Points.

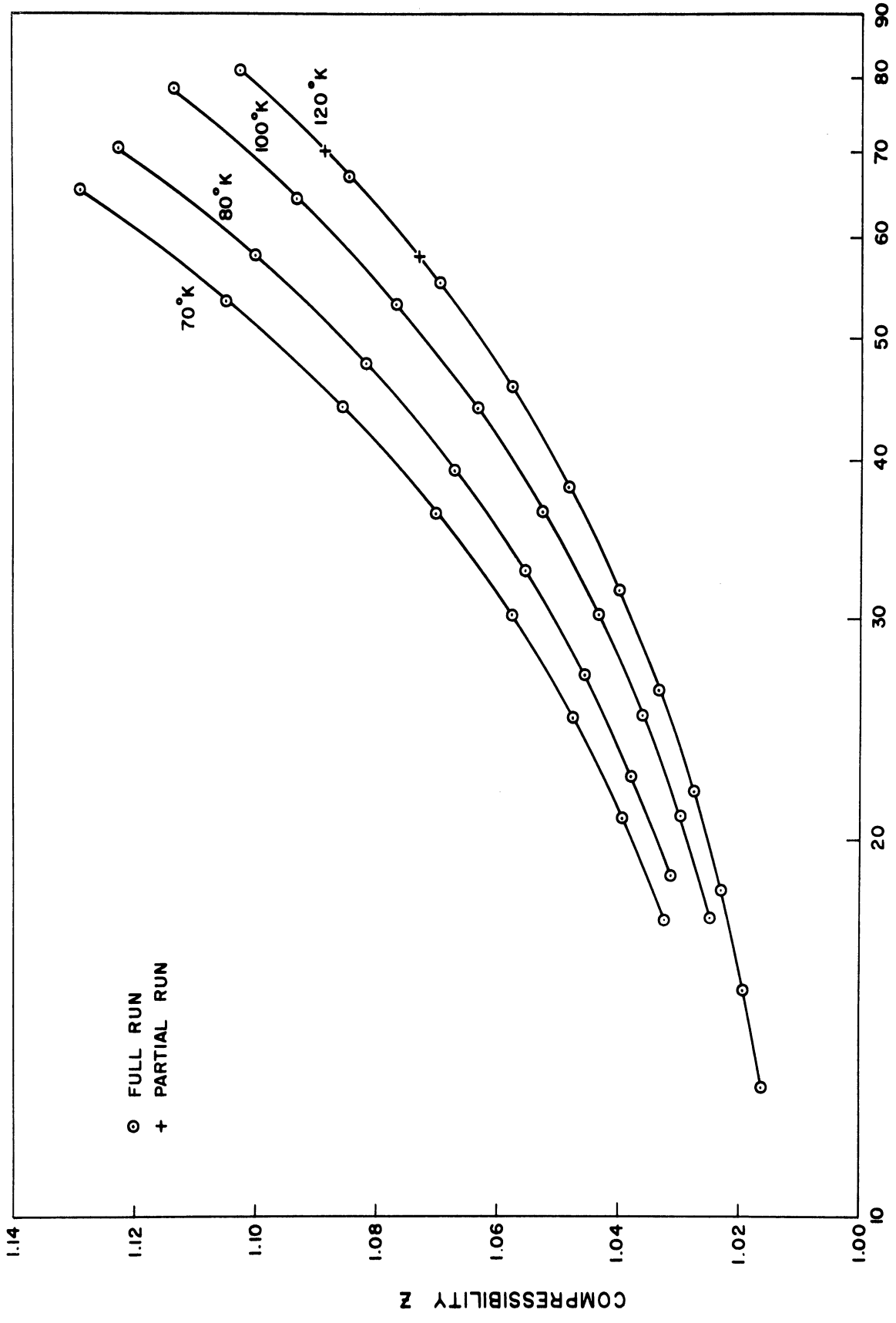

Figure 22. Compressibility Diagram For Helium Showing The Low Pressure Experimental Points.

TABLE 3

COMPARISON OF SELECTED VALUES OF COMPRESSIBILITY

FOR HELIUM TO PUBLISHED VALUES

T = 70° K

Reference	Pressure (atm)		
	20	50	100
This work	1.03788	1.09700	1.20060
Holborn and Otto (33), (34), (35)	1.03520	1.09383	1.19690
Mann (49) (Compilation)	1.03653	1.09619	1.20002

T = 80° K

Reference	Pressure (atm)		
	20	50	100
This work	1.03440	1.08472	1.17445
Holborn and Otto (33), (34), (35)	1.03199	1.08423	1.17654
Mann (49) (Compilation)	1.03381	1.08771	1.18051

TABLE 3 (CONT'D)

COMPARISON OF SELECTED VALUES OF COMPRESSIBILITY FOR HELIUM TO PUBLISHED VALUES

T = 100° K

Reference	Pressure (atm)		
	20	50	100
This work	1.02841	1.07198	1.14508
Holborn and Otto (33), (34), (35)	1.02682	1.06938	1.14460
Mann (49) (Compilation)	1.02938	1.07489	1.15172

T = 120° K

	Pressure (atm)		
	20	50	100
This work	1.02526	1.06293	1.12519
Holborn and Otto (33), (34), (35)	1.02294	1.05906	1.12182
Mann (49) (Compilation)	1.02579	1.06506	1.13092

2. Second and Third Virial Coefficients

The values of the second and third virial coefficient for each isotherm were obtained by least squares fitting the points with densities less than half the critical density to the equation

$$v(Z - 1) = B + C/v \qquad (124)$$

The values obtained for the second and third virial coefficients of helium are listed in Table 4.

TABLE 4

EXPERIMENTAL SECOND AND THIRD VIRIAL COEFFICIENTS FOR HELIUM

Temperature °K	Second Virial Coefficient B (cc/gm)	Third Virial Coefficient C (cc^2/gm^2)
70	2.608	14.32
80	2.690	12.56
100	2.883	12.26
120	3.106	9.809

Figure 23 shows a comparison between the values of the second virial coefficient from this work to values obtained by previous investigators. Figure 23 shows that the values of the second virial coefficient for the 80 and 100° K isotherms of helium show satisfactory agreement with published values. The values for the 70 and 120° K isotherms are slightly too large and do not form a smooth curve with the 80 and 100° K values as they should. This inconsistancy is attributed to lack of low pressure

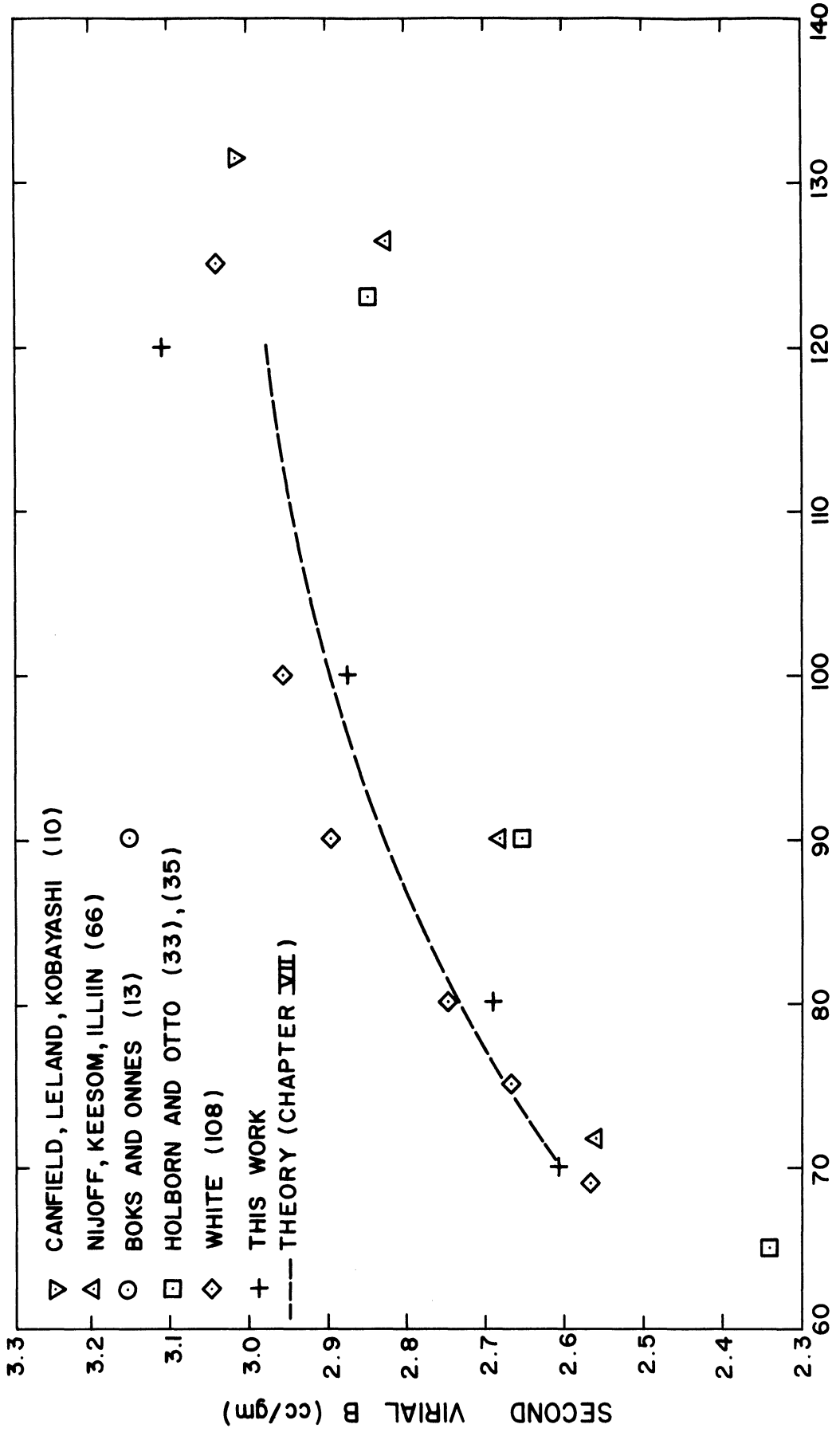

Figure 23. Comparison of Experimental Values of the Second Virial Coefficient of Helium.

data for the helium isotherms. The helium data was taken with the intention of using the method described in reference (10) to reduce the data. Since the low pressure data points are ignored when this method is used it was not considered necessary to take them. In using this method N_o was varied until a minimum deviation from linearity was obtained for points below half the critical density on a virial plot. In approaching the true value of N_o from below with this method the second virial coefficient for the 80° K isotherm of helium came out to be about 3.1 cc/gm. On the other hand, if an initial value of N_o that was greater than the true value was used the minimum deviation in linearity occurred for N_o too large and the second virial coefficient came out to be about 2.44 (cc/gm) for the 80° K isotherm of helium. The region between 2.44 and 3.1, where all of the published values lie, was inaccessable unless the density limit is increased to around 0.8 of the critical density. It was apparent upon observing the data for this higher density limit that considerable forcing of the data was present. It was this dilemma which ultimately led to the technique discussed in Chapter III for reduction of Burnett data. Unfortunately the new technique requires accurate low pressure data. The data on helium terminates at about the maximum point on a β-plot as can be seen in Figure 7. The fact that the data does not continue to lower densities makes it possible to obtain a nearly linear isotherm for erroneous values of P_o/Z_o and N_o . Thus even using the new technique it is possible to obtain a false answer although the degree of variation of the answer has been considerably reduced. This problem does not arrise in the

neon data where lower pressures were taken and about twice as many points are available below the density limit of four-tenths the critical density. In addition to the considerations given above it should also be pointed out that the small value of the cell constant used in this work seriously limits the accuracy to which the virial coefficients can be determined due to the buildup of experimental error with the number of expansions.

B. Experimental Results for Neon

1. Compressibilities

The isotherms of neon were investigated using high purity neon supplied by Linde Company. Impurities in the neon were oxygen in the amount of 1 ppm and helium in the amount of 15 ppm.

The experimentally determined values of the compressibilities for neon are listed in Table 5 along with the computed values of the specific volumes. Each isotherm for neon was determined by making a single run from 300 atmospheres down to about 7 atmospheres.

Figure 24 shows the experimental points for neon and demonstrates that the data are consistent.

Table 6 gives a comparison of selected values of the compressibility to published values. The values in Table 6 for the data of Holborn and Otto were obtained by plotting Z against T and drawing a smooth curve between the points. Only the 65, 90 and 123° K isotherms were studied by them over the range of this research. Thus the interpolated values in Table 6 are not very accurate and serve only as a rough comparison. The average deviation of the compressibilities of this work from the values listed in Table 6 for the results of Holborn and Otto is about 2%.

TABLE 5

EXPERIMENTAL RESULTS FOR NEON

T = 70° K			T = 80° K		
P(atm)	Z = Pv/RT	v(cc/gm)	P(atm)	Z = Pv/RT	v(cc/gm)
302.5444	1.27578	1.20013	301.6140	1.25022	1.34825
201.1379	1.01210	1.43210	216.3159	1.07020	1.60921
149.0674	0.89524	1.70923	166.1444	0.98122	1.92095
118.1366	0.84686	2.04019	133.0937	0.93837	2.29324
97.2274	0.83197	2.43535	109.3310	0.92026	2.73780
81.6516	0.83404	2.90712	91.0234	0.91471	3.26861
69.2561	0.84448	3.47034	76.4044	0.91667	3.90240
58.9992	0.85879	4.14271	64.3973	0.92244	4.65912
50.3235	0.87444	4.94538	54.3665	0.92977	5.56261
42.9013	0.88991	5.90360	45.9233	0.93768	6.64133
36.5347	0.90468	7.04750	38.7807	0.94540	7.92927
31.0483	0.91780	8.41304	32.7298	0.95262	9.46698
26.3430	0.92960	10.0432	27.6038	0.95924	11.3029
22.3139	0.93999	11.9892	23.2603	0.96505	13.4949
18.8712	0.94900	14.3123	19.5856	0.97018	16.1120
15.9367	0.95672	17.0856	16.4790	0.97460	19.2367
13.4429	0.96338	20.3962	13.8561	0.97840	22.9674
11.3265	0.96899	24.3483	11.6434	0.98160	27.4215
9.5353	0.97382	29.0661	9.7805	0.98446	32.7395
8.0208	0.97787	34.6982	8.2123	0.98692	39.0888
6.7438	0.98149	41.4215	6.8930	0.98903	46.6695

TABLE 5 (CONT'D)

EXPERIMENTAL RESULTS FOR NEON

T = 100° K			T = 120° K		
P(atm)	Z = Pv/RT	v(cc/gm)	P(atm)	Z = Pv/RT	v(cc/gm)
304.2405	1.24211	1.65993	304.7889	1.23859	1.98269
232.6842	1.13411	1.98167	239.0719	1.15994	2.36718
184.1213	1.07144	2.36596	191.4889	1.10930	2.82640
148.9023	1.03457	2.82491	155.5557	1.07600	3.37483
122.0946	1.01290	3.37299	127.5737	1.05370	4.02978
100.9979	1.00047	4.02749	105.2952	1.03849	4.81191
84.0062	0.99363	4.80905	87.2889	1.02800	5.74593
70.1102	0.99020	5.74233	72.5757	1.02064	6.86130
58.6309	0.98879	6.85678	60.4697	1.01547	8.19324
49.0917	0.98859	8.18755	50.4512	1.01170	9.78378
41.1338	0.98911	9.77663	42.1355	1.00898	11.6831
34.4771	0.98995	11.6741	35.2140	1.00694	13.9513
28.9013	0.99091	13.9400	29.4441	1.00541	16.6598
24.2283	0.99192	16.6456	24.6269	1.00417	19.8941
20.3086	0.99282	19.8764	20.6036	1.00323	23.7565
17.0217	0.99365	23.7343	17.2411	1.00248	28.3687
14.2673	0.99451	28.3410	14.4303	1.00195	33.8763
11.9583	0.99536	33.8418	12.0791	1.00153	40.4534
10.0211	0.99601	40.4104	10.1135	1.00136	48.3073
8.3973	0.99661	48.2539			

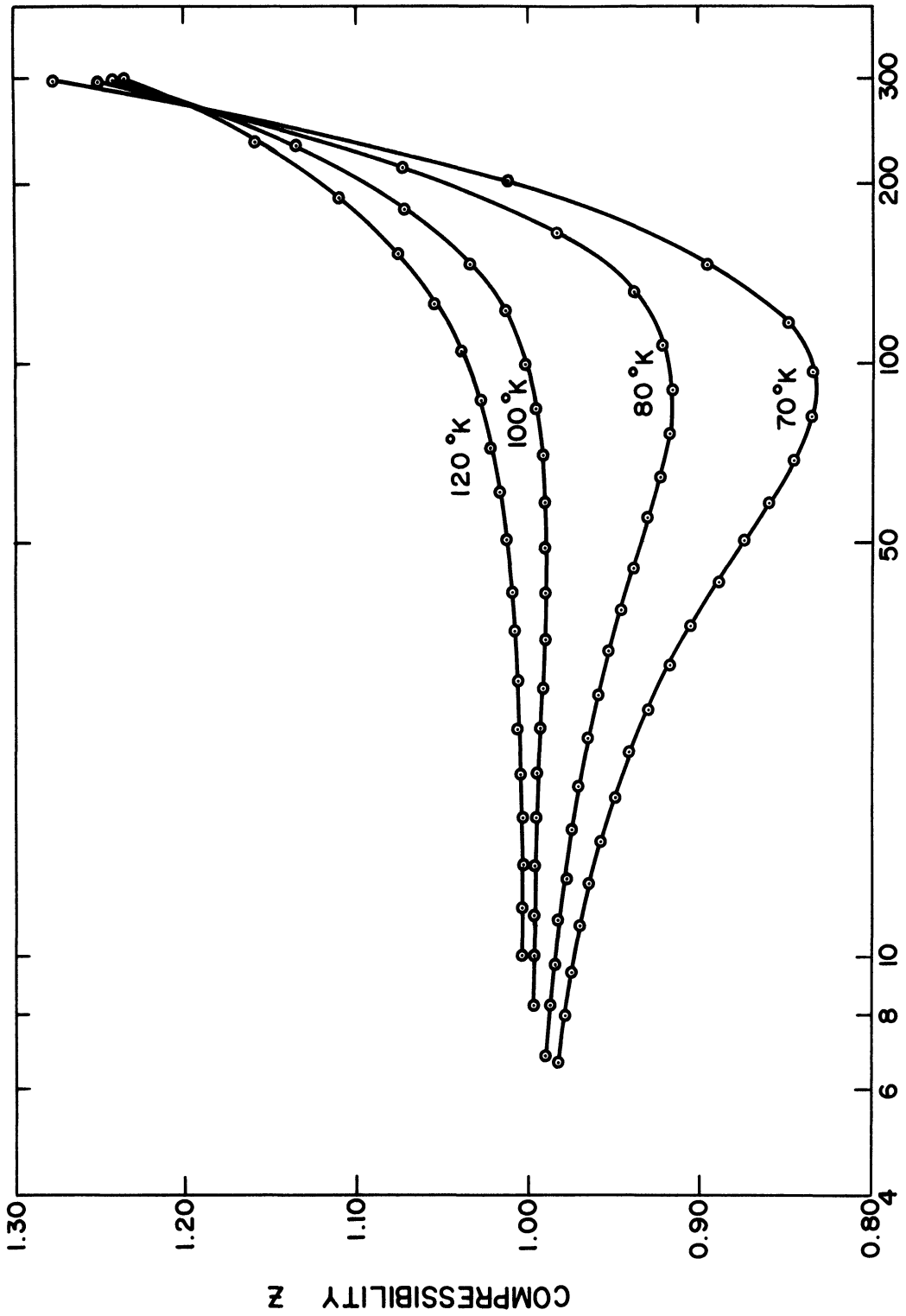

Figure 24. Compressibility Diagram For Neon Showing The Experimental Points.

TABLE 6

COMPARISON OF SELECTED VALUES OF COMPRESSIBILITY

FOR NEON TO PUBLISHED VALUES

T = 70° K

Reference	Pressure (atm)			
	20	50	100	200
This work	0.94611	.87501	0.83251	1.00953
Holborn and Otto (31)	0.9402	0.8587	0.7590	-------
McCarty, Stewart and Timmerhaus (59) (Compilation)	0.9400	0.8686	0.8251	0.9869

T = 80° K

Reference	Pressure (atm)			
	20	50	100	200
This work	0.96977	0.93347	0.91650	1.03913
Holborn and Otto (31)	0.9647	0.9236	0.8880	-------
McCarty, Stewart and Timmerhaus (59) (Compilation)	0.9644	0.9285	0.9129	1.0334

TABLE 6 (CONT'D)

COMPARISON OF SELECTED VALUES OF COMPRESSIBILITY

FOR NEON TO PUBLISHED VALUES

T = 100° K

Reference	Pressure (atm)			
	20	50	100	200
This work	0.99296	0.98857	1.00001	1.09068
Holborn and Otto (31)	0.9906	0.9825	0.9940	-------
McCarty, Stewart and Timmerhaus (59) (Compilation)	0.9875	0.9833	0.9981	1.0964

T = 120° K

Reference	Pressure (atm)			
	20	50	100	200
This work	1.00310	1.01157	1.03524	1.11807
Holborn and Otto (31)	1.0010	1.0067	1.0300	-------
McCarty, Stewart and Timmerhaus (59) (Compilation)	0.9973	1.0054	1.0319	1.1226

The comparison of this work to the compilation of McCarty, Stewart and Timmerhaus shows an average deviation of about 0.6%. Figure 25 presents a graphical comparison of this work to the calculated results of McCarty, Stewart and Timmerhaus. It is clear from this comparison that their isotherms are displaced from those of this research by a constant factor. Also the zero pressure limits of their isotherms is not unity as they should be.

2. Second and Third Virial Coefficients

The values of the second and third virial coefficients were obtained by least squares fitting the points with densities less than four-tenths the critical density to Equation (124).

The values obtained for the second and third virial coefficients are listed in Table 7.

TABLE 7

EXPERIMENTAL SECOND AND THIRD VIRIAL COEFFICIENTS

FOR NEON

Temperature °K	Second Virial Coefficient B (cc/gm)	Third Virial Coefficient C (cc^2/gm^2)
70	-0.789	0.824
80	-0.531	0.783
100	-0.179	0.706
120	+0.049	0.647

Figure 26 presents a graphical comparison of the second virial coefficients obtained in this research to the results of previous investigators. The values of the second virial coefficient for neon from this research compare favorably with those of Holborn and Otto.

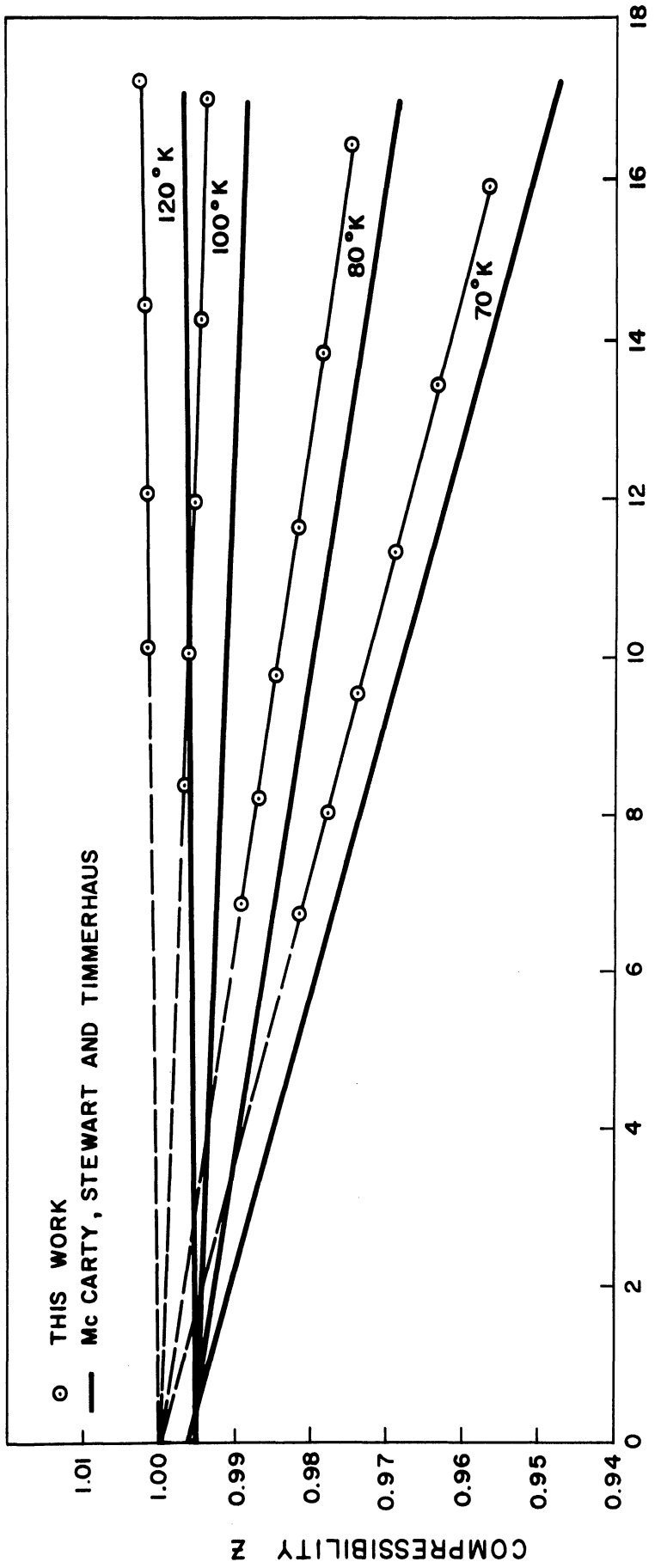

Figure 25. Comparison of This Work To The Compilation of McCarty, Stewart and Timmerhaus(59).

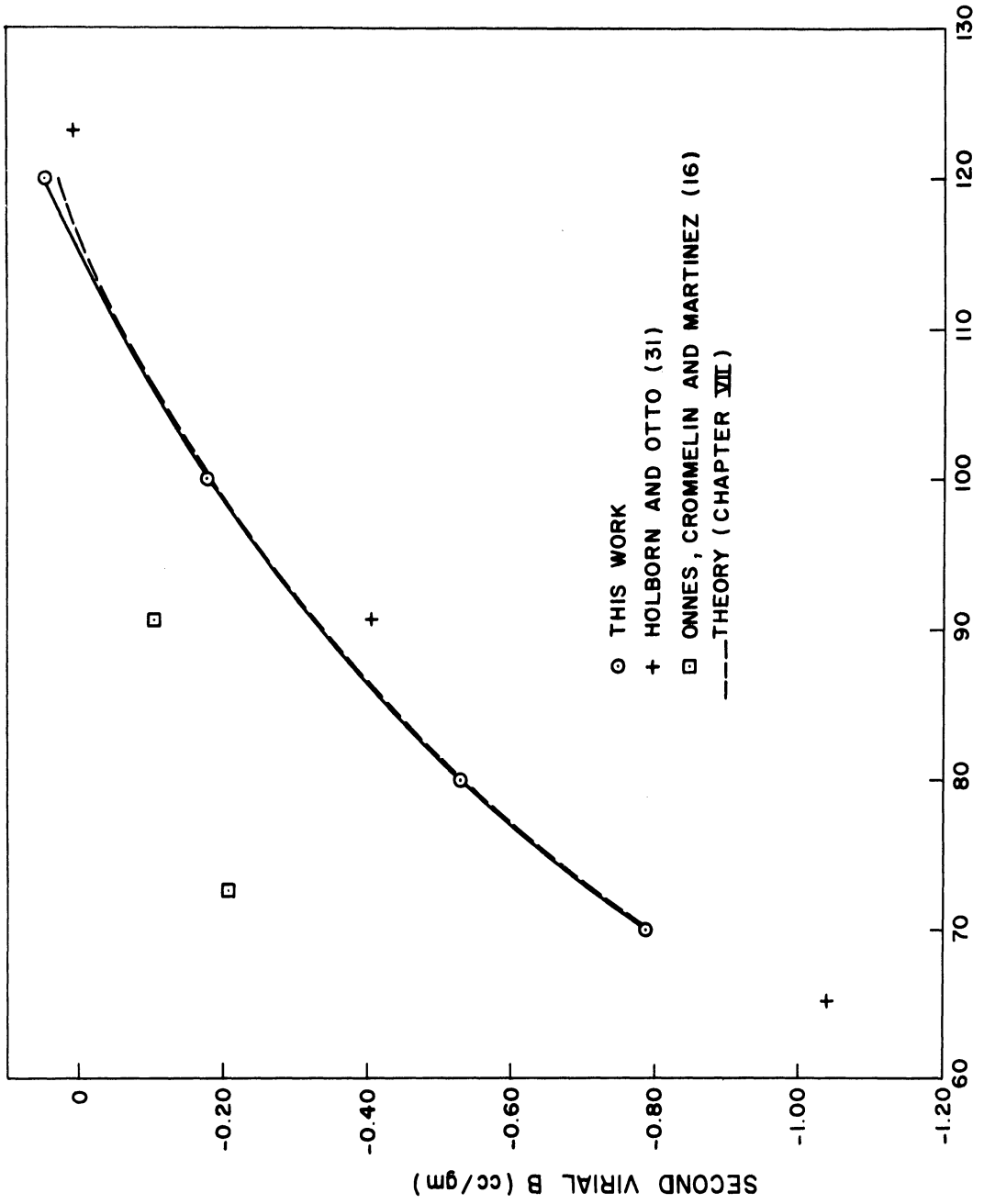

Figure 26. Comparison of the Experimental Values of the Second Virial Coefficient of Neon.

VII. THEORETICAL AND EMPIRICAL CORRELATIONS

A. Determination of Intermolecular Parameters for the Lennard-Jones 6-12 Potential

The theoretical expression for the second virial coefficient including quantum corrections is presented in Chapter III, section F. Equations (57) through (64) were programmed for solution on the IBM 7090 digital computer. Vaules of σ and ϵ based on the results of previous work were used as starting values.

These values were then modified by determining the shift in the ordinate and abscissa on a plot of $\ln B_{exp}$ against $\ln T$ necessary to cause this plot to coincide with a plot of $\ln B^*$ against $\ln T^*$. The variations in σ and ϵ were determined from Equations (65) and (66) which can be written as

$$\ln B_{exp} = \ln B^* + \ln b^\circ \tag{125}$$

and

$$\ln T = \ln T^* + \ln \epsilon/k \tag{126}$$

The values of ϵ and σ obtained from the above procedure for neon and helium are listed in Tables 8 and 9. The theoretical curves of the second virial coefficient as a function of temperature for neon and helium are shown in Figures 23 and 26.

B. Fit of the Experimental Data to the Leiden Expansion

1. Helium

Each isotherm of helium was least squares fitted to the Leiden expansion of Z in a polynomial in density. The coefficients resulting

TABLE 8

RESULTS OF THE DETERMINATION OF σ AND ϵ

FOR HELIUM WITH QUANTUM CORRECTIONS

σ = 2.60 Å

ϵ/k = 9.78° K

Λ^* = 2.69

T °K	T*	B*	B^*_{cl}	B^*_I	B^*_{II}	B^*_o	B_{calc}(cc/gm.
70	7.1576	.4716	.3828	.01442	-.0001947	.0002799	2.613
80	8.1801	.4947	.4190	.01208	-.0001392	.0002291	2.741
100	10.2252	.5229	.4647	.009055	-.0000804	.0001639	2.897
120	12.2702	.5379	.4910	.007191	-.0000519	.0001247	2.980

TABLE 9

RESULTS OF THE DETERMINATION OF σ AND ϵ

FOR NEON WITH QUANTUM CORRECTIONS

σ = 2.782 Å

ϵ/k = 34.82 °K

Λ^* = 0.5935

T °K	T*	B*	B^*_{cl}	B^*_I	B^*_{II}	B^*_o	B_{calc}(cc/gm)
70	2.0103	-.5856	-.6193	.09907	-.007025	.001880	-.7884
80	2.2975	-.3944	-.4211	.07845	-.004612	.001539	-.5309
100	2.8719	-.1398	-.1583	.05422	-.002347	.001101	-.1881
120	3.4463	+.0207	+.0067	.04076	-.001382	.0008377	+.02782

from the fit are listed in Table 10. In observing Table 10 it is apparent that the fit is well within the expected experimental error. It should be noted that the coefficients in Table 10 are not true virial coefficients, but empirical coefficients obtained by fitting the data to the Leiden expansion.

2. Neon

Each isotherm of neon was least squares fitted to the Leiden expansion and the coefficients listed in Table 11 were obtained. As was the case for helium the fit is well within the expected experimental error. And as was stated for helium the coefficients in Table 11 are not true virial coefficients, but empirical coefficients necessary to fit the data to the Leiden expansion.

C. Fit of the Experimental Data to the Berlin Expansion

Each isotherm of neon and helium was least squares fitted to the Berlin expansion of Z in a polynomial in pressure. The coefficients which resulted for each isotherm are listed in Tables 12 and 13. Tables 14 through 17 show a point by point comparison of the experimental compressibilities for helium to those computed from the Berlin expansion. It is apparent that the 80° K isotherm of helium shows a large variation compared to the other three isotherms. It is felt that this is due to the overall accuracy of the data for this isotherm. The 80° K isotherm of helium was the first isotherm studied and a smooth repeatable technique of taking the data had not been fully developed.

TABLE 10

LEIDEN COEFFICIENTS FOR HELIUM

$$Z = A + B\rho + C\rho^2 + D\rho^3 + E\rho^4 + F\rho^5 + G\rho^6$$

Density in (gm/cc)

Temperature (°K)	Standard Deviation	A	B	C	D	E	F	G
70	$.405 \times 10^{-4}$	0.999637	2.65968	12.2893	18.9290	144.414	-55.0248	- - -
80	$.488 \times 10^{-3}$	1.00037	2.64376	14.6551	-56.3750	1001.16	-4889.81	9802.75
100	$.367 \times 10^{-4}$	0.999684	2.93280	10.0783	26.0415	42.2053	45.4363	- - -
120	$.203 \times 10^{-4}$	0.999925	3.13063	7.83890	42.3823	-63.3062	227.480	- - -

TABLE 11

LEIDEN COEFFICIENTS FOR NEON

$$Z = A + B\rho + C\rho^2 + D\rho^3 + E\rho^4 + F\rho^5 + G\rho^6$$

Density in (gm/cc)

Temperature (°K)	Standard Deviation	A	B	C	D	E	F	G
70	0.115×10^{-3}	0.998950	-.741799	.241041	2.49833	-5.06805	5.29583	-1.54645
80	0.121×10^{-3}	1.00013	-.535049	.845095	-0.671967	3.01108	-3.61031	2.13445
100	0.453×10^{-4}	0.999861	-.172746	.674702	-0.453964	3.36785	-4.99988	3.21807
120	0.519×10^{-4}	0.999479	.075942	.280106	1.69360	-2.97270	4.23309	-2.03686

TABLE 12

BERLIN COEFFICIENTS FOR HELIUM

$$Z = A' + B'P + C'P^2 + D'P^3 + E'P^4 + F'P^5 + G'P^6$$

Pressure in Atmosphere

Temperature (°K)	Standard Deviation	Coefficient A'	B'x10^3	C'x10^6	D'x10^9	E'x10^{12}	F'x10^{15}	G'x10^{18}
70	0.265x10^{-3}	1.00061	1.80897	2.96340	-13.2222	30.1403	-35.1756	16.2242
80	0.601x10^{-3}	1.00360	1.46855	3.96361	-20.0961	50.4692	-62.0908	29.4334
100	0.396x10^{-4}	0.99954	1.43890	0.234588	-0.726644	0.216244	0.818254	-0.683837
120	0.316x10^{-4}	1.00001	1.26602	-0.161639	0.240920	-0.512839	0.340978	- - -

TABLE 13

BERLIN COEFFICIENTS FOR NEON

$$Z = A' + B' P + C' P^2 + D' P^3 + E' P^4 + F' P^5 + G' P^6$$

Pressure in Atmosphere

Temperature	Standard Deviation	A'	B'x10^3	C'x10^5	D'x10^6	E'x10^9	F'x10^{11}	G'x10^{14}
70	.377x10^{-3}	0.998479	-2.49453	-1.14477	0.276765	-0.697925	-0.139693	0.496004
80	.156x10^{-3}	0.998532	-1.41019	-0.448470	0.169866	-0.807773	0.158826	-0.113610
100	.516x10^{-4}	0.99573	- .386214	0.234405	0.024086	-0.095574	0.010881	--------
120	.817x10^{-4}	0.999991	0.098132	0.307911	-0.012608	0.107566	-0.040149	0.050817

A comparison of compressibilities for neon computed from the Berlin expansion to experimental values is presented in Tables 18 through 21.

D. Values of Compressibility for Even Values of Pressure

The Berlin Expansion for each isotherm of neon and helium was used to compute values of the compressibility for even values of pressure for the full range of the experimental data. The results of these computations are presented in Tables 22 and 23.

TABLE 14

FIT OF THE 70°K ISOTHERM OF HELIUM TO THE BERLIN EXPANSION

P(atm)	Z exp	Z calc	Z exp - Z calc	% deviation
684.8179	2.38703	2.38709	-.00006	-.00239
575.2362	2.17780	2.17746	.00034	.01573
477.0025	1.98494	1.98556	-.00062	-.03098
408.8116	1.84789	1.84796	-.00007	-.00355
346.0660	1.71950	1.71911	.00039	.02281
301.4177	1.62691	1.62645	.00046	.02812
259.2827	1.53844	1.53832	.00012	.00749
228.6351	1.47372	1.47379	-.00007	-.00482
199.1316	1.41104	1.41133	-.00029	-.02057
177.2556	1.36451	1.36484	-.00033	-.02394
155.8527	1.31895	1.31925	-.00030	-.02305
139.7372	1.28472	1.28492	-.00020	-.01557
123.7492	1.25078	1.25090	-.00012	-.00978
111.5619	1.22502	1.22504	-.00002	-.00178
99.3494	1.19934	1.19923	.00011	.00923
89.9440	1.17961	1.17945	.00016	.01385
80.4433	1.15988	1.15957	.00031	.02630
65.5593	1.12903	1.12874	.00029	.02612
53.7108	1.10481	1.10451	.00030	.02710
44.1820	1.08549	1.08529	.00020	.01833
36.4628	1.07001	1.06992	.00009	.00806
30.1718	1.05755	1.05755	-.00000	-.00020
25.0185	1.04743	1.04753	-.00010	-.00960
20.7789	1.03908	1.03937	-.00029	-.02775
17.2845	1.03240	1.03270	-.00030	-.02910

The Average Per Cent Deviation For the Fit is 0.016%

TABLE 15

FIT OF THE 80°K ISOTHERM OF HELIUM TO THE BERLIN EXPANSION

P(atm)	Z exp	Z calc	Z exp - Z calc	% deviation
693.3695	2.21331	2.21344	-.00013	-.00591
601.2871	2.05939	2.05883	.00056	.02721
492.1884	1.87656	1.87726	-.00070	-.03721
433.8434	1.77490	1.77565	-.00075	-.04232
362.1074	1.64925	1.64843	.00082	.04971
323.3245	1.58022	1.57930	.00092	.05819
274.2133	1.49211	1.49157	.00054	.03609
247.1254	1.44302	1.44299	.00003	.00194
212.1853	1.37949	1.37996	-.00047	-.03404
192.5948	1.34369	1.34438	-.00069	-.05141
166.9379	1.29679	1.29751	-.00072	-.05528
152.3615	1.27013	1.27075	-.00062	-.04894
133.0322	1.23480	1.23518	-.00038	-.03088
121.9451	1.21469	1.21477	-.00008	-.00618
107.0731	1.18756	1.18742	.00014	.01185
86.8495	1.15102	1.15045	.00057	.04927
70.8718	1.12237	1.12160	.00077	.06858
58.1139	1.09975	1.09892	.00083	.07534
47.8305	1.08162	1.08096	.00066	.06102
39.4923	1.06718	1.06666	.00052	.04890
32.6789	1.05524	1.05518	.00006	.00586
27.0986	1.04566	1.04593	-.00027	-.02616
22.5058	1.03777	1.03844	-.00067	-.06483
18.7183	1.03142	1.03235	-.00093	-.09042

The Average Per Cent Deviation For the Fit is 0.041%

TABLE 16

FIT OF THE 100°K ISOTHERM OF HELIUM TO THE BERLIN EXPANSION

P(atm)	Z exp	Z calc	Z exp - Z calc	% deviation
685.9706	1.96335	1.96333	.00002	.00088
596.0191	1.84474	1.84481	-.00007	-.00388
503.0904	1.71951	1.71942	.00009	.00518
442.7845	1.63667	1.63666	.00001	.00065
379.2859	1.54826	1.54826	.00000	.00030
337.2588	1.48891	1.48899	-.00008	-.00545
292.2335	1.42483	1.42483	.00000	.00008
261.9459	1.38129	1.38130	-.00001	-.00044
228.9879	1.33360	1.33362	-.00002	-.00131
206.5452	1.30100	1.30099	.00001	.00071
181.8324	1.26498	1.26494	.00004	.00312
164.8037	1.24004	1.24004	-.00000	-.00002
145.8905	1.21241	1.21234	.00007	.00545
132.7315	1.19305	1.19306	-.00001	-.00068
118.0002	1.17145	1.17146	-.00001	-.00101
107.6887	1.15632	1.15635	-.00003	-.00226
96.0702	1.13935	1.13932	.00003	.00256
78.6122	1.11376	1.11376	-.00000	-.00022
64.5923	1.09325	1.09327	-.00002	-.00178
53.2492	1.07670	1.07672	-.00002	-.00166
44.0156	1.06324	1.06327	-.00003	-.00260
36.4623	1.05223	1.05228	-.00005	-.00502
30.2599	1.04324	1.04328	-.00004	-.00345
25.1502	1.03587	1.03587	.00000	.00042
20.9281	1.02978	1.02975	.00003	.00294
17.4326	1.02477	1.02469	.00008	.00767

The Average Per Cent Deviation For the Fit is 0.0023%

TABLE 17

FIT OF THE 120°K ISOTHERM OF HELIUM TO THE BERLIN EXPANSION

P(atm)	Z exp	Z calc	Z exp - Z calc	% deviation
692.8584	1.81597	1.81597	-.00000	-.00017
518.3546	1.62214	1.62211	.00003	.00175
396.7062	1.48243	1.48250	-.00007	-.00439
309.0784	1.37927	1.37926	.00001	.00079
244.2293	1.30160	1.30155	.00005	.00421
195.1435	1.24208	1.24205	.00003	.00244
157.3013	1.19579	1.19581	-.00002	-.00169
127.6941	1.15939	1.15941	-.00002	-.00183
104.2411	1.13043	1.13044	-.00001	-.00073
99.1653	1.12411	1.12415	-.00004	-.00366
85.4788	1.10716	1.10717	-.00001	-.00076
81.3971	1.10206	1.10209	-.00003	-.00317
70.3492	1.08834	1.08834	-.00000	-.00022
67.0455	1.08422	1.08422	-.00000	-.00037
58.0692	1.07302	1.07302	-.00000	-.00003
55.3808	1.06970	1.06966	.00004	.00367
45.8487	1.05776	1.05773	.00003	.00249
38.0308	1.04798	1.04793	.00005	.00446
31.5946	1.03990	1.03985	.00005	.00459
26.2807	1.03319	1.03317	.00002	.00179
21.8844	1.02764	1.02764	.00000	.00017
18.2393	1.02301	1.02305	-.00004	-.00354
15.2130	1.01918	1.01923	-.00005	-.00496
12.6974	1.01605	1.01606	-.00001	-.00067

The Average Per Cent Deviation for the Fit is .0022%

TABLE 18

FIT OF THE 70° K ISOTHERM OF NEON TO THE BERLIN EXPANSION

P(atm)	Z exp	Z calc	Z exp - Z calc	% deviation
302.5444	1.27578	1.27578	-.00000	-.00030
201.1379	1.01210	1.01197	.00013	.01235
149.0674	.89524	.89600	-.00076	-.08438
118.1366	.84686	.84573	.00113	.13323
97.2274	.83197	.83179	.00018	.02200
81.6516	.83404	.83452	-.00048	-.05708
69.2561	.84448	.84501	-.00053	-.06294
58.9992	.85879	.85905	-.00026	-.03017
50.3235	.87444	.87438	.00006	.00684
42.9012	.88991	.88971	.00020	.02266
36.5347	.90468	.90424	.00044	.04903
31.0483	.91780	.91759	.00021	.02263
26.3429	.92960	.92953	.00007	.00761
22.3138	.93999	.94001	-.00002	-.00231
18.8712	.94900	.94910	-.00010	-.01013
15.9367	.95672	.95689	-.00017	-.01791
13.4429	.96338	.96353	-.00015	-.01516
11.3265	.96899	.96915	-.00016	-.01620
9.5353	.97382	.97389	-.00007	-.00685
8.0208	.97787	.97787	-.00000	-.00048
6.7438	.98149	.98122	.00027	.02755

The Average Per Cent Deviation For the Fit is .0289%

TABLE 19

FIT OF THE 80° K ISOTHERM OF NEON TO THE BERLIN EXPANSION

P(atm)	Z exp	Z calc	Z exp - Z calc	% deviation
301.6140	1.25022	1.25022	.00000	.00003
216.3159	1.07020	1.07021	-.00001	-.00117
166.1444	.98122	.98116	.00006	.00650
133.0937	.93837	.93843	-.00006	-.00633
109.3310	.92026	.92019	.00007	.00722
91.0234	.91471	.91495	-.00024	-.02587
76.4044	.91667	.91675	-.00008	-.00898
64.3973	.92244	.92227	.00017	.01836
54.3665	.92977	.92957	.00020	.02120
45.9233	.93768	.93749	.00019	.02076
38.7807	.94540	.94531	.00009	.00908
32.7298	.95262	.95266	-.00004	-.00410
27.6038	.95924	.95932	-.00008	-.00797
23.2603	.96505	.96522	-.00017	-.01715
19.5856	.97018	.97035	-.00017	-.01789
16.4790	.97460	.97478	-.00018	-.01822
13.8561	.97840	.97855	-.00015	-.01570
11.6434	.98160	.98176	-.00016	-.01607
9.7805	.98446	.98446	-.00000	-.00018
8.2123	.98692	.98674	.00018	.01838
6.8930	.98903	.98865	.00038	.03824

The Average Per Cent Deviation For the Fit is .0331%

TABLE 20

FIT OF THE 100° K ISOTHERM OF NEON TO THE BERLIN EXPANSION

P(atm)	Z exp	Z calc	Z exp - Z calc	% deviation
304.2405	1.24211	1.24211	.00000	.00000
232.6842	1.13411	1.13411	.00000	.00010
184.1213	1.07144	1.07145	-.00001	-.00123
148.9023	1.03457	1.03454	.00003	.00326
122.0946	1.01290	1.01291	-.00001	-.00128
100.9979	1.00047	1.00049	-.00002	-.00198
84.0062	.99363	.99365	-.00002	-.00152
70.1102	.99020	.99019	.00001	.00069
58.6309	.98879	.98879	.00000	.00028
49.0917	.98859	.98859	.00000	.00022
41.1338	.98911	.98907	.00004	.00422
34.4771	.98995	.98990	.00005	.00493
28.9013	.99091	.99089	.00002	.00243
24.2283	.99192	.99190	.00002	.00179
20.3085	.99282	.99288	-.00006	-.00627
17.0217	.99365	.99379	-.00014	-.01400
14.2673	.99451	.99461	-.00010	-.00966
11.9583	.99536	.99533	.00003	.00311
10.0210	.99601	.99596	.00005	.00487
8.3973	.99661	.99651	.00010	.01014

The Average Per Cent Deviation For the Fit is .0036%

TABLE 21

FIT OF THE 120° K ISOTHERM OF NEON TO THE BERLIN EXPANSION

P(atm)	Z exp	Z calc	Z exp - Z calc	% deviation
304.7889	1.23859	1.23860	-.00001	-.00050
239.0719	1.15994	1.15988	.00006	.00545
191.4889	1.10930	1.10947	-.00017	-.01554
155.5557	1.07600	1.07592	.00008	.00741
127.5737	1.05370	1.05356	.00014	.01319
105.2952	1.03849	1.03846	.00003	.00272
87.2889	1.02800	1.02807	-.00007	-.00652
72.5757	1.02064	1.02076	-.00012	-.01192
60.4697	1.01547	1.01553	-.00006	-.00635
50.4512	1.01170	1.01173	-.00003	-.00335
42.1355	1.00898	1.00894	.00004	.00420
35.2140	1.00694	1.00686	.00008	.00809
29.4441	1.00541	1.00530	.00011	.01094
24.6269	1.00417	1.00412	.00005	.00473
20.6036	1.00323	1.00323	.00000	.00027
17.2411	1.00248	1.00254	-.00006	-.00620
14.4303	1.00195	1.00201	-.00006	-.00643
12.0791	1.00153	1.00161	-.00008	-.00751
10.1135	1.00136	1.00129	.00007	.00738

The Average Per Cent Deviation For the Fit is .0068%

TABLE 22

VALUES OF COMPRESSIBILITY FOR HELIUM

FOR EVEN VALUES OF PRESSURE

P(atm)		TEMPERATURE (° K) 70	80	100	120
	v cc/gm				
10	v	146.22155	167.05729	207.85583	249.10711
	Z	1.01899	1.01866	1.01395	1.01265
20	v	74.46615	84.81940	105.40945	126.10496
	Z	1.03788	1.03440	1.02841	1.02526
30	v	50.56913	57.43824	71.26328	85.10180
	Z	1.05722	1.05072	1.04290	1.03785
40	v	38.63447	43.76747	54.19194	64.59847
	Z	1.07694	1.06752	1.05743	1.05040
50	v	31.48312	35.57814	43.95036	52.29512
	Z	1.09700	1.08472	1.07198	1.06293
60	v	26.72221	30.12752	37.12354	44.09180
	Z	1.11733	1.10225	1.08657	1.07543
70	v	23.32633	26.24037	32.24788	38.23138
	Z	1.13789	1.12004	1.10117	1.08791
80	v	20.78287	23.32922	28.59160	33.83529
	Z	1.15865	1.13803	1.11579	1.10036
90	v	18.80710	21.06784	25.74815	30.41545
	Z	1.17956	1.15619	1.13043	1.11278
100	v	17.22827	19.26060	23.47362	27.67899
	Z	1.20060	1.17445	1.14508	1.12519
110	v	15.93775	17.78311	21.61278	25.43955
	Z	1.22173	1.19279	1.15973	1.13756
120	v	14.86316	16.55251	20.06214	23.57287
	Z	1.24294	1.21118	1.17439	1.14992
130	v	13.95446	15.51152	18.75008	21.99295
	Z	1.26419	1.22960	1.18905	1.16225
140	v	13.17589	14.61926	17.62542	20.63833
	Z	1.28548	1.24801	1.20371	1.17456
150	v	12.50130	13.84580	16.65064	19.46397
	Z	1.30678	1.26641	1.21836	1.18685
160	v	11.91107	13.16874	15.79760	18.43606
	Z	1.32809	1.28478	1.23301	1.19912
170	v	11.39021	12.57099	15.04479	17.52876
	Z	1.34939	1.30312	1.24764	1.21136
180	v	10.92711	12.03926	14.37548	16.72197
	Z	1.37068	1.32141	1.26226	1.22358
190	v	10.51258	11.56309	13.77644	15.99981
	Z	1.39194	1.33965	1.27687	1.23578
200	v	10.13931	11.13415	13.23713	15.34960
	Z	1.41317	1.35785	1.29145	1.24796
210	v	9.80136	10.74568	12.74899	14.76104
	Z	1.43438	1.37600	1.30602	1.26012
220	v	9.49391	10.39218	12.30501	14.22574
	Z	1.45554	1.39410	1.32057	1.27225
230	v	9.21296	10.06910	11.89943	13.73674
	Z	1.47667	1.41216	1.33509	1.28436
240	v	8.95520	9.77267	11.52743	13.28825
	Z	1.49776	1.43018	1.34958	1.29644
250	v	8.71783	9.49971	11.18497	12.87540
	Z	1.51882	1.44816	1.36405	1.30850
260	v	8.49851	9.24755	10.86863	12.49409
	Z	1.53983	1.46611	1.37849	1.32054

TABLE 22

VALUES OF COMPRESSIBILITY FOR HELIUM
FOR EVEN VALUES OF PRESSURE (CONT'D)

		TEMPERATURE (° K)			
P(atm)	v cc/gm	70	80	100	120
270	v	8.29522	9.01391	10.57550	12.14079
	Z	1.56081	1.48403	1.39290	1.33255
280	v	8.10625	8.79681	10.30309	11.81252
	Z	1.58174	1.50193	1.40728	1.34454
290	v	7.93013	8.59459	10.04923	11.50667
	Z	1.60264	1.51981	1.42163	1.35651
300	v	7.76557	8.40576	9.81209	11.22101
	Z	1.62350	1.53767	1.43594	1.36844
310	v	7.61145	8.22906	9.59002	10.95356
	Z	1.64432	1.55553	1.45023	1.38036
320	v	7.46680	8.06335	9.38162	10.70263
	Z	1.66511	1.57337	1.46448	1.39224
330	v	7.33076	7.90765	9.18563	10.46671
	Z	1.68585	1.59121	1.47869	1.40410
340	v	7.20255	7.76108	9.00097	10.24447
	Z	1.70656	1.60904	1.49288	1.41593
350	v	7.08152	7.62285	8.82666	10.03474
	Z	1.72724	1.62686	1.50702	1.42774
360	v	6.96705	7.49226	8.66184	9.83647
	Z	1.74787	1.64468	1.52114	1.43951
370	v	6.85861	7.36869	8.50574	9.64872
	Z	1.76846	1.66248	1.53521	1.45126
380	v	6.75572	7.25157	8.35766	9.47068
	Z	1.78901	1.68028	1.54926	1.46298
390	v	6.65794	7.14038	8.21700	9.30158
	Z	1.80951	1.69805	1.56327	1.47467
400	v	6.56488	7.03466	8.08320	9.14076
	Z	1.82997	1.71581	1.57724	1.48633
410	v	6.47619	6.93399	7.95575	8.98761
	Z	1.85038	1.73353	1.59118	1.49797
420	v	6.39153	6.83798	7.83422	8.84157
	Z	1.87073	1.75123	1.60509	1.50957
430	v	6.31063	6.74628	7.71817	8.70216
	Z	1.89103	1.76888	1.61897	1.52114
440	v	6.23320	6.65857	7.60725	8.56892
	Z	1.91126	1.78648	1.63281	1.53268
450	v	6.15901	6.57455	7.50112	8.44144
	Z	1.93144	1.80403	1.64662	1.54420
460	v	6.08783	6.49396	7.39946	8.31935
	Z	1.95154	1.82151	1.66040	1.55568
470	v	6.01946	6.41654	7.30198	8.20229
	Z	1.97157	1.83892	1.67415	1.56714
480	v	5.95372	6.34207	7.20844	8.08996
	Z	1.99153	1.85625	1.68786	1.57856
490	v	5.89043	6.27035	7.11858	7.98207
	Z	2.01141	1.87350	1.70155	1.58996
500	v	5.82943	6.20119	7.03220	7.87835
	Z	2.03120	1.89065	1.71521	1.60132
510	v	5.77060	6.13443	6.94909	7.77856
	Z	2.05092	1.90770	1.72883	1.61266
520	v	5.71379	6.06990	6.86905	7.68247
	Z	2.07054	1.92464	1.74243	1.62397
530	v	5.65889	6.00749	6.79192	7.58988
	Z	2.09009	1.94148	1.75600	1.63525

TABLE 22

VALUES OF COMPRESSIBILITY FOR HELIUM

FOR EVEN VALUES OF PRESSURE (CONT'D)

P(atm)	v cc/gm	TEMPERATURE (° K) 70	80	100	120
540	v	5.60580	5.94706	6.71754	7.50060
	Z	2.10954	1.95822	1.76953	1.64651
550	v	5.55442	5.88853	6.64575	7.41445
	Z	2.12891	1.97485	1.78304	1.65774
560	v	5.50466	5.83179	6.57641	7.33126
	Z	2.14821	1.99138	1.79652	1.66894
570	v	5.45647	5.77678	6.50940	7.25088
	Z	2.16742	2.00783	1.80997	1.68012
580	v	5.40977	5.72344	6.44459	7.17318
	Z	2.18657	2.02419	1.82338	1.69127
590	v	5.36450	5.67174	6.38187	7.09801
	Z	2.20566	2.04048	1.83677	1.70240
600	v	5.32063	5.62164	6.32112	7.02527
	Z	2.22470	2.05674	1.85012	1.71352
610	v	5.27811	5.57313	6.26226	6.95483
	Z	2.24370	2.07298	1.86344	1.72461
620	v	5.23693	5.52622	6.20518	6.88659
	Z	2.26269	2.08922	1.87673	1.73568
630	v	5.19706	5.48093	6.14979	6.82045
	Z	2.28168	2.10552	1.88997	1.74674
640	v	5.15850	5.43729	6.09601	6.75632
	Z	2.30070	2.12191	1.90318	1.75778
650	v	5.12124	5.39536	6.04375	6.69411
	Z	2.31977	2.13845	1.91635	1.76881
660	v	5.08529	5.35520	5.99294	6.63375
	Z	2.33893	2.15519	1.92947	1.77982
670	v	5.05068	5.31691	5.94351	6.57515
	Z	2.35821	2.17220	1.94255	1.79083
680	v	5.01743	5.28057	5.89538	6.51826
	Z	2.37765	2.18955	1.95558	1.80183

TABLE 23

VALUES OF COMPRESSIBILITY FOR NEON

FOR EVEN VALUES OF PRESSURE

TEMPERATURE (° K)

P(atm)	v cc/gm	70	80	100	120
10	v	27.68238	32.01054	40.49397	48.85133
	Z	.97266	.98414	.99597	1.00127
20	v	13.46336	15.77149	20.18591	24.47035
	Z	.94611	.96977	.99296	1.00310
30	v	8.72996	10.36678	13.42621	16.35167
	Z	.92022	.95616	.99067	1.00544
40	v	6.37647	7.67547	10.05452	12.29826
	Z	.89619	.94391	.98918	1.00827
50	v	4.98064	6.07249	8.03863	9.87083
	Z	.87501	.93347	.98857	1.01157
60	v	4.06737	5.01544	6.70101	8.25636
	Z	.85748	.92518	.98889	1.01535
70	v	3.43225	4.27139	5.75119	7.10647
	Z	.84418	.91925	.99017	1.01959
80	v	2.97231	3.72347	5.04387	6.24698
	Z	.83549	.91581	.99245	1.02432
90	v	2.62976	3.30647	4.49826	5.58113
	Z	.83160	.91490	.99573	1.02953
100	v	2.36937	2.98104	4.06582	5.05087
	Z	.83251	.91650	1.00001	1.03524
110	v	2.16829	2.72197	3.71565	4.61923
	Z	.83804	.92054	1.00527	1.04144
120	v	2.01090	2.51235	3.42709	4.26156
	Z	.84787	.92689	1.01149	1.04815
130	v	1.88609	2.34037	3.18582	3.96078
	Z	.86152	.93539	1.01864	1.05535
140	v	1.78573	2.19754	2.98160	3.70465
	Z	.87842	.94587	1.02667	1.06304
150	v	1.70365	2.07762	2.80688	3.48420
	Z	.89790	.95813	1.03555	1.07119
160	v	1.63518	1.97590	2.65602	3.29267
	Z	.91927	.97196	1.04522	1.07980
170	v	1.57669	1.88876	2.52466	3.12487
	Z	.94178	.98717	1.05562	1.08882
180	v	1.52539	1.81344	2.40943	2.97677
	Z	.96474	1.00355	1.06670	1.09823
190	v	1.47920	1.74774	2.30767	2.84517
	Z	.98750	1.02093	1.07841	1.10799
200	v	1.43659	1.68995	2.21724	2.72750
	Z	1.00953	1.03913	1.09068	1.11807
210	v	1.39654	1.63871	2.13641	2.62170
	Z	1.03046	1.05800	1.10347	1.12843
220	v	1.35850	1.59294	2.06378	2.52606
	Z	1.05012	1.07743	1.11671	1.13904
230	v	1.32234	1.55179	1.99820	2.43921
	Z	1.06863	1.09730	1.13038	1.14988
240	v	1.28833	1.51458	1.93873	2.36000
	Z	1.08642	1.11756	1.14441	1.16091
250	v	1.25717	1.48079	1.88456	2.28752
	Z	1.10431	1.13815	1.15879	1.17214
260	v	1.22994	1.45000	1.83505	2.22098
	Z	1.12361	1.15906	1.17348	1.18357
270	v	1.20811	1.42189	1.78966	2.15979
	Z	1.14611	1.18031	1.18847	1.19523
280	v	1.19357	1.39622	1.74794	2.10347
	Z	1.17426	1.20193	1.20376	1.20717
290	v	1.18861	1.37281	1.70952	2.05164
	Z	1.21114	1.22397	1.21935	1.21947
300	v	1.19594	1.35150	1.67410	2.00404
	Z	1.26063	1.24653	1.23526	1.23226

APPENDIX A

LIST OF PHYSICAL CONSTANTS

Local gravitational acceleration	$g = 32.1618$ ft/sec^2
Standard gravitational acceleration	$g_s = 32.1740$ ft/sec^2
Universal Gas Constant	$R = 82.0575$ liter-atm/gm mole °K
Planck's Constant	$h = 6.6252 \times 10^{-34}$ joule-sec
Boltzman's Constant	$k = 1.3804 \times 10^{-23}$ joule/°K
Avogadro's number	$\tilde{N} = 6.0249 \times 10^{23}$ molecules/gm mole
Molecular weight of Helium	4.003 gm/gmmole
Molecular weight of Neon	20.183 gm/gmmole
Density of Mercury at 0 °C	$\rho_{hg} = 13.5951$ gm/cm^3
Standard atmosphere	14.6959 lbf/in^2
Absolute Zero of Temperature	- 273.15°C

BIBLIOGRAPHY

1. Armstrong, E. N., Oil Gas J., 45, 82-4 114, (Dec.,1946), (B).

2. Basinski, Z. S., and Christian, J. W., Advances in Cryogenic Engr., Vol. 2, Plenum Press, New York, (1960), (Des).

3. Beattie, J. A., Rev. Sci. Instr., 2, 458, (1931), (TC).

4. Bedjai, G., Volff, C. L., and Canjar, L. N., Advances in Cryogenic Engr., Vol. 1, Plenum Press, New York, (1960), (Des).

5. Birmingham, B. W. Brown, E. H., Class, C. R., and Schmidt, A. F., Advances in Cryogenic Engr., Vol. 1, Plenum Press, New York, (1954), (Des).

6. Boato, G., and Casanova, G., Physica 27, 571-89, (1961), (Thy).

7. Brandt, L. W., Stoud, L., and Deaton, W. M., Advances in Cryogenic Engr., Vol. 1, Plenum Press, New York, (1954), (TC).

8. Burnett, E. S., J. App. Mech., 58, A136, (1936), (B).

9. Burt, F. P., Trans. Faraday Soc., Vol. 6, 19-26, (1910), (NPvt).

10. Canfield, F. D., Leland, T. W., Kobayashi, R., Advan. Cryog. Eng. 8, p. 146, Plenum Press, New York, 1963, (B).

11. Cattel, R. A., and others, U.S. Bur. Mines, Pet. Invest. 3616, 13-14, (1942), (B).

12. Clement, J. R., and Quinnel, E. H., Rev. Sci. Instr., 24, 545, (1953), (TC).

13. Cook, D., Can. J. Chem., 35, 268, (1957), (B).

14. Cook, G. A., Argon, Helium and the Rare Gases., 2 vols. Interscience Publishers, New York, (1961), (HePvT).

15. Crain, R. W., Jr., P-v-T Behavior in the Argon-Nitrogen System, PhD dissertation in Mechanical Engineering, Univ. of Mich, Ann Arbor, Michigan, (1965), (B).

16. Crommelin, C. A., Martinez, J. P., and Onnes, H. K., Commun. Phys. Lab. Univ. Leiden, 154a, (1919), (NPvT).

17. Davis, E. T., Instruments 24, 642, (1951), (TC).

18. Dauphinee, T. M., and Preston-Thomas, H., Rev. Sci. Instr., 25, 844, (1954), (TC).

19. Dauphinee, T. M., MacDonald, D. K. C., and Preston-Thomas, H., Proc. Roy. Soc., A, 221. 267, (1954), (TC).

20. DeBoer, J. Physica,24, 590-597, (1958), (Thy).

21. DeBoer, J., and Michels, A., Physica,5, 945, (1938), (Thy).

22. Fulk, M. M., Reynolds, M. M., and Park, O. E., Advances in Cryogenic Engr., Vol 1, Plenum Press, New York, (1960), (Des).

23. Goodwin, R. D., Advances in Cryogenic Engr., Vol. 4, Plenum Press, New York, (1958), (TC).

24. Grilly, E. R., Cryogenics 2, No. 4, 226, (1962), (Des).

25. Gropper, L., Phys. Rev.,55, 1095-7, (1939), (Thy).

26. Harper, R. C., Jr., An Investigation of the Compressibility Factors of Gaseous Mixtures of Carbon Dioxide and Helium, PhD dissertation in chemistry, Univ. of Penn., Philadelphia, Pa., (1956), (B).

27. Harper, R. C., Jr., and Miller, J. G., J. Chem. Phys., 27, (1957), (B).

28. Heuse, V. W., and Otto, J., Ann. Physik,2, 1012, (1929), (NPvT).

29. Hirschfelder, J. O., Curtiss, C. F., and Bird, R. B., Molecular Theory of Gases and Liquids, Wiley, New York, (1954), (Thy).

30. Holborn, L., and Otto, J., Z. Physik,38, 359-67, (1926), (NPvT).

31. Holborn, L., and Otto, J., Z. Physik,33, 1-12, (1925), (NPvT).

32. Holborn, L., and Otto, J., Z. Physik, 23, 77, (1924), (NPvT).

33. Holborn, L., and Otto, J., Z. Physik, 30, 320, (1924), (HePvT).

34. Holborn, L., and Otto, J., Z. Physik, 33, 1, (1925), (HePvT).

35. Holborn, L., and Otto, J., Z. Physik, 38, 359-367, (1926), (HePvT).

36. Holborn, L., and Otto, J., Z. Physik, 23, 77, (1924), (NHePvt).

37. Hoover, A. E., Canfield, F. B., Kobayashi, R., and Leland, T W., Jr., J. Chem. Eng. Data 4, 569, (1964), (Thy).

38. Jacobs, R. B., Richards, R. J., and Schwartz, Advances in Cryogenic Engr., Vol. 1, Plenum Press, New York, (1954), (Des).

39. Johnston, H. L., Hood, C. B., Jr., Bigeleisen, J., Powers, R. W., and Ziegler, J. B., Advances in Cryogenic Engr., Vol. 1, Plenum Press, New York, (1960), (Des).

40. Keesom, W. H., Helium, 36-8, Elsevier Press, Amsterdam, (1942), (HePvT).

41. Keyes, F. G., Ind. Eng. Chem., 23, 1375, (1931), (Des).

42. Keyes, F. G., Ind. Eng. Chem., 23, 1375, (1931), (TC).

43. Kilpatrick, J. E., Keller, W. E., and Hammel, E. F., Phys. Rev., 97, 9-12, (1955), (Thy).

44. Kramer, G. M., and Miller, J. G., J. Phys. Chem., 61, 785, (1957), (B).

45. Lennard-Jones, J. E., and Cook, W. R., Proc. Roy. Soc. London, A115, 334, (1927), (HePvT).

46. Lennard-Jones, J. E., Proc. Roy. Soc. London, 106, 463, (1942), (Thy).

47. Liston, M. D., Rev. Sci. Instr.,17, 194, (1946). (TC).

48. MacCormack, K. E., and Schneider, W. G., J. Chem. Phys., 18, 1269-72, (1950), and J. Chem. Phys.,19, 845-8, (1951), (B).

49. Mann, D. B., NBS Tech. Note 154, (1962).

50. Margenau, H., Phys. Rev.,36, 1782-90, (1930), (Thy).

51. Margenau, H., Phys. Rev., 36, 1782-90, (1930), (Thy).

52. Martinez, J. P., and Onnes, H. K., Commun, Phys. Lab. Univ. Leiden, 164, (1923), (HePvT).

53. Mason, C. E., Trans. ASME, 60, 327, (1938), (TC).

54. Mason, C. E., and Philbrick, G. A., Trans. ASME, 62, 295, (1940), (TC).

55. Mason, E. A., Rice, W. E., J. Chem. Phys., 22, 843, (1954), (Thy).

56. Masson, I., and Dolley, L. G. F., Proc. Roy. Soc. London, A103, 524, (1923), (Thy).

57. Mathewson, R. C., Advances in Cryogenic Engr., Vol. 2, Plenum Press, New York, (1960), (Des).

58. McCarty, R. D., and Stewart, R. B., Cryogenic Engineering Report K-1, R-293, (1963), (NPvT).

59. McCarty, R. D., Stewart, R. B., and Timmerhaus, K. D., Paper No. C-3, 1962, Cryogenic Engin. Conf., (NPvT).

60. Michels, A., and Gibson, R. O., Ann. Physik, Vol., 87, 850, (1928), (NPvT).

61. Michels, A., Wassenaar, T., and Louwerse, P., Physica, 26, 539, (1960), (NPvT).

62. Mueller, W. H., Leland, T. W., Jr., and Kobayashi, R., A.I.Ch.E. J., 7, 267, (1961), (B).

63. Nicholson, G. A., and Schneider, W. G., Can. J. Chem., 33, 589-96, (1955), (NPvT).

64. Nijhoff, G. P., Keesom, W. H., and Illiin, B., Commun. Phys. Lab. Univ. Leiden, 188c, (1927), (HePvT).

65. Nijhoff, G. P., Keesom, W. H., Commun. Phys. Lab. Univ. Leiden, 188b, (1927), (HePvT).

66. Nijhoff, G. P., Keesom, W. H., and Illiin, B., Leiden Suppl.,64c, (1928), (Thy).

67. Oiski, J., J. Sci. Research Inst., 43, 220-31, Tokyo, (1949), (NPvT).

68. Onnes, H. K., and Crommelin, C. A., Commun. Phys. Lab. Univ. Leiden, 147d, (1915), (NPvT).

69. Onnes, H. K., Commun. Phys. Lab. Univ. Leiden, 102a, (1927), (HePvT).

70. Onnes, H. K., Commun. Phys. Lab. Univ. Leiden, 102c, (1908), (HePvT).

71. Onnes, H. K., Commun. Phys. Lab. Univ. Leiden, 71, (1901), (Thy).

72. Onnes, H. K., Commun. Phys. Lab. Univ. Leiden, 151a, (1917), (Des).

73. Onnes, H. K., and Boks, J. D. A., Commun. Phys. Lab. Univ. Leiden, 170a, b, (1924), (HePvT).

74. Palacios, J., and Onnes, H. K., Commun. Phys. Lab. Univ. Leiden, 164, (1923), (HePvT).

75. Penning, F. M., and Onnes, H. K., Commun. Phys. Lab. Univ. Leiden, 165c, (1923), (HePvT).

76. Pfefferle, W. C., Jr., PhD dissertation in Chemistry, Univ. of Penn., Philadelphia, Pa., (1952), (B).

77. Pfefferle, W. C., Jr. Goff, J. A., and Miller, J. F., J. Chem. Phys., 23, 509, (1955), (B).

78. Ramsey, W., and Travers, M. S., Phil. Trans of Royal Soc., 197A, 47, (NPvT).

79. Reynolds, M. M., Brown, J. D., Fulk, M. M., Park, O. E., and Curtis, G. W., Advances in Cryogenic Engr., Vol. 1, Plenum Press, New York, (1960). (Des).

80. Sachse, H. B., Electronics Inds., 16, 55, (1957), (TC).

81. Schamp, H. W., Jr., Mason, E. A., Richardson, A. B. C., and Altman, A., Phys. Fluids, 1, No. 4, 329, (1958), (Thy).

82. Scheider, W. G., Can J. Research, B27, 339-52, (1949), (B).

83. Schneider, W. G., and Duffie, J. A. H., J. Chem. Phys., 17, 751-54, (1949), (B).

84. Scott, Russell, B., Cryogenic Engineering, (1959), (Des).

85. Silberberg, I. H., Kobe, K. A., and McKetta, J., J. of Chem. and Engin. Data, Vol. 4, No. 4, (1959), (B).

86. Silberberg, I. H., McKetta, J. J., and Kobe, K. A., J. Chem. Eng.,Data, 4, 314, (1959), (B).

87. Silberberg, I. H., McKetta, J. J., and Kobe, K. A., J. Chem. Eng., Data, 4, 323, (1959), (B).

88. Smith, M. C., and Rabb, D., Advances in Cryogenic Engr., 1, (1954), (Des).

89. Stevens, A. B., and Vance, H., Oil Weekly, 106, 21026, (June 8, 1942), (B).

90. Sulzer, P. G., Proc. I.R.E., 43, 701, (1955), (TC).

91. Tanner, C. C., and Masson, J., Proc. Roy. Soc. London, A122, 283, (1929), (Thy).

92. Tanner, C. C., and Masson, J., Proc. Roy. Soc. London, A126, 268-88, (1929-30), (Thy).

93. Van Agt, F.P.G.A.J., and Onnes, H. K., Commun. Phys. Lab. Univ. Leiden, 176b, (1925), (HePvT).

94. Van Wylen, G. J., Lady, E. R., and Clark, J. A., Cryogenic Engin. Fundamentals, Univ. of Mich., (1962), (Des).

95. Waite, H. J., Advances in Cryogenic Engr., Vol. 1, Plenum Press, New York, (1960), (Des).

96. Wartel, W. S., PhD dissertation in chemistry, Univ. of Penn., Philadelphia, Pa., (1954), (B).

97. Watson, G. M., and others, Ind. Eng. Chem., 46, 362-4, (1954), (B).

98. West, E. D., and Ginnings, D. C., Rev. Sci. Instr., 28, 1070, (1957), (TC).

99. Whalley, E., Lupien, Y., and Schneider, W. G., Can. J. Chem., 31, 722-33, (1953), and Can. J. Chem, 33, 633-6, (1955), (B).

100. Whalley, E., and Schneider, W. G., J. Chem. Phys.,23, 1644, (1955), (Thy).

101. Woodard, K. A., Advances in Cryogenic Engineering, Vol. 1, Plenum Press, New York, (1960), (Des).

102. Yendall, E. F., Advances in Cryogenic Engineering, Vol. 4, Plenum Press, New York, (1960), (NPvT).

103. Yntema, J. L., and Schneider, W. G., J. Chem.Phys., 18, 641, (1950), (B).

104. Zimmerman, R. H., and Beitler, S. R., Trans. Am. Soc. Mech. Engr., 74, 945-51, (1952), (B).

105. Kaminsky, J., and Blaisdell, B. E., "The Determination of the Internal Volume of Steel Capillaries for Measurements with Gases," R.S.I., Vol. 10, (Feb.,1939).

106. Allen, C. W., Astrophysical Quantities, Univ. of London, The Athlone Press, (1955).

107. Thompson, L. G. D., Hawkins, C., and Perry, R., Research Report, USAF Air Base Gravity Network.

108. White, D., Rubin, T., Camky, P., and Johnston, H. L., The Virial Coefficients of Helium from 20 to 300° K, J. of Physical Chemistry, 64, 1607 (1960).

Des Design.

NPvT Neon P-v-T data.

HePvT Helium P-v-T data.

Thy Theory.

B Burnett device.

TC Temperature control.